ABSTRACT

Title of Document:	DEVELOPMENT OF A NEW TYPE OF COMPOSITE MATERIAL: A GLASS BASED LAMINATED CERMET
	Dennis P. Brown, Master of Science
Directed By:	Dr. Manfred Wuttig, Department of Material Science and Engineering

This thesis is concerned with developing a revolutionary composite – a majority glass based laminated cermet[1,2] or GMET (**G**lass-**Met**al Laminate.) A GMET exhibits extraordinary qualities: strength to density ratio's up to 80% greater than 6061 aluminum alloy, and uniquely, bulk toughness/fracture toughness similar to that alloy, and astonishingly, tensile failure morphologies that are identical to 6061 aluminum alloy.

Using glass in the laminate creates another crucial advantage: this class of composites can be manufactured using hot rolling – a processing technique that could lend itself to rapid production of high layer density, large area composites in a cost effective manner.

It will be demonstrated that GMETs offer excellent protection capabilities versus kinetic, and superior capabilities against shaped charged weapons at weights lower than that achieved using current metal or ceramic armors. This class of composites will be shown to withstand multi-ballistic impacts over the same contiguous area.

---

[1] Cermet: **Cer**amic – **met**al

[2] The use of glass for the ceramic phase of a cermet laminate in this thesis is the first ever-documented example of this type of composite. This assertion has been certified by Dr. Wadsworth, (Director of Oak Ridge Laboratory) and Dr. Nieh (Professor, UT Materials Science Department ORNL Metals and Ceramics Division) both world-renowned researchers in the fields of metal/composite laminates. (Private e-mail)

DEVELOPMENT OF A NEW TYPE OF COMPOSITE MATERIAL:

A GLASS BASED LAMINATED CERMET

by: Dennis P. Brown[1]

2006

Thesis submitted to the Faculty of the Graduate School of the
University of Maryland, College Park in the partial fulfillment
Of the requirements for the degree of
Master of Science

Advisory Committee:
Dr. M. Wuttig, Chair
Dr. A. Christou
Dr. I. K. Lloyd
Dr. A. L. Roytburg
Dr. A. Dasgupta
Dr. B. Lawn, NIST

---

[1] Currently employed at the Naval Research Laboratories, Nike Laser Physics Section, Washington DC

Dedication

I would like to dedicate this thesis work to my loving Daughter,

Jeannette Danielle Lorena Maisano-Brown

With all my love

Acknowledgements

Table of Contents

Introduction

Similar and Dissimilar Metal Lamination

Two-dimensional multiple layered structured composites designed to increase the tensile strength and/or toughness of materials has a long history. The ancient technique of metallurgical processing of low and high carbon iron plates to form laminated structures is well documented for both Damascus (ref. 1), and Japanese folded steels (ref. 2.) Problems of cross diffusion at the elevated temperatures used to form these types of similar metal laminates places severe constraints on the minimum layer thickness and ultimate layer density that these metallic composites can achieve by rolling and/or fold processing (ref. 2.)

Relative to the cold or hot roll forming of dissimilar metal plates with the goal of creating high layer density laminates, these processes are not practical for a number of reasons: first, chemical bonding problems related to interface oxides tend to prevent the layers between the dissimilar metals from achieving good adhesion. Secondly, differential coefficient of temperature expansion (CTE) mismatch between the two different metals will often cause the layers in the laminated structure to break apart during any significant temperature cycling. Third and most critically, the processing problems of differential work hardening and strain rate response between the two different metallic phases places severe limits on the final layer thickness and densities that these types of dissimilar laminated metals can achieve under hot or cold roll processing (ref. 3).

To overcome these process limitations for hot roll production of dissimilar laminates, a non-metallic phase must be considered. Specifically, use of an oxide glass[1] as the second phase in the ceramic-metal laminated composite. The use of a glass phase within the matrix will allow the creation of a new class of laminated composite[2], and these special materials will be referred to as GMETs[3] in this thesis.

Classical Laminated Cermets

A cermet (**cer**amic-**met**al) is a material that uses both ceramic and metal phases to create the composite. More recently laminated cermets - where the metal and ceramic phases form plates or layers that alternate within the composite, have been created by other researchers (ref. 4, et. al.) – see fig. 1.
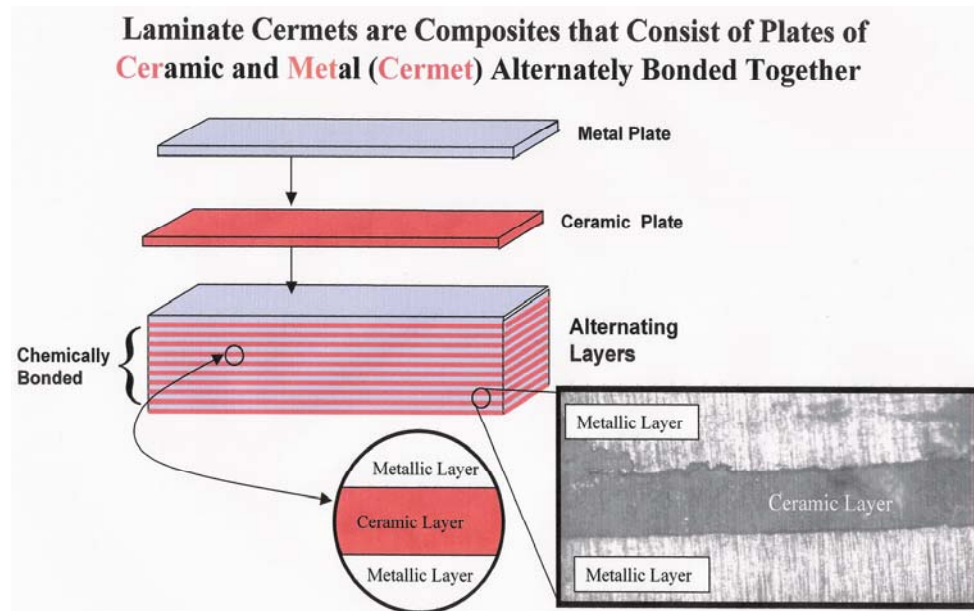
Fig. 1: Laminated cermet schematic and (**insert**) an image of an actual laminate layer

---

[1] In this thesis, unless otherwise noted, all references to 'glass' are meant to mean an oxide glass

[2] The use of glass for the ceramic phase of a cermet laminate in this thesis is the first ever-documented example of this type of composite. This claim has been certified by Dr. Wadsworth, (Director of Oak Ridge Laboratory) and Dr. Nieh (Professor, UT Materials Science Department ORNL Metals and Ceramics Division) both world renowned researchers in the fields of metal/composite laminates. (Private e-mail)

[3] GMET: **G**lass-**Met**al Laminate

The primary advantage of using a metal/ceramic combination in any laminated structure is that the metallic component can, if the layers are thin enough and the system layer density is sufficient, provide the composite with considerably greater toughness compared to that of even toughened ceramics and the ceramic phase could, by careful selection of materials, impart to the overall composite a greater bulk strength compared to that of the singular metal phase and possibly, lower the overall density of the composite (ref. 5, 6, 7, 8 and 9.)

The major drawback for this specific class of composites is that there is no true mass production technique that can rapidly manufacture the high densities and ultra-thin layers required or produce large area laminated plates in a cost effective manner. As a consequence, these types of laminates have been little more than laboratory curiosities.

This thesis research was started with the express intent of overcoming this lack of a more rapid and cost effective method for creating this class of laminate cermets.

For many of the same reasons that hot rolling fails for dissimilar metals, crystalline-based laminated cermets cannot readily be created using any common mass-production methodologies. Ceramics, like metals, exhibit strain rate/work hardening effects that prevent the flow matching of the two different phases when being deformed under hot rolling. Due to ceramics brittle nature, cold rolling is not feasible.

For reasons that will be elaborated on in greater detail later in this thesis, a new type of laminated cermet – one based on glass – was developed permitting the creation of an entirely new type of laminated composite: a GMET.

These GMETs, while mostly glass by volume (88 – 95%), have exhibited tensile yield strengths greater than 6061-aluminum alloy (currently, a 22% - 80% improvement.)

One very significant discovery made in this thesis is that GMETs exhibit not just a thirty to sixty percent improvement in overall bulk toughness as achieved by researchers with many crystalline based laminated cermets (ref. 4, 8.) but rather, GMETs offer a revolutionary improvement in composite's bulk toughness. GMET's constructed for this thesis routinely exhibit an improvement in fracture toughness of nearly two orders of magnitude and almost one order of magnitude improvement in overall toughness compared to bulk oxide glasses. Incredibly, these GMETs have demonstrated tensile **elongation failure modes that are *identical*** to 6061 Al alloy.

From previous researchers' work (ref. 10) and experimental results obtained from this thesis, the toughness improvement and elongation properties of the GMETs are most probably due to the presences of a special glass that has the unique ability to support true plastic deformation even at room temperatures. This conjecture is based on extensive experimental testing using tensile, four-point bend, and torsion deformations of different GMETs performed at room temperature and after careful inspection of glass areas that were heavily stressed/deformed using visible and polarized white light.

It will be demonstrated in this thesis that GMETs offer superior armor protection performance compared to either metals or ballistic grade ceramics versus man portable weapons: assault rifles (caliber 7.62 mm; ref. 11) and RPG's (ref. 12, and 13.)

Experimental evidence will be presented that demonstrates that a hot rolling technique can be used to process this new type of glass based laminated cermet.

Thesis: Primary Objectives

The initial goal of this research was to overcome a lack of a scalable production methodology for laminated cermets. For reasons that will be discussed more fully later in

this thesis, if a GMET is used and a number of material processing parameters can be carefully controlled, then hot rolling, a common manufacturing process, could readily be adapted for production of these special laminates.

Relative to the new manufacturing technique - the simultaneous rolling of a glass and metal – a number of material science and engineering issues such as matching the coefficient of thermal expansion (CTE), and creating high strength chemical bonding between the ceramic (oxide glass) and metal phases would need to be addressed for all temperature ranges and material phases used in the hot roll process. Regardless of the manufacture technique chosen, the resulting cermet laminate will need to exhibit toughness values similar to that of a metal in order to be of significant use in load bearing or multi-hit resistant ballistic applications.

To ensure that the overall strength to density ratio was high enough to be of use in aerospace applications, an aluminum alloy (6061; @ 2.7 gm/cm^3) was selected as the primary metal phase in the composite for this thesis effort. Copper was also used for its ease of machineability and high melting point compared to the softening point of the glass (480 - 500 C.) The special glass used for this thesis has a density of 2.5 gm/cm^3.

Another critical objective was to fully demonstrate that a glass and aluminum based cermet laminate could stop all major handheld ballistic weapon threats (7.62 mm rounds) at a weight that a soldier could readily endure while not compromising bulk toughness or true multi-hit defeat capabilities for a contiguous plate.

As possible vehicle armor the composite was tested, under a successful Navy SBIR contract (N00014-04-M-0393), against shaped charged warheads (a. k. a.: RPG's) the

most deadly man portable anti-armor weapon in existence and the GMET composite was shown to be superior to all existing armor on a weight bases.

Applications

As a result of this thesis work, a new type of high strength to density, easy to work and metal-like tough GMET has been developed that could have numerous applications where high end light metal alloys or difficult to manufacture/assemble composites are often exploited.

In the aerospace industry GMETs can be used as fully load bearing capable, high strength to density and high performance radiation and micro-meteor protection structural materials. With the addition of boron and/or lithium to the GMET matrix, this composite would be 15 - 25% lower in density than 6061 aluminum alloys while retaining both the improved strength and bulk toughness capabilities of this composite.

On a weight bases, neutron protection similar to plastic and proton radiation protection two to three times greater than plastic can be achieved when using the boron/lithium in the glass. Since aluminum volume is minimized (< 12%) in the composite, GMETs will produce very few secondary particles (neutrons and protons) when radiated by high-energy galactic cosmic rays (GCR), or solar particle events (SPE) compared to existing aluminum alloys.

Versus hyper-velocity impacts (10^{+} km/s), this GMET when used as a load bearing structural component would provide significantly improved non-parasitic protection for all space vehicles – manned or robotic.

Critically, GMETs, unlike any ceramic or most composites, exhibits very metal-like behavior in their bulk toughness response to impacts and especially important, in their tensile/torsional failure modes.

Processing techniques such as cutting, and drilling using typical metal blades/bits is fully permissible on the GMET and standard aerospace assembly methods such as riveting, hot forming and possibly edge welding can be used with this composite. Amazingly, for a mostly glass based composite, significant room temperature bending can be endured without observable cracking within the glass matrix.

For the automobile industries GMETs offer a lower weight composite compared to aluminum for the manufacture of body components and panels that can still readily be hot formed into near net shape. Since these composites are extremely tough, most automobile assembly methods can be used.

Relative to civilian police and military sectors as a high performance, low-density ballistic armor due to the fact that GMETs exhibit superior multi-hit stopping power compared to any existing ballistic grade ceramic.

GMETs are a type of ceramic based composite that provides the best, on a weight bases, hyper-velocity metal jet defeat protection of any existing material. For applications where low weight vehicle armor is required, GMETs are ideal since this composite can easily be cut/drilled edged welded or bolted as needed for assembly; for personal armor GMETs can readily be hot formed into complex curves and shapes for creating better fitting components that will not compromise the composites protection capabilities.

Chapter 1

Methodology to Mass Produce Laminated Cermets

Background

The novel processing idea developed for this thesis research relative to GMET production exploits the fact that for short time periods when a metal undergoes shear deformation, this type of material tends to closely approximate constant volume flow, which is very similar to Newtonian fluid flow. Oxide glasses, when heated to or above their working range, are classic Newtonian fluids under deformation. This overlap of Newtonian flow characteristics of these dissimilar materials opens up the possibility that the shear induce flow of a metal might be made to match that of a glass – that is, if a number of other physical parameters can be suppressed or made to match.

Except for very high temperature processing, metals work harden under deformation to some extent, and this problem for laminate hot rolling of dissimilar materials in a composite must be addressed. Using glass as one phase in the laminate will further suppress this problem since glass does not work harden.

Matching the three-dimensional flow of a glass with a metal under hot roll deformation would still appear unworkable since metallic flow for large deformations is non-Newtonian but elastic-plastic. Using the principle of near constant volume conservation of metals undergoing idealized metallic shear strain ($\tau = G\gamma$; where G is the shear modulus), it can be shown, to first order, that the constrained two dimensional shear-induced deformation of a differential metallic volume element is essentially identical to the viscous flow of a differential liquid glass element when process conditions are carefully controlled. (The basic physical and mathematical details on

8

metal/glass flow matching are discussed in the section entitled "Flow Matching of a Metal and Glass Under Shear Stress", page 17.)

The key to getting a metal to behave in a viscous-like manner when deformed is to use encapsulated (hydrostatic) hot rolling; also, if the metal phase is then rolled at temperatures above 0.4 the metal's melting point (T_{mp}), strain hardening by the metal phase during processing is strongly suppressed.

Hot rolling is not only an excellent example of a shear deformation process but as demonstrated by the metal industry a practical methodology to mass produce materials that are most often in the form of large area, rectangular plates. Since GMETs can consist of assemblies of these types of glass and metal plates, the possibly of adapting such a process to permit the low-cost, and rapid production of large area laminates might be feasible if the previously mentioned processing issues are overcome.

Shear Processing of a GMET: Metallic Newtonian Flow

Hot roll forming of laminated cermets grew out of the experiments of other researcher's who used metallic hot torsion testing to demonstrate that metals can exhibit highly viscous-like flow when heated and deformed under pure shear (ref. 14 and 15).

Torsion data graphs displayed in fig. 2 show that the torsional deformation response to angular displacement of a metal at 980 C is relatively flat (nearly constant in its yield) and supports a great deal of shear deformation before failure. That is, the behavior of the metal sample that was heated to 980 C and deformed under shear closely mimics the deformation behavior of a Newtonian-like fluid.

9
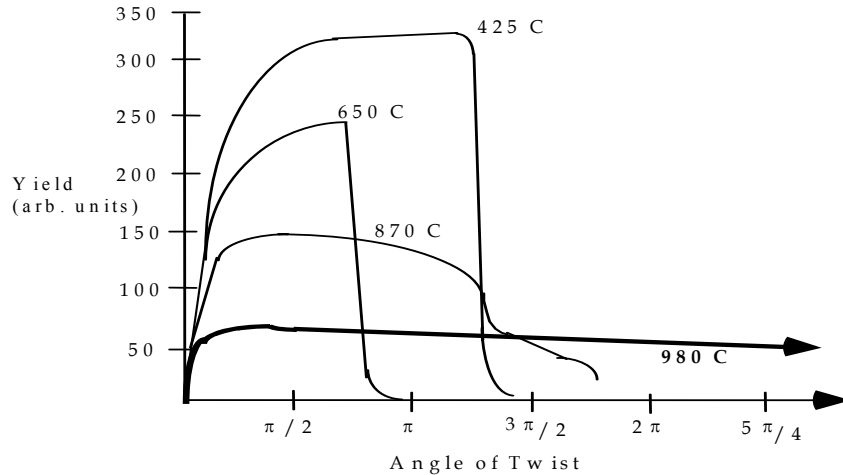
Fig 2: Data for hot torsion testing of steel (from Dieter; Mech. Met.; Third ed., Chapter 10, Sec 6, pp 346)

In hot torsion experiments this metal's deformation flow response is nearly identical to what the material would exhibit under hot rolling conditions. These two operations differ in absolute magnitude of the stress forces required to initiate deformation/flow, but the overall behavior of the deformation flow is related in a one-to-one manner.

Importantly, the response of a glass while in its very soft or 'plastic-like' state to a hot torsion test would be very similar to that of the 980 C metal – that is, have a similar overall shape relative to the applied stress to strain displacement. The two phases would differ in that the glass flow would be exactly horizontal (strain rate or m-value equals one) while the metal would show some negative slope (m < 1).

This relationship between the behavior of a metal when experiencing a torsional deformation (especially under a shear deformation) to the Newtonian-like flow of a glass leads to the distinct possibility that the gross compressive deformation response of a glass and metal could be made to match, under hot rolling, if other issues such as CTE mis-match, bonding, and temperature dependent plastic flow matching could be satisfied.

10

Rolling Induced Deformation of a Metal and Glass: Background Theory

All metals and most crystalline ceramics have some range of ductility - that is, the ability of the substance to permanently deform past their elastic range without cracking or exhibiting bulk failure. This material property is highly dependent on temperature. As is well known, many metals have a ductile working range from below room temperature up, and nearly to their melting points.

Ceramics, on the other hand, generally only exhibit a ductile range when heated to temperatures near their melting points (generally 0.8 T_{mp} and above).

Since these materials can be deformed in these temperature ranges, they all experience deformation rate effects relative to the applied force. Generally, work hardening during deformation also plays a significant role as well, but this effect will be ignored for now.

The strain rate exponents for many common ceramics have been roughly determined[4] and using these values a rough sketch of the 'ductility' map of these materials could then be determined for comparison purposes.

As the processing temperature of the ceramic is raised (near 0.8 T_{mp} softening temperature), the ceramics poor ductility response suddenly, and rapidly improves until a maximum value is reached (and strain rate response reaches a metal-like value of 0.3 or more) before melting effects become detrimental and lead to bulk failure. The ductility graph of a ceramic would be a rather narrow Gaussian in overall shape with its center near but somewhat after the softening point temperature (see fig. 3).

---

[4] "Superplasticity", Nieh, Wadsworth, and Sherby; Cambridge Press, Chapter 6, pp. 197

While a glass does not really have a ductile response in the classical definition of the term, it does have gross characteristics that resemble such a response. For short (finite) deformations, a glass does exhibit all criteria of a ductile response that is nearly identical to that of a metal. This idea can be considered a useful extension of the concept of ductile ranges.

Using the idea of ductile response by a glass (for short time periods), the maximum range of possible deformation would roughly cover the known mechanical viscosity working ranges of between 7.2 and 10.2 poise. Below 7.2 poise the glass rapidly becomes extremely liquid-like and would not meet the general criteria for successful working by most rolling processes. For values of 10.2 poise and above, cracks and crushing of the glass will occur for any significant deformations or strain rates.
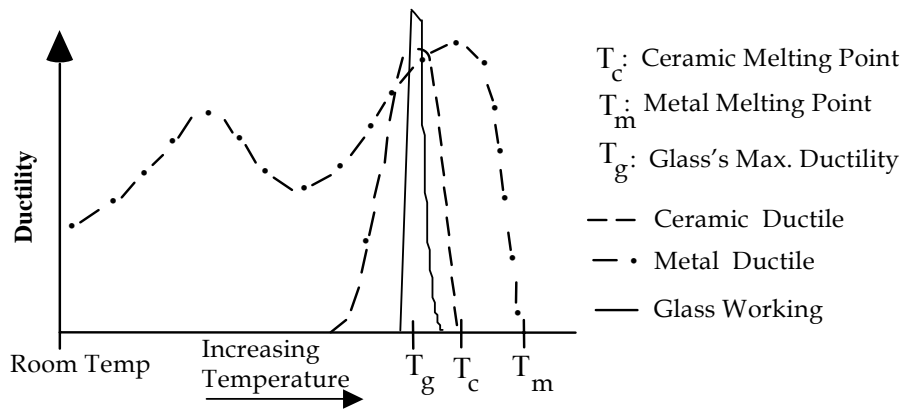
Fig. 3: Ductility of a metal, glass and ceramic as a function of temperature

To map a glass's ductile range, the viscosity of the material must be carefully considered. Since a glass exhibits a rapidly falling 'ductile-like' response above 7.2 poise, its graph of 'apparent ductility' versus process temperature would quickly fall from its ideal value over a *very* narrow temperature range. Note that all the material

ductility graphs displayed in fig. 3 are normalized so that they melt/soften at roughly similar temperatures – for simultaneous hot rolling of two dissimilar materials such as glass and metal, the two material's ductile flow properties will need to closely match at the desired processing temperature.

The ductility plot for a metal displayed in fig. 3 (the metallic graph is based on a titanium alloy) is not a simple function of the temperature. This metal, like many other metallic substances, has considerable ductile response even at room temperature. Of course, a complete study of the ductile response of a metal must include detailed microscopic examination and study of crystals or dislocation structures after processing as well as detection of any cracking or brittle failure. These defects can be created/caused by using the incorrect total deformation, or system strain rate, or alloying elements, or temperature to name a few of the more common process parameters. Relative to metals, the overall ductility curve is also controlled by strain hardening, and to lesser extent, numerous other physical parameters (grain boundaries, defeats, impurities, and crystal size to name a few of the most important.)

Ceramics can readily exhibit some of these effects, through these parameters are far smaller and not all have anywhere near the same impact on a given deformation process as these factors do relative to a metal. Of course, oxide glasses will never exhibit any grain boundary, strain hardening, or rate effects when deformed over its narrow working range temperature, and this aspect of glass behavior is of crucial importance for the ability of a GMET to be hot roll formed.

More on this aspect of processing cermets will be covered later in this chapter.

Strain Rate Exponents

Ceramics and especially glasses cannot be worked unless temperatures near or above their softening points are reached. To understand how the flow of a metal (which is a non-Newtonian fluid) and a glass (which is a Newtonian fluid to a high degree) compare, the gross stress to strain equations of these two materials must be examined in more detail.

Ignoring work hardening effects (i.e. for moderate deformations above $0.4\ T_{mp}$), the stress to strain equation for any generalized metallic substance can be written in the following form:

$$\sigma \ = \ C\ \dot{\varepsilon}^{\ m} \qquad \text{where the strain rate } '\dot{\varepsilon}' \text{ is } d\varepsilon / dt \qquad \text{Eq. 1}$$
$$\text{and } '\varepsilon' \text{ is the strain response of the material.}$$

Where 'm' is referred to as the strain rate sensitivity exponent. In general, 'm' can be determined for any solid but deformable substance by experimental means. Now, for a given applied force and no work hardening, the stress can be rewritten in terms of pressure to cross-sectional area as:

$$\sigma \ = \ P/A \ = \ C\dot{\varepsilon}^{\ m} \qquad \text{where "P" is the applied force,}$$
$$\text{and "A" is the cross-sectional area}$$

Then the time rate of change of the cross-sectional area of a deforming sample is then given as:

$$-\frac{dA}{dt} \ = \ \left[\left(\frac{P}{C}\right)^{1/m}\right]\left(\frac{1}{A^{(1-m)/m}}\right) \qquad \text{Eq. 2}$$

A plot of this differential relation for various m-values (Eq. 2) demonstrates how the cross sectional area of a material changes for various m-values of materials (applied force is fixed) – see fig. 4.

In general, the overall response of the sample's cross-sectional area change under deformation is just an inverse exponential function that is dependent on the strain rate parameter 'm'.
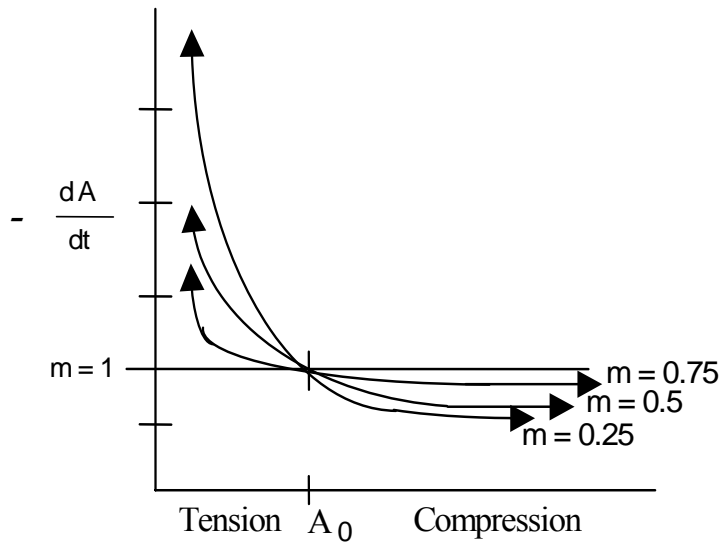
Fig. 4: Plot of the dependence of the cross-sectional area to strain rate exponent for metals. From "Mechanical Metallurgy", George Dieter, Chapter 8, sec. 6, pp. 300

In fig. 4, the series of curves to the left side of 'A$_0$' (initial cross-sectional area of the sample under no applied force) represent the area being deformed under a tensile force; and the series of curves to the right side of 'A$_0$' are the material's cross-sectional response to compressive deformation forces.

For a true Newtonian substance (the curve m = 1), the time rate of change of the area is a constant. That is, the area reduces or increases depending on whether it is in tension or compression at some linear rate regardless of the sample's previous work history (i.e.

the flow response of the material is not being controlled by work hardening, dislocations, or other internal innate physical factors.)

For most metals at elevated temperatures (where m-values range from 0.1 to 0.3, the rate the area decreases (for tension) will be a function that is highly dependent on the innate m-value of the material (for a fixed temperature, and with no work hardening effects). For moderate to low temperature processing, the material's strain-induced cross-sectional change in area is highly affected by any previous deformation (i.e. work hardening where m = 0.0001 – 0.09). For high temperature processing the strain rate exponent is the dominant controlling factor in this relationship.

Notice from the graphs in fig. 4 that the change in area for a metal when it is deformed under *compression* is not nearly as sensitive to variations of m-values (0.25, 0.5, 0.75, 1.0) as when the deformation is caused by tensional deformations.

This is the primary reason most metals can sustain extremely large rolling deformations since the process induces purely shear displacements (a compressive, semi-constant volume state of deformation). For compression deformations, all m-value curves differ very little in their slope when compared to the plots displayed on the tensile side of the graph. In fact, all the compressive curves begin to more closely mimic the 'm = 1.0' plot (but offset) as 'm-values' increase. This indicates that metals, in general, should closely obey the previous strain rate equation (Eq. 1) for high temperature processing (> 0.4 T_{mp}) and exhibit a flow response under compression that is very similar to that of a Newtonian like fluid; furthermore, when the metallic phase is deformed under shear and at elevated temperatures the flow response, even for large strains, will be very similar to Newtonian or glass like flow.

Flow Matching of a Metal and Ceramic

The procedure by which the problem of differential flow matching of a metal and ceramic can be overcome is by the precise control of two key physical parameters that are, to first order, independent of one another for roll deformation of glass and metal phases. That is the strain rate response (m-value) of the metal to deformation, and the temperature-controlled flow response of the glass (viscosity.)

For any metal undergoing a deformation at elevated temperature (> 0.4 T_{mp}), the strain rate has a major control on the plastic flow response of these types of materials. For this reason, the strain rate can be used to adjust the deformation induced flow response of a metal during hot rolling.

Glass, on the other hand, is relatively strain rate insensitive under deformation; it is a nearly perfect Newtonian fluid. Temperature can readily be exploited to control the flow response of the glass phase since the ductile response of a metal is only moderately sensitive to this parameter (for moderate temperature changes of +/- 25 C.) A glass's ductile response is significantly changed by even small variations in temperature (+/- 5 C and see fig. 3 and fig. 73, p. 137.)

Flow Matching of a Metal and Glass under Shear Deformation

The issue of matching the compressive induced flow of the glass and metal phases for a laminate composite during hot rolling is the critical challenge that must be addressed in order for these unique composites to be rapidly manufactured by this process – especially for high layer density laminates to be created in a simple and cost effective manner.

The central premise of the concept is that in hot roll deformation the flow of a metal and glass can be made to closely match for very specific environmental processing

parameters of temperature and strain rate. This can be demonstrated, to first order, by a

simple appeal to elementary deformation theory of ideal metal and glass volume elements

undergoing shear deformation – see fig. 5.

Shear Strain   Shear Strain

$$\tau_{glass} = \eta \frac{dv'}{dy} \quad \text{where } v' = u'/t_0 \qquad \tau_{Metal} = G \frac{du}{dy}$$
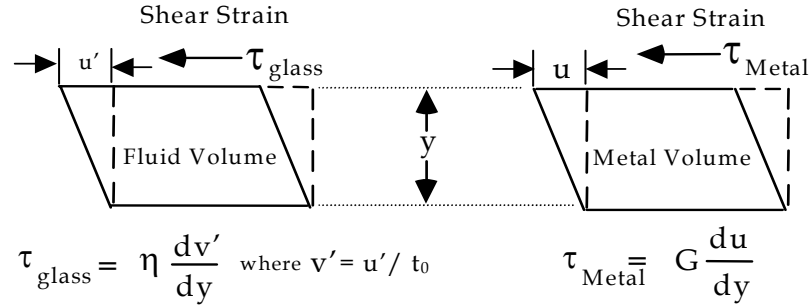
For the metal's differential element heated to a process
temperature s.t. $T > 0.4\ T_{mp}$:

$$u = v * t \Big|_{t \approx Const} \quad \text{then} \quad \frac{du}{dy} \Rightarrow t_0 \frac{dv}{dy} \qquad \therefore \ \tau_{Metal} = G \frac{dv}{dy}$$

By careful selection of process
temperature, glass and metal: $$\tau_{Glass} = \tau_{Metal}$$

Then for the case where the system is
laminated, we have $v = v'$, so $$\Rightarrow \eta(T) \cong t_0\, G = G/(\dot{\varepsilon})$$

Fig. 5: Relationship between the viscous flow of glass and the shear deformation of a
metal

In the shear diagram displayed in fig. 5, "τ" is defined as the applied shear stress that

initiates deformation on either the glass (viscous fluids can support shear) or metal

differential elements; "v'" is the displacement velocity of the glass for a given shear force

and "u" is the shear displacement of the metallic volume; "η" is the fluid's viscosity

(depends very strongly on temperature), and "G" is the shear modulus coefficient of the

metal at the processing temperature (which less strongly depends on temperature

compared to glass but is sensitive to strain rate.)

18

Strain rate for the system is indirectly given by the variable 't' which is a direct measure of the time needed for the deformation processes to displace the differential glass and metal volume elements for the given shear forces (τ_{glass} and τ_{metal}).

The magnitude of the shear forces required to deform two differential volume elements was quantified in the force diagram displayed in fig. 5 to be:

$$\tau_{glass} = \eta \ (dv'/dy), \text{ for the glass, and } \tau_{metal} = G \ (du/dy) \text{ for the metal}$$

The change in shape of both these differential volume elements are constant volume deformations due to the fact that fluids are, by definition incompressible, and in shear metallic deformation is a constant volume process for short time periods and moderate strain rates.

Under hot rolling when the deformation period is fairly short and the processing is performed at elevated temperatures ($T_{process} > 0.4 \ T_{mp}$), non-shear deformation effects can be ignored. Then the deflection velocity of the differential metallic volume element will be approximately constant over the time period 't' for which the shear is being applied. This permits the metal's displacement, due to the applied shear force, to be rewritten in terms of an average velocity ($u = v * t$.)

Then rewriting the metal's differential displacement using the chain rule (see fig. 5):

$$(du/dy) \Rightarrow (d/dy) \ (v * t) = [t * dv/dy + v * dt/dy]$$

The system's strain rate is fixed (i.e., 't', the time to deform the system is a constant and independent of the 'y' variable), this displacement term becomes:

$$du/dy = t \ (dv/dy)$$

When the two volume elements are strongly bonded and thin (so interface effects are significant), then under shear processing the displacements of the two materials will be highly constrained (i.e. v' ≅ v due to interface bonding and that the glass and metal support shear forces across their cross-sections). Under these conditions, to first order, the flow rate of the glass ($\eta(T)$) will match the metal's shear modulus ($G(\varepsilon, T)$) times the deformation period 't_0'; that is:

$$\eta(T) \cong [t_0 * G(\dot{\varepsilon}, T)] \qquad \text{Eq. 3}$$

For the desired process temperature both the viscosity of the glass (for a fixed temperature) and the metal's shear modulus values are fixed by the nature of the materials selected.

Equation 3 allows the system's strain rate to be calculated by noting that in the previous equation 't_0' is just the inverse of the strain rate. Solving for this value yields:

$$\dot{\varepsilon} = G(\dot{\varepsilon}, T)/\eta(T) \text{ where '}\dot{\varepsilon}\text{' is the strain rate} \qquad \text{Eq. 4}$$

For specific materials and substituting known physical parameters into equation 4, the rolling strain rate required to match the flow of the glass with the metal phase will be obtained. For example: copper at 526 C has a rolling shear yield of about 28 MN/cm^2 (see data graph, p. 137, fig. 74), and using the special sealing glass will have a viscosity of 7.8 poise at this temperature. These processing parameters will required a strain rate of:

$$\dot{\varepsilon} = [28 * 10^6 \text{ N/m}^2 \, / \, 1.0 * 10^{7.8} \text{ N-sec/m}^2] = 0.4/\text{sec}$$

For this strain rate, the glass should exhibit a shear induced total elongation nearly identical to that of the metal when rolled. Now, if the Poisson response of the two materials is nearly identical, and spreading effects lateral to the rollers is ignored (or

20

constrained by design), and then the two materials will exhibit nearly identical three-dimensional elongation values under hot roll deformation.

This calculated value for the system strain rate does not account for work hardening effects in the metal phase, which in reality will have a strong influence on the desired flow. The assumption of constant volume deformation for the metal phase during shear flow in a rolling system is not completely accurate – rolling, while a shear processing technique does not truly conserve volume during deformation and is only valid relative to the initial and final volume elements; this approximation should be sufficient for first order calculations to get the system's required initial deformation parameters for the two phases when the other parameters are known.

For hot rolling the strain rate calculated using these simple equations should give a shear induced elongation response of the composite for a glass phase that is fully embedded in the copper that more or less follows that of the metal.

More exact calculations using Kelvin-Voigt evolution equations for the visco-plasticity relative to the strain rate response matching between the glass and metal would provide a much more precise approximation to real shear deformation of the system under rolling and this approach will be addressed in a future paper.

As will be demonstrated in both the rolling and torsional deformation experiments for a metal, and glass the overall behaviors of these two substances are, in fact, very similar regardless of any theoretically calculated values (which are always approximations for real material flow properties in any case.)

Besides deformation flow matching in the direction of rolling between a metal and glass during processing, there are other important considerations such as chemical

bonding, matching of the coefficient of thermal expansion between the phases over all process temperatures, and finding a glass system that also exhibits the required viscosity values needed for processing a specific metal in a desired temperature range.

Relative to bonding between the proprietary sealing glass and either copper or aluminum, we have solved this issue. In fact, we have been unable to induce failure between the bulk metal and glass at their interface within the laminate structures by shock cooling in water for the copper/glass laminates pre-heated to 550 C.

For CTE matching, the primary sealing glass almost exactly matches copper from 850 C to room temperature (see the CTE chart, fig. 6) as well as closely following, somewhat offset but in a fairly linear manner, the aluminum over its range. A viscosity to temperature graph that is nearly identical to the specially modified sealing glass (see fig. 73, located on page 137, in the Appendix section.)
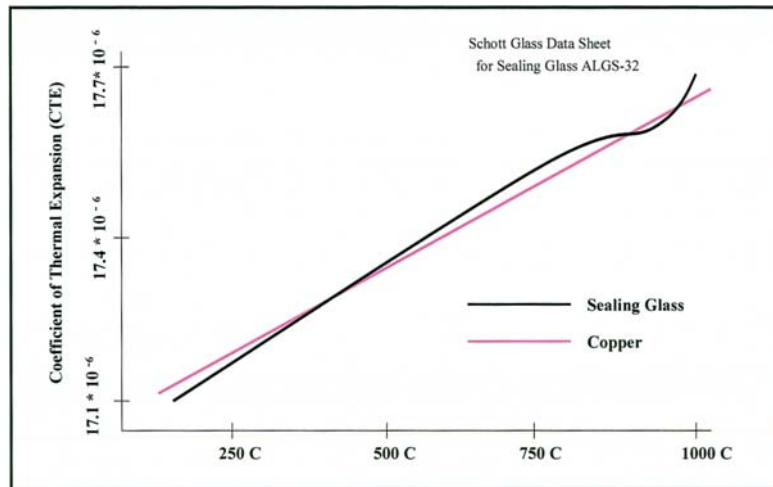
Fig. 6: Coefficient of thermal expansion of the sealing glass and Cu versus temperature

The Poisson ratio of the special sealing glass is 0.27 and one of the metallic phases (copper) for rolling has a value of 0.29. This near matching of Poisson values further simplifies and improves the roll induced flow matching between the two phases, especially as the layers get thinner and interface bonding effects begin to dominate between and across the layers (ref. 16.)

In creating high layer density cermet laminates, a glass plate is encapsulated within a metal phase (forming an initial 'three layer' sandwich structure.) The GMET sandwich was created by taking a metal case and pouring liquefied glass (750 – 800 C) into the center of the metal case – fig. 7.

This glass filled assembly was allowed to air cool to room temperature. Following this, the laminated system was reheated to the processing temperature (between 450 C – 525 C) and rolled using the required system strain rate to thin and elongate the assembly.
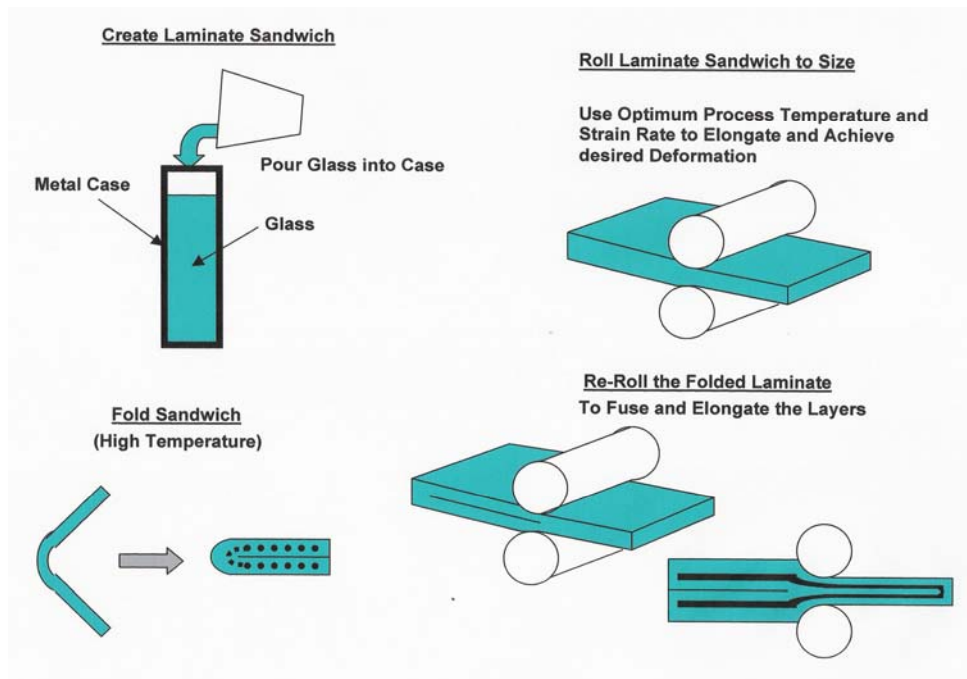
Fig. 7: Generalized schematic of hot rolling process to increase layer density

Then, in order to create more and thinner layers, the previously rolled assembly is folded onto itself, reheated and re-rolled (fig. 7 & 8.) Depending on the number of layers and desired thickness, this process could be continued as long as planar layer stability is maintained.

For example, the total number of layers created in a laminate by rolling and folding is given by the relation '$2^n + k_{n-1}$,' where n is the number of rolling and folding cycles executed, and 'k_{n-1}' is the number of layers existing in the laminate before that given folding iteration. After one rolling/folding operation (n = 1, and where $k_{n-1} = 3$ for the number of starting layers), the final number of layers becomes five - see fig. 8.
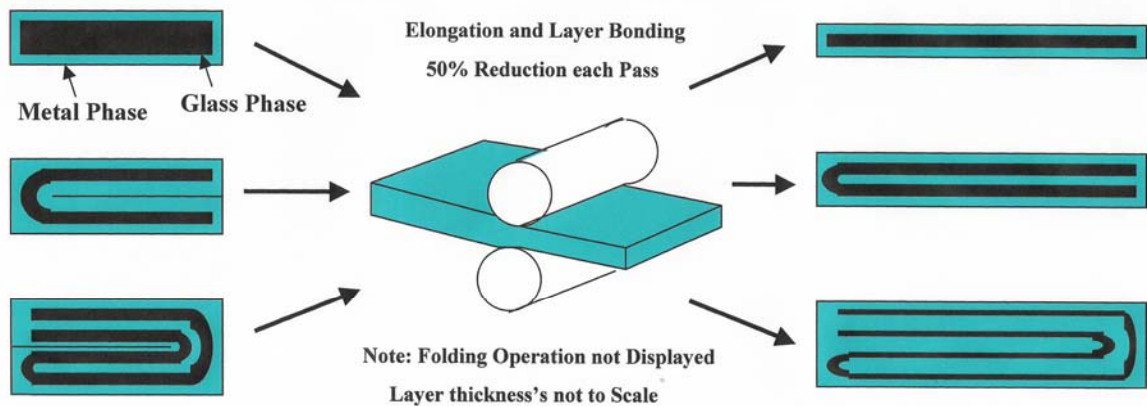
Layer density increase by rolling and folding is given by: $k_{i+1} = 2^n + k_i$ where k_i is the previous number of layers and n is the iteration.

n = 1	n = 2	n = 3	n = 4	n = 5	n = 6	n = 7
$k_0 = 3$	$k_1 = 5$	$k_2 = 9$	$k_3 = 17$	$k_4 = 33$	$k_5 = 65$	$k_6 = 129$
$k_1 = 2^1 + 3$	$k_2 = 2^2 + 5$	$k_3 = 2^3 + 9$	$k_4 = 2^4 + 17$	$k_5 = 2^5 + 33$	$k_6 = 2^6 + 65$	$k_7 = 2^7 + 129$
$k_1 = 5$	$k_2 = 9$	$k_3 = 17$	$k_4 = 33$	$k_5 = 65$	$k_6 = 129$	$k_7 = 257$

Fig. 8: Layer multiplication by rolling/fold operations for a single glass encapsulated laminated being rolled and folded twice (total number of layers, $k_2 = 9$.) The folding operation is not displayed but would occur after each roll pass

For roll reductions of 50%, the folding operation will then restore the laminate approximately back to its original thickness, while nearly doubling the laminate's total number of layers.

After six rolling and folding operations starting with a metal/glass/metal laminate about 1.3 cm thick (each glass/metal layer about 0.43 cm thick), the final laminate would have 129 layers each only about 10 microns thick– creating a metal layer thicknesses for an arbitrary ceramic based laminate that allows for the maximum possible bulk toughness (ref. 9).

Suppressing Secondary Rolling Issues

Issues relating to transverse flow effects, system work hardening and finite flow mismatch between the phases must also be accounted for and suppressed.

Transverse flow forces (which run perpendicular to the rolling direction) cannot be balanced for both glass and metal phases simultaneously during roll deformation since a glass will not be significantly constrained by frictional forces with the rollers. This problem can more readily be addressed by encapsulating the glass phase within the metal phase before rolling. Then the metallic phase, which will be constrained by fictional forces in the transverse rolling direction will strongly confine the glass volume in a manner such that the deformation induced flow of the glass will only occur in the rolling direction.

A fully encapsulated glass phase will tend to be subjected to near hydrostatic deformation forces during most of the rolling process – a condition that will further enhance flow matching between the two phases during shear deformation (see fig. 9.)
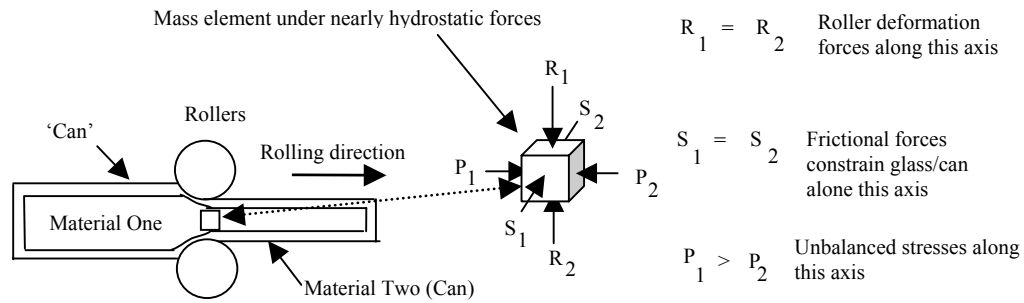
Fig. 9: Schematic of rolling of canned materials and a volume element with stress forces

Only the forces on the volume element along the direction of rolling are never in equilibrium during the rolling process, and these forces cause the glass and metal layers to elongate in the rolling direction. The encapsulating metal phase, due to frictional forces with the rollers will prevent the interior material (glass or ceramic) to undergo uncontrolled transverse flow.

Deformation Flow of Encapsulated Laminates

The process where one material is canned or encapsulated within another for rolling is a common industrial process used to create some types of specialty metals and some types of ceramics in the form of powders. The primary advantage to encapsulated rolling of materials is that the process tends to lower the deformation forces required to process the materials and stabilizes the flow of the different materials within case. This latter aspect has important implications for the rolling process since the stress fields experienced by any material subjected to deformation by rolling within the case, to first order approximation, a highly hydrostatic process. Of course, the 'can' must be stronger than the encapsulated phase and/or have a higher melting point for hot processing.

For the situation where a two-phase system is laminated and rolled, the materials in this structure would normally experience different total deformations, and as a consequence would exhibit both differential lateral widening and elongation lengths (similar to steel and copper for instance.)

This problem is primarily caused by the differential shear yield of each phase.

When one of the phases is completely canned or encased within another (see fig. 9), the inner phase's total deformation is strongly constrained by the outer cladding in all directions. These constraining forces cause the two phases to more closely match one another's flow deformation during the rolling process. This is a common practice used to create many types of two-phase materials; for instance, copper encased steel for wire drawing.

Of course, in reality, some mutual accommodation will occur and the inner material will cause deformation in the cladding. But to first order the inner material's ability to flow will be highly influenced or controlled by the cladding.

Relative to the differential work hardening between two phases there is a parameter that can be adjusted to compensate for this factor. When the system work hardens during rolling, the metal's shear yield increases and for a two phase laminate these changes will cause differential or non-uniform flow by the two materials.

The strain rate can then be adjusted so as to decrease the metal's shear-induced yield in a manner that permits the two phases to match their flow rates.

Examining the data displayed in fig. 10, the yield of a metal significantly decreases at lower strain rates (m-value.)
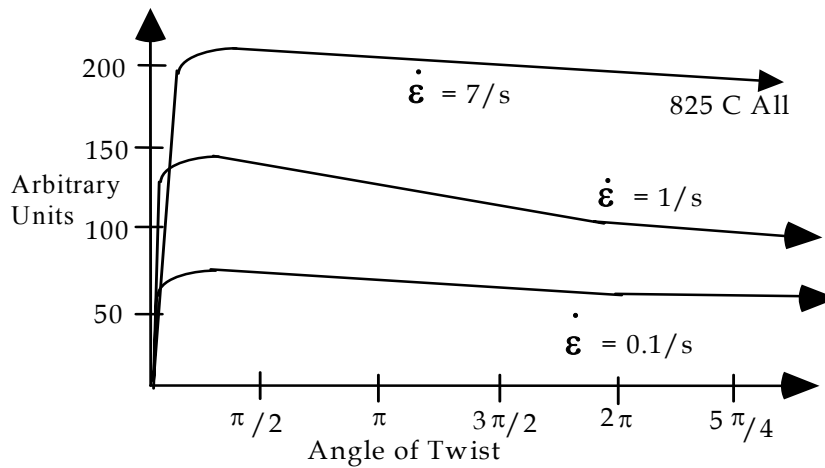
Fig. 10: Strain rate effects on flow of steel (for constant temperature); from ASM Journal; chapter 9, sec. 8

In order to compensate for any increase in work hardening in the metal phase while rolling a laminate structure (glass and metal), the rolling strain rate can be lowered for the next pass.

In this manner, the flow response of the metal, even if modified by work hardening can be made to match the glass simply by re-adjusting the strain rate. Then if the glass's viscosity needs to be increased or decreased to improve performance of the glass relative to the deformation conditions, the yield of the metal and, hence, the flow response can be made to match the glass once again by simply changing the deformation strain rate.

As partly demonstrated on mathematical and partly on experimental grounds, flow matching of a glass and metal under rolling deformation can be made to closely match if the system strain rate and temperature are used to control the shear yield of each component. Encapsulation can be exploited to further aid in offsetting minor differences in the flow reposes between the phases for larger/thicker laminate systems.

An interesting aspect of rolling laminates is that this type of operation should become more stable as the layer thickness within the composite decreases (ref. 3.) This is due to the fact that as layer thickness is reduced, interfacial-bonding effects will tend to dominate the bulk flow of both phases. So as each phase experiences deformation forces, continuity across the boundary will tend to require that any given layer accommodate the flow of the two layers that are adjacent and bonded to it. This interface continuity factor will tend to cause laminate structures in rolling deformation to become more stable as the layer thickness decreases – especially if the two materials exhibit similar Poisson ratios.

This is precisely the effect needed by the rolling process to maintain layer structure integrity within the laminate. (Aside: For the high CTE glasses, the Poisson ratios have values of 0.27 – 0.28. Metals typically have Poisson ratio's from 0.26 (aluminum) to 0.30 (copper) and up to 0.33 (steel.)

The issue of rolling deformation flow of a metal and glass still must be made to match to some as yet non-determined extent in order to allow the laminated system to be repeatedly rolled. This requirement can only be meet when the glass exhibits a viscosity between 7.2 to 10.2 poise. Otherwise the glass phase will not be sufficiently plastic for non-destructive rolling.

For the aluminum sealing glass this condition is best satisfied for copper in the glass's softening range of 450 – 550 C. In this temperature range, the metal has a relatively low shear induced yield and readily flows under roll deformation (see fig. 73, p. 137.) In this process temperature range the sealing glass does not crack nor act too fluid-like and can easily be rolled. More importantly, the glass readily forms/grows an oxide interface system (see chapter 4.)

One other important consideration for processing under roll forming is the number of metal layers, and their total thickness. As previously discussed, this layer density issue can have a major impact on the bulk toughness of the laminate. Metal layer density alone will have little, if any effect on the glass phase's fracture toughness – that is solely an innate property of the glass and can only be addressed by chemically modifying the glass.

These issues and how they can be dealt with will be discussed more fully later in this thesis.

In summation, the ability to exploit a hot rolling process to rapidly manufacture high layer density metal-glass laminates with layers approaching ten microns is a unique idea that if practical, could allow this class of laminates to be created almost as easily as any rolled metal. Such a development could allow this oxide glass based cermet laminate to be commercially viable with other common composites and even some high-end alloys.

Chapter 2

Hot Shear Processing of Glass/Metal Composites

Hot Rolling Glass Laminates

A series of metal and glass test samples were hot rolled using the strain rate value that was derived from equation 4 (pg. 20; process temperature was optimized for the glass). These tests were conducted to determine if the flow parameters for a glass and metal under shear could in fact be made to match in a real hot rolling environment. The test GMETs were made from 20 mm square copper plates (99.98 % purity) that were 2.6 mm thick. A circular depression 14.0 – 14.2 mm in diameter and 1.2 – 1.5 mm deep was milled into one side of each copper plate.

The special Al sealing glass[*] was melted (@ 750 - 800 C) and poured into the previously heated (5 minutes @ 500 C) circular machined depression. The samples were then removed wrapped in insulation to allow for a semi-controlled but rapid cooling rapid. The samples were encased in a steel foil envelope to keep from adhering to the rollers and rolled at 525 C - see fig. 11.

Fig. 11: Left: Unrolled cermet (glass diameter 14.2 mm, depth 1.7 mm) Center: Cermet encased in steel foil envelope before rolling; Right: Roll deformed glass core Cu plate

---

[*] This proprietary glass consists of Schott aluminum sealing glass (ALGS-32) with a special set of modifiers that were developed by the author

The rolling reductions/elongation results for the GMETs are displayed in Table 1.

#	Reduction (mm) & (%)	System Strain and Strain Rate	Glass Elongation (mm)	Cu Elongation (mm)	Cu Elong (%)	Glass Elong (%)	Difference (%)
CuG 1	2.48-1.85 = 0.63 (25%)	0.29 & 0.45	19.1-14.1 = 5.0	26.8-20.0 = 6.8	35	34	1
CuG 2	2.47-1.82 = 0.66 (26%)	0.31 & 0.46	17.8-14.0 = 3.8	25.8-20.4 = 5.4	26	27	1
CuG 3	2.48-1.90 = 0.58 (23%)	0.27 & 0.43	19.9-14.0 = 5.9	28.4-20.2 = 8.2	41	42	1
CuG 4	2.45-1.87 = 0.58 (24%)	0.31 & 0.43	18.2-14.0 = 4.2	27.2-20.4 = 6.8	33	30	3
CuG 5	2.48-1.84 = 0.64 (26%)	0.30 & 0.45	18.7-14.1 = 4.6	27.1-20.4 = 6.7	33	33	0
CuG 6	2.50-1.84 = 0.66 (26%)	0.31 & 0.44	18.7-14.2 = 4.5	27.3-20.4 = 6.9	34	32	2
CuG 7	2.47-1.87 = 0.60 (24%)	0.28 & 0.44	17.9-14.1 = 3.8	25.7-20.0 = 5.7	28	27	1

Table 1: Hot rolling results for single pass reduction of seven copper/glass composites (unrolled and rolled thicknesses values, with differences, are displayed in the 'Composite thickness reduction' column)

In table 1, the elongation differences between the copper and the glass phases were measured to be between 0% and 3% in the direction of rolling after undergoing single pass roll reduction deformations of between 23% and 26% (Lateral elongations of both the glass and copper were very small and showed no appreciable differences.)

Images of two hot rolled and one unrolled encapsulated glass/Cu samples are displayed in fig. 12.

Fig. 12: Two rolled metal/glass composites (left and center) and one unrolled cermet (far right.) Rolled samples had a 23 – 26% total reduction at a strain rate of about 0.45/sec for a processing temperature of 525 C

These processing results demonstrate that roll forming of copper containing glass is feasible. The fact that there were some small differences in elongation between the two phases after rolling was not surprising. In these tests, the glass phase was not fully encapsulated, and as a result, the copper exhibited strain-hardening effects that were not fully compensated for relative to the composite during rolling. The author believes this is the first example of a glass being simultaneously hot rolled with a metal.

The United States Patent Office has awarded the author a patent (no. 5,900,097) for the concept of using hot rolling to match the shear deformation-induced flow of glass or ceramic to metal in order to create cermet laminates.

The rolling conditions were optimized for the glass flow to match the copper's deformation as close as possible. The strain rate was fixed at 0.45/sec and process temperature was 525 C. Copper plates were (99.8% pure.) A single pass reduction of about 25% was made. The glass used was a variation on a commercial aluminum sealing glass (Schott ALGS-32). Both the width of the metal and glass phases, due to roller friction on the copper, severely limited the lateral spread of the composite during deformation and these values differed very little from the initial widths (< 0.2 mm.)

Elongations in the rolling direction of both the glass and copper showed very similar values - all within 3% of each other (reference Table 1).

The composite's rolling strain is given by: $\varepsilon = \ln (H_0/ H_f)$, where '$H_0$'is the initial plate thickness, and 'H_f' is the final plate thickness.

The system's actual strain rate can be calculated (approximately) by using:

$$\dot{\varepsilon} = \frac{V_r}{H_0} \left[\frac{2(H_0 - H_f)}{R} \right]^{1/2}$$

Where 'V_r' is the roller velocity (linear feed of 5 mm/s) and the roller diameter is 50 mm. No attempt was made to slow cool the rolled samples from 525 C to room temperature after removal from the rolling mill/furnace system since the two phases have nearly identical CTE's.

From the elongation differences in Table 1, the glass phase showed nearly identical total roll induced elongations as that of the copper. This experiment demonstrates that under the correct processing conditions (temperature, and strain rate) the shear induced flow of a glass does in fact match that of a metal under constrained rolling (glass encapsulated by copper.)

These results confirm that the first order model for glass/metal flow under shear deformation is approximately valid. This modest experiment demonstrates that the hot rolling formation of glass and copper composites is practical.
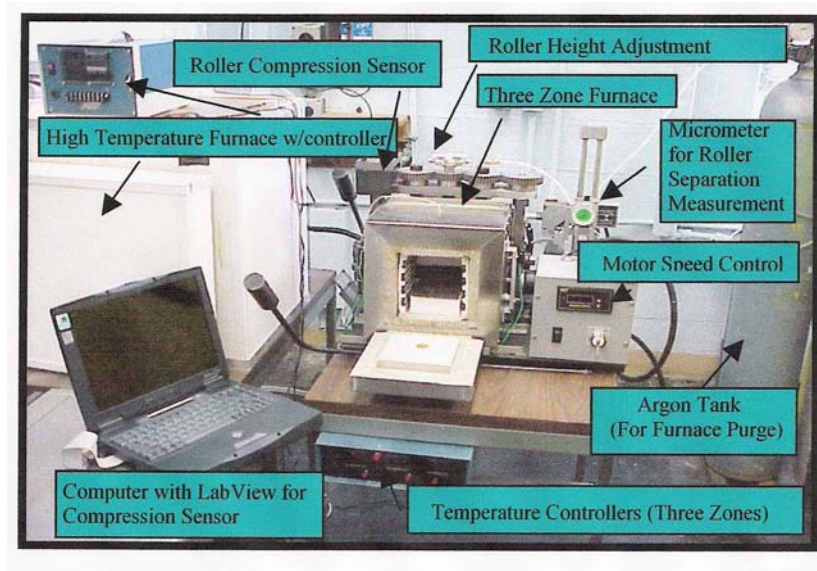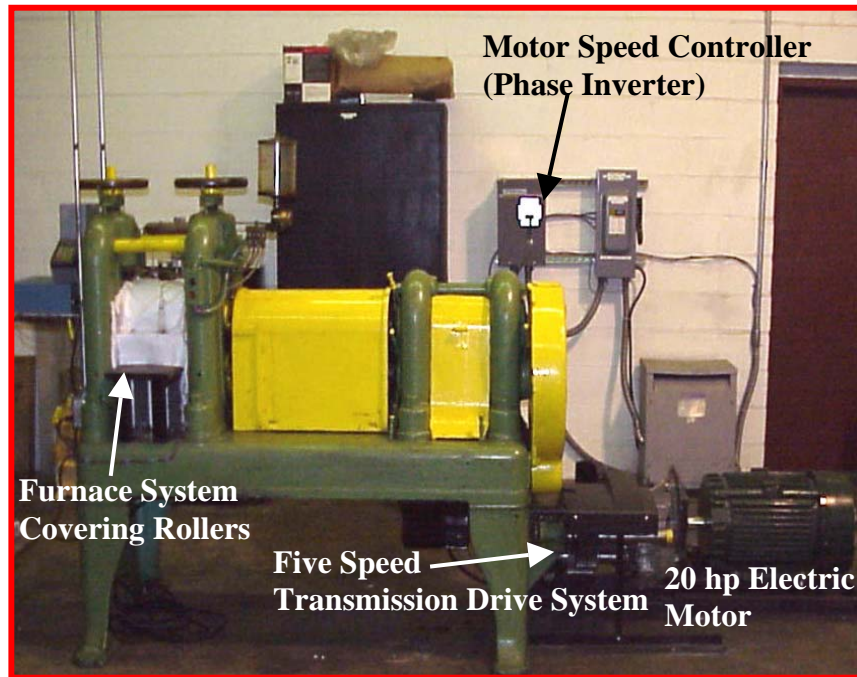

Fig. 13: (Upper) Three-ton hot rolling system used for the large Al/glass samples - this mill can handle plates up to 15 cm wide and up to three cm thick. (Lower) Small research hot rolling mill used for the copper/glass samples.

Fracture Toughness of GMET Under Compression

Many ceramics and all glasses have low toughness values compared to metals. One way to improve the toughness of a ceramic or glass is to place the phase in compressive loading. For example, ordinary oxide glass (with or without structure modifiers) has a bulk toughness of only 0.01 kJ/m^2. Yet, if the glass is placed under a compressive stress of 400 MN/m^2 via compressive loading (i.e. sealing glass with a CTE of 17.6 bonded to Al with a CTE of 22.5 and temperature change of over 400 C), the glass can exhibit an apparent "toughness" improvement of over 20 kJ/m^2.

Exploiting the previously mentioned thermal expansion differential between materials, the ceramic or glass layers can be placed under large compressive stress to allow the overall 'toughness' of the laminate system to be significantly improved.

This phenomenon on toughening a ceramic phase by placing it between two materials with greater CTE's was first formally proposed for patenting by the thesis author in 1998. This mechanism of laminate toughening is now covered under this patent (no. 5,900,097). Interestingly, for such an obvious technique, only lately have armor scientist started to explore this important CTE property relative to laminate structures (ref. 5).

For the Al/glass based GMETs, the existing mis-match in the CTE between the two materials will place the glass phase in a large compressive state of stress and due to the good interface bonding, this should only enhance the overall toughness and tensile strengthen properties of the laminate. This partly explain the high tensile loading strengths of these samples (but not the copper samples that have a CTE that almost exactly matches that of the glass.)

Exploiting this CTE mis-match property has many advantages for laminates, as long as the metal and glass phases exhibit good bonding. The ability to adjust the loading between the phases is very simple. Different alloys can be used to make large changes in the metal's CTE. This concept is also covered in the patent for the process.

A significant benefit of laminating a glass with a metal is that the metallic layer will protect the defect free glass surface from abrasive wear and dirt or chemical attack. Such a protected surface will allow the laminate to better withstand environmental exposures without degradation of initial tensile yield capabilities of the glass.

Processing Toughness of GMETs

A hot rolled fully encapsulated GMET based on Al was hot rolled using the three ton rolling system. This GMET was sectioned using a metal-toothed band saw (fig. 14.)
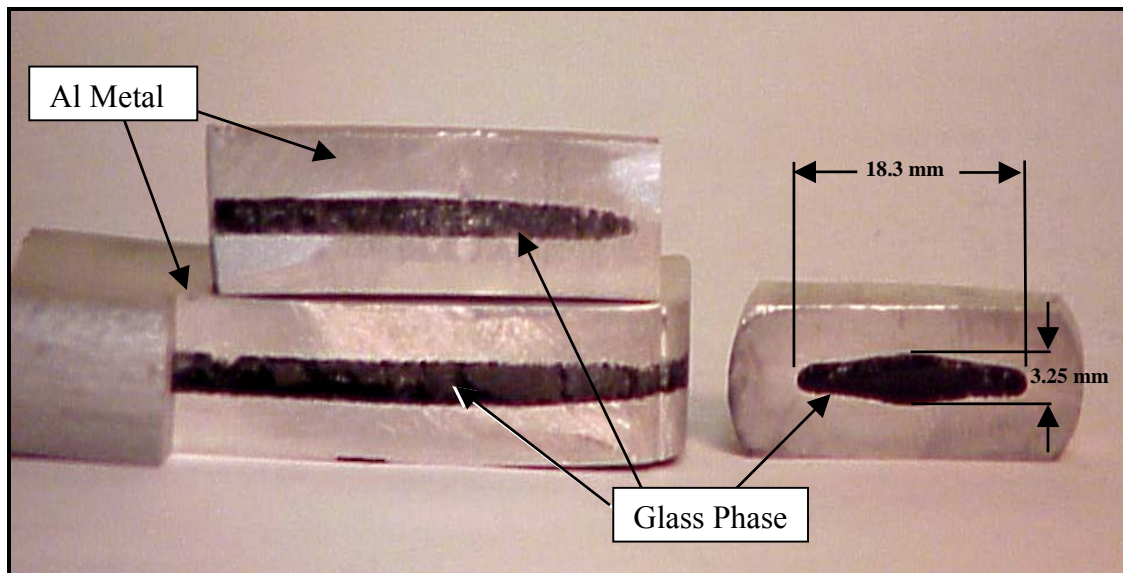

Fig. 14: Encapsulated glass cermet sectioned with a standard metal blade band saw

Sample was originally a circular aluminum rod that was bored out (approx. 10 mm diameter) and filled with liquid glass (@ 750 C.) The samples were pre-heated to 525 C,

and immediately processed using rollers that were heated to 350 C. The samples underwent three hot rolling passes (re-heated each time to 525 C) for a total reduction of about 40%. One of the rolled specimens was sectioned in order to determine the deformation dimensions of the glass. A standard metal blade machine shop band saw was used to cut the cermet. No effort was taken to band cut the sample in any manner to preserve the glass phase – feed rate was similar to that supported by aluminum metal. The cermet was sectioned as if it was a pure aluminum rod – see fig. 14 & 15 for images of the sections.

In the image of the sectioned cermet (fig. 15), repeated cuts have been made on this sample as well but they are parallel. The sample displayed in fig. 14 & 15 was cut twice to create a laminate section that had a total thickness of only 7.5mm (both sides having been cut to form the section.)
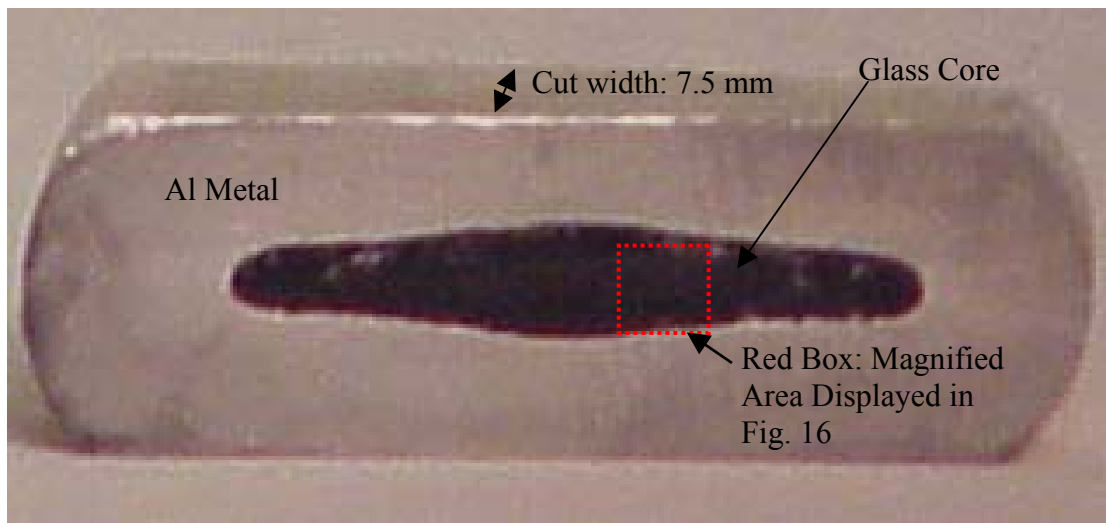

Fig. 15: Encapsulated glass cermet sectioned with a standard metal blade saw band; red box region is the highly magnified area displayed in fig. 16.

The glass phase (approx. 46% sapphire Al_2O_3) has not shattered nor exhibited any significant breakage; chipping and cracking is extremely minor and under 80 μm in depth (see fig. 16.)

Magnified images of the rolled cermet sample (displayed in fig. 14, far right) that had close parallel cuts using the metal band saw are displayed in fig. 16. Note that the glass surfaces cut by the metal grade saw blade exhibit no unusual damage – the glass appears as if a diamond blade cut it. The saw blade teeth exhibited no sign of abnormal wear. One sample was even cut twice in a manner such that the cuts were at right angles and still the glass phase did not crumble, breakup or show signs of significant cracking (see fig. 14, sample on the bottom, left.)

This GMET, due to its extraordinary toughness, can be cut and diced using simple metal saw blades. This cermet in a manner similar to toughen ceramics can be drilled or even machined. This unique property (for an amorphous glass) strongly tends to indicate that the glass is extraordinarily tough. While some shallow surface cracking exists, apparently a powerful arresting effect in the glass phase is occurring preventing these cracks from propagating into the bulk volume.

The image glass surface (fig. 16) for the core region in the Al/glass laminate is still partly transparent strongly indicating that this ceramic phase is still amorphous.

This GMET was cut at room temperature with a standard shop grade steel blade running at 1.0 m/s speed; the blade had 6 teeth/cm, was 0.6 mm thick, and the cermet feed rate was 3 - 5 mm/s. The magnified image of the glass surface (see fig. 16) was rough polished using a standard shop buffing wheel.
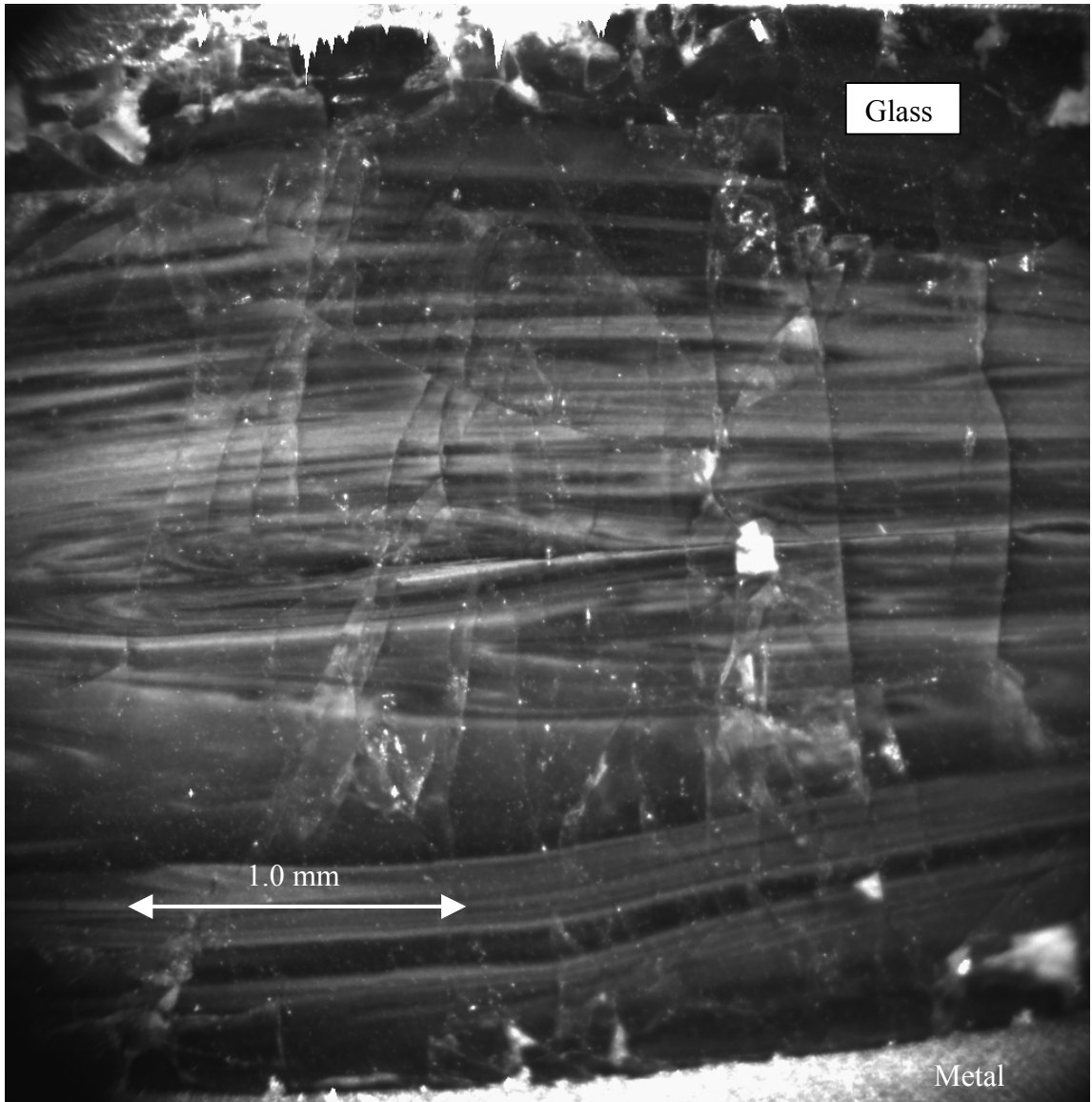
Fig. 16: Magnified image of the cross-section of the glass area as cut by a metal band saw at room temperature (area has only been polished using a machine shop buffer to confirm clarity) in the hot rolled cermet. Cracks extend only 40 – 80 µm into the sample (crack depth measured using a Zygo interferometer.) Any chips reached similar depths. Original GMET was hot rolled. White regions are caused by over saturated pixel regions in the camera array

This narrow glass-metal laminate section demonstrates the very impressive processing toughness of the glass phase – especially considering that a large tooth-cutting blade was used.

The fact that normal metal-like processing of the glass phase is not just possible but practical will allow many standard aerospace assembling/processing techniques to be exploited with this composite. Unlike most composites used in aerospace applications – especially glass or carbon fiber systems – this composite can be treated very much like an aluminum alloy for processing (metal tooth saw blade for cutting, and drilling with standard metal working equipment.)

Drilling of one sample was performed with no noticeable damage to either the drill bit or within the drill hole. The glass did not breakup or crumble after the drill bit was removed.

To further test the overall toughness of the glass phase, a glass layer (1.5 mm thick) spanning a washer (hole diameter 10 mm) was created. A metal nail (approx. 3 mm diameter) driven by a manual hammer was used to punch a hole through the glass as the washer was mounted within a vise and the layer was free standing. The punched walls of the hole were smooth and the large freestanding glass layer did not crack or show any signs of significant damage around the hole area. This experiment further demonstrated that the glass phase could endure extreme damaged without secondary cracking or breakage outside of the impacted area.

Due to this GMET's innate toughness, riveting and even bolting should be feasible for laminated sections. Due to the fact that the glass phase is encapsulated within a metal case, edge welding should be possible when joining the metal-to-metal sections of a laminate structure.

Chapter 3

Plastic Deformation of Oxide Glass Cermets

Hot Torsion Testing of a GMET

Glass filled copper tube cermet torsion test specimens were created (see fig. 17.) These samples consisted of 1.25 cm inside diameter thin walled (0.75 mm) copper tubes that were filled with the special aluminum sealing glass. Each glass filled copper tube had a narrow nearly 'metal-free' ring gap area machined around the tube's center creating an almost freestanding section of glass across the center section of the tube assembly. Short 1.2 cm diameter copper rods were used as end plugs for these glass filled tubes (the end plugs were simple Cu rods cut about 2 cm in length.)
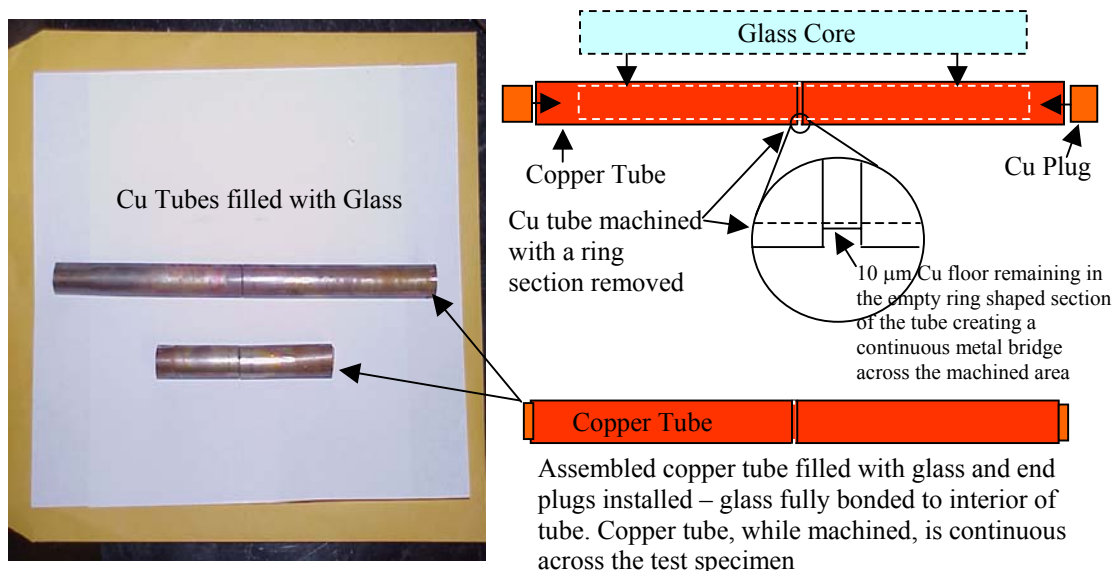
Fig 17: Glass filled copper tubes (commercial grade Cu pipe) used for torsion testing (Left image: top specimen: cermet rod is 30 cm long; bottom specimen: cermet rod is 14 cm long.) The machined ring area almost reaches to the glass's surface, creating a nearly free section of glass at the mid-point of the assembly. The inner glass core (0.5 inch diameter) extends nearly to the ends of the copper tubes where room was left to install short copper plugs to facilitate filling with liquid glass

The Cu plugs were used for mounting purposes in the torsion tester (to allow the end of the cermet tubes to be strongly clamped by the instrument's grips and to keep the liquid glass contained in the tube assembly until cooled down.) The tube was mounted vertically, with the lower end plugged, and liquid glass (@820 C) was poured in to partly fill the tube. Assemblies air-cool to room temperature.

The outer surface of the copper tube was machined with a ring like grove 1.5 mm wide and 0.65 mm deep at the midpoint region of the tube (machine work performed after filling and cool down – see fig. 17.). Since the cut was 0.65 mm deep and the tube's walls are 0.75 mm thick, the cut ring section on the copper tube almost extended down to the glass's outer surface. This 'semi-gap' region in the copper tube surface partly decouples the copper tube in a manner that either side of the tube griped in the torsion yester permits most of the twisting force to be focused into the glass core at this location.

This permitted the glass core section in the Cu tube to carry much of the load (instead of the Cu walls) and more accurately measure the twist effects of the glass phase near the center cut region. This machined ring in the tube significantly reduced the copper wall's dominating the overall torque readings. Conversely, the system torque was mostly concentrated in the glass rod at this location of the assembly, allowing a more accurate measure of the torsion deformation on the glass phase in the GMET.

Torsion Test

The glass filled copper tubes and rods were mounted in a computer controlled torsion tester (see fig. 18.) Two different gauge length test samples were created depending on whether a room temperature or elevated temperature test was to be performed on the glass section (longer samples were needed to fit the furnace.) Temperatures tested were

22 C, 300 C, and 500 C. Instrument torque speed was 5º per minute. Temperature control

(for the heated samples) was better than +/- 5 C.
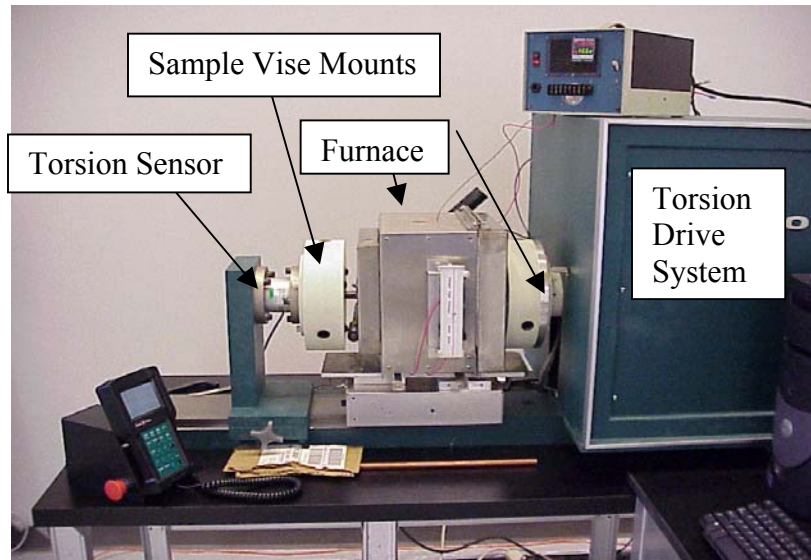
Fig 18: Torsion tester with furnace (author constructed) installed

Torsion Data

Raw torsion test data for the rod and glass filled copper assemblies are displayed in

fig. 19 – fig. 22. The data for all the cermet and copper rods are summarized in Table 2.
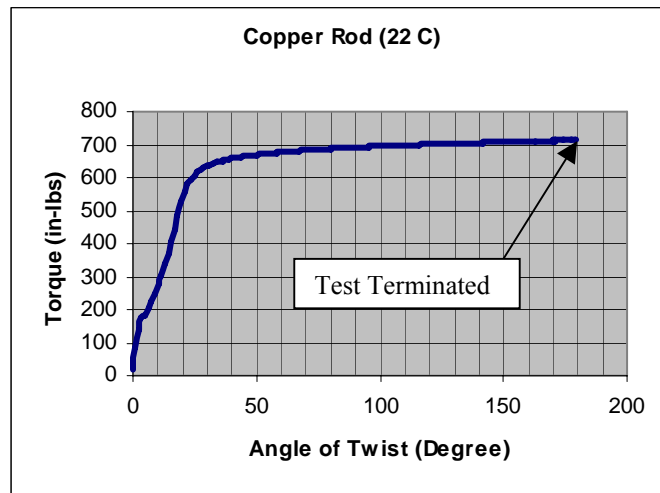
Fig 19: Torsion test of a copper rod specimen (0.5 inch diameter) performed at room
temperature (22 C). The copper's ultimate yield is just over 700 in-lbs.
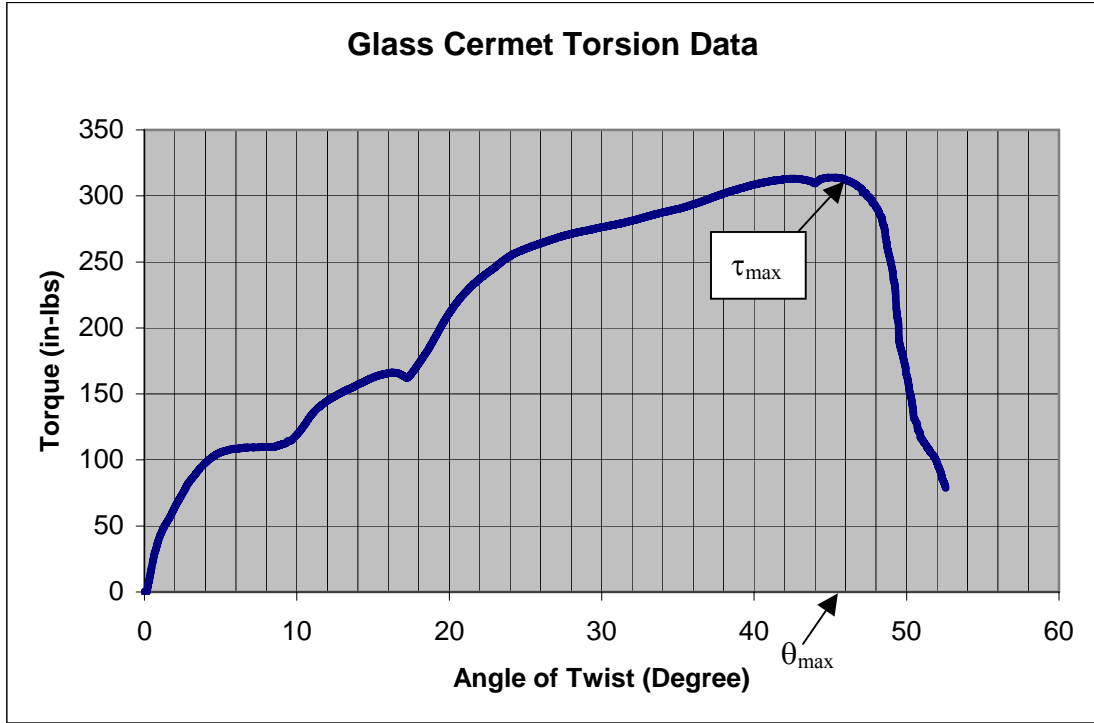
Fig 20: Torsion test of a glass filled cermet specimen at room temperature (22 C.) Note maximum yield value of about $\tau = 315$ in-lbs @ $\theta = 45.8$ degree
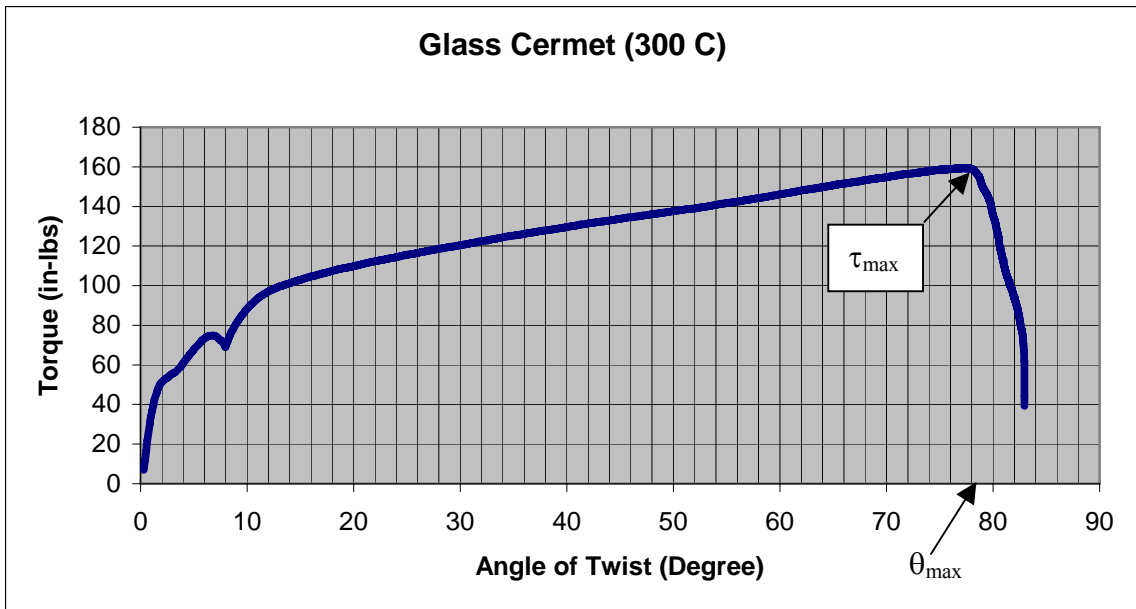
Fig 21: Torsion test of a glass filled cermet specimen at 300 C. Maximum yield of about 160 in-lbs at about 78.5 degree
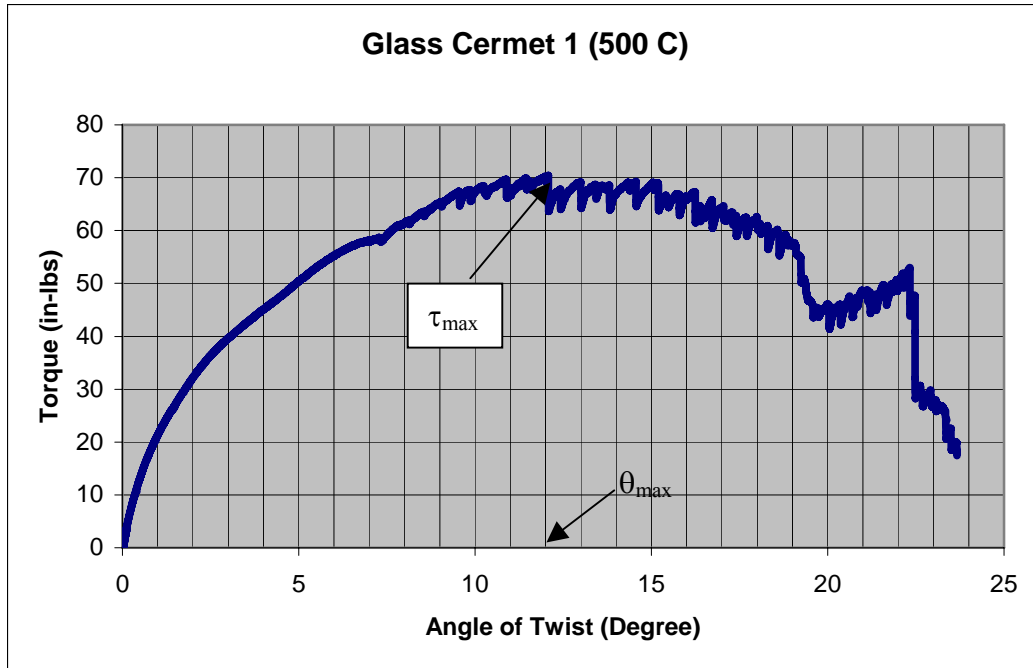
Fig 22: Torsion test of cermet specimen at 500 C; yield 70 in-lb at about 12 degree

Material	Temperature(C)	θ_{max} (Degree's)	τ_{max} (Torque)	Yield (MN/m^2)
Copper	22	180	700$^+$ in-lb	**147.6**
Cermet 1	500	12	70 in-lb	14.8
Cermet 2	300	78	60 in-lb	33.7
Cermet 3	22	45	315 in-lb	**66 .2**

Table 2: Torsion Test Data (Cu or Glass rod diameter: 0.5 in; strain rate: 5 degree/min)

A number of interesting properties from the torque test specimens are immediately apparent: first, and very surprisingly the room temperature GMET (fig. 20) behaved under torsion deformation in a manner very consistent with metal rather than what is

46

generally observed for an ultra-brittle material like glass. That is, the overall cermet assembly appeared to act in a manner more consistent with metallic or plastic-like flow properties.

Certainly, the metal walls of the tube for the cermet played a role in these large twisting results. The overall response of the cermet by the glass phase is the most dominate component in the rotational torque displacement since the metal walls are not continuous between the mounting grips and very thin; also, and a significant component of the total rotational strain for the system must be sustained by the glass phase for a number of reasons.

First, since the sealing glass bonds so strongly to the copper (interface bond strength is well above the yield strength of copper), the two phases are strongly locked together - stress forces from the rotation are readily transmitted throughout the glass phase; especially since the copper tube's walls are only about 0.75 millimeters thick and hard tempered in the grip/mounting regions. Secondly, the copper tube was machined in a manner that created two almost independent glass filled metal tube sections that were only connected by a 1.5 mm wide gap in the metal wall that created an almost free standing glass bridge allowing the greatest torque forces to be concentrated on this free standing section of glass rod (this aspect of the force loading was confirmed by the fact that all the cermet tube assemblies fully failed in the glass volume located at the ring gap located at the center of the tube assembly.)

The copper tube's outer surface showed no obvious signs of significant rotation deformation independent of the inner glass rod – the interface never failed in any experiment. Since the inner glass phase did not break free of the copper wall both

systems had to share in the rotation. This was further confirmed by the fact that lateral surface scratches on the copper tube showed no obvious signs of permanent rotational deformation and where still straight after twist testing was complete; also, the development of rotation induced stress bands along the tube's surface were not observed unlike the solid copper rod that had extensive stress branding (and of course, greater total twist.)

Looking at the raw data graphs for the room temperature (22 C) cermet (fig. 20), the torque force due to the angle of twist rises fairly uniformly as a function of angle, which is more consistent with metallic behavior rather than that of an extremely brittle substance like glass (where an extremely steep rise, over a very short angle of twist, followed by immediate and complete failure would be more typical.) Further, the maximum sustained torque occurs at an amazingly high total angle of twist exceeding 45 degrees, and resulted in a torque yield of over 315 in-lbs. Various plateaus in the graph may be the results of limited crack and/or plastic flow with corresponding stress reductions in the cermet assembly.

As mentioned previously, since the glass metal interface between the copper tube and glass rod has not suffered any significant failure, the glass volume near the copper tube's inner walls must be highly strained. So the maximum sustained torque force by the cermet is almost half the yield for the non-heat treated semi-hardened copper rod of identical dimensions (see graph of copper rod torsion data, fig. 19.)

More impotently, after the peak ultimate shear yield was exceeded, the sample did not instantly fail in a manner consistent with a highly brittle material but still offered

significant, although rapidly decreasing, resistance for almost three more degrees of subsequent twist (for over thirty-six seconds after peak yield failure.)

The data from the glass-based cermet tested at 300 C (see fig. 21) is also consistent with the data from the room temperature results. The over all shear yield is, of course, lower but still very high - more than half of that of the room temperature test. As expected, since the glass was far less viscous, the total angle of twist is substantially greater than that obtained for the room temperature sample – by almost a facture of two.

Considering this test was conducted at 300 C (the glass softens near 480 C so the viscosity would be: > 14 Poise), these results are inexplicable for any ordinary glass (which always has an exponential response to viscosity with respect to temperature changes.)

The torsion results for the glass at its softening temperature 500 C (fig. 22) are as expected – the yield is very low and supports only a small angle of twist (less than 15 degree's) before 'failure; this indicates that around the softening point of the GMET, the composite acts very much like a semi-liquid glass; that is, the glass's ability to sustain a torque force quickly falls due to the fact that the soft glass core must support all the load.

Analysis of the Torsion Test Data

The shear yield 'τ_y' in MN/m^2 (after unit conversion) for the cermet can be obtained by using the following relationship relative to the maximum torsion force achieved and the rod's cross-sectional area:

τ_y = 3(Max. torque (in-lbs))/(2π r^3) where 'r' is the radius of the rod (0.25 in)

The maximum shear yield value for the room temperature glass based cermet (see Table 2) is an impressive 66.2 MN/m^2 which is nearly half the value for hardened copper

(147 MN/m^2.) Interestingly, the value obtained for the GMET is in excellent agreement with the previously obtained tensile yield (shear yield, for metals, is generally given as 0.57 times the tensile yield. For tensile test of one specific Cu walled glass based GMET, the yield was found to be about 120 MN/m^2: this results in a theoretical shear yield of $120 * 0.57 = 68.4 \text{ MN/m}^2$.)

This shear yield value of the glass filled metal tube is in excellent agreement with the calculated shear yield value obtained for the GMET from the tensile testing of both copper or aluminum/glass samples but not for the solid copper rod; while these two independent test results are fully consistent, it is nonetheless surprising because the two types of experiments – tensile versus torsion - are so radically different in how forces are distributed across the glass cores.

For tensile tests, the forces are fairly uniform, to first order, across the glass's core cross-sectional area. In torsion tests, the shear forces go from zero at the center to a maximum at the surface.

That is, the shear strain (γ) is a function of distance (r) across the cylinder times the displacement angle or amount of twist (θ) per unit length: '$\gamma = r\,\theta$'.

The differential torque is then defined as: $dM = 2\pi r^2\,\tau\,dr$.

Integrating this will yield the maximum surface torque (M_t.) Changing variables of integration and limits ($r_1 = \gamma_1$, $r_2 = \gamma_2$) of the integrand, and using: $dr = d\gamma/\theta$ yields:

$$M_t = (2\pi/\theta^3) \int \tau\,\gamma^2\,d\gamma \;|_{\text{from }\gamma1\text{ to }\gamma2}$$

By Nadai[5], assuming that the shear stress in the cylinder only depends on the local shear strain, the integral depends only on the upper limit (γ_2) of integration.

---

[5] A. Nadai, Theory of Flow and Fracture, vol. 1, 2nd Ed., McGraw-Hill, 1950, p. 349

Differentiating the equation with respect to the twist angle per unit length yields:

$$\tau_{Surface} = (1/2\pi a^3) [3M_t + \theta (dM_t / d\theta)]$$

or

$$\tau_{Surface} = (M_t/2\pi a^3) (3 + dlnM_t / dln\,\theta)$$

This equation yields the maximum surface torque on the specimen. Using the graph of the specimen torque versus twist angle, the maximum surface shear that the sample has endured can be obtained using a geometric method. This technique requires that the inflection point for the torque versus angle per unit length curve be determined (where the inflection point of the curve is given as $dM_t/d\theta = 0$).

A fitted curve must be used with the torque plot since the measured data has various slope changes due to the glass phase partly failing and than regaining resistance until significant failure occurred. In fig. 23, the central region of the plot has been expanded, truncated, and displayed. A curve has been fitted so as to provide the best inflection point fit for the torque data. The angle scale has been normalized for the specimen gauge length (10 cm).

From the data in the graph displayed in fig. 23, $dM_t/d\theta = CB/DB$, and $DB = \theta$. Using this graph the torque yield value for the inflection point on the curve is about 215 MN/m^2.

Using the mathematical and graphical derivation from Dieter[6], the maximum surface shear stress is geometrically given from the torque curve as:

$$\tau_{Surface} = [1/(2\pi a^3)][(BC + 3AC)] \text{ where a} = 0.5 \text{ in}$$

---

[6] G. Dieter, 'Mechanical Metallurgy', McGraw-Hill Book Co., Third Edition, 10-3

Where the inflection point and vertical white line form the point 'C', the intersection of the horizontal white dashed line with the vertical white line forms the point 'B', and the point 'A' is located at the angle of displacement value of 5.5 θ/in and the vertical white line. Using these points, 'M_t' is the length of the white line AC (215 in-lbs) and BC is 140 in-lbs.
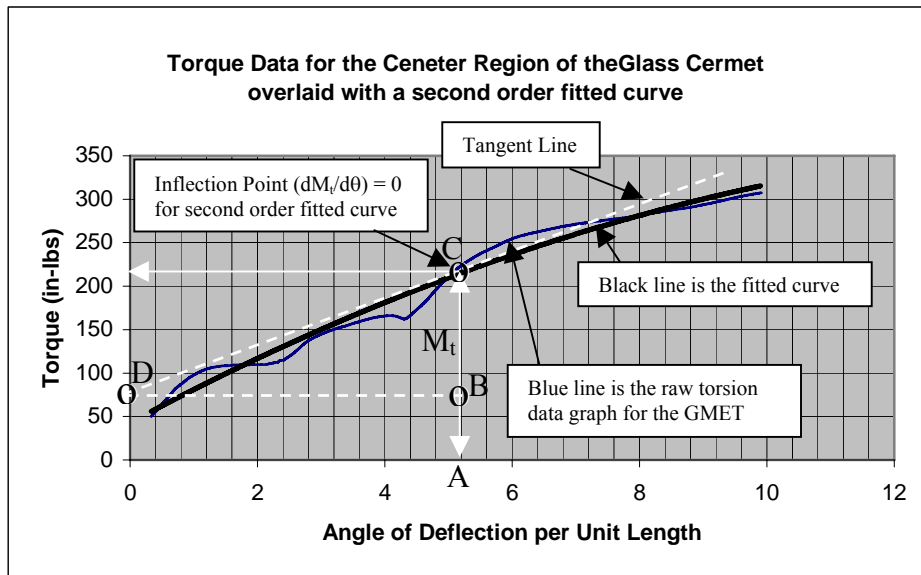
Fig. 23: Truncated and modified center data region of the room temperature torsion glass cermet curve (blue line) with a second order curve (black line) fit to the data set. Inflection point displayed and various data intercept points defined by the fitted curve are displayed. Displacement angle scale has been normalized for the specimen gauge length (10 cm)

Then the maximum surface torque values for the glass cermet is:

$$\tau_{Surface} = [1/(2\pi a^3)][(140) + 3(215)] = 1020 \text{ lbs/in}^2 = 7.0 \text{ MN/m}^2$$

Using this same method for the copper rod (22C), the maximum surface yield is found to be:

$$\tau_{Surface} = 1912 \text{ lbs/in}^2 \text{ or } 13.2 \text{ MN/m}^2 \text{ (see page 138, 'Curve fitted Cu Rod Torque Data')}$$

The maximum sustained surface shear for the glass-based cermet is impressively high considering that this value is 53% of the shear yield found for semi-hardened copper. This high surface yield value for the glass based composite is especially impressive considering that the stress forces for the torsional test specimen occur where most ceramics/glasses are typically their weakest – the surface location where micro-cracks are more likely to exist and more ready to propagate due to the concentration effect of the stress field. Normally, ceramics and especially glasses cannot support any significant rotational nor tensile deformations due to the previously discussed crack propagation issues. These results, from a perspective of standard material dynamics relative to the typical properties of normal glass are inexplicable.

In a manner very similar to the tensile and four-point bend test data (p. 80, Four-point Testing) for the GMETs, these results are all consistent and lead to the conclusion that these special laminates have very metal like bulk properties or conversely, exhibit significant plastic behavior similar to that of metals: yield, failure modes under tension, and twist as well as overall bulk toughness and fracture toughness that is more similar to metallic properties than any known ceramic/glass.

These torsion tests for the glass composite are extraordinary and without detail atomic structural maps of the lattice using x-ray diffraction of the glass both in the unstrained and strained states, along with precise crack propagation studies for the glass (r-curves), the mechanism that is allowing for these extremely unusual metal like behaviors by the glass phase is not easily determined using just bulk property tests.

The torsion test results do provide convincing evidence that this new composite has room temperature mechanical deformation properties that have never been previously

documented for any know glass/ceramic based composite and strongly indicates that this glass composite behaves in a manner more consistent with bulk metals rather then ceramics or typical oxide glasses.

These results, combined with the ability of this glass to be successfully cut without any significant damage/failure by a metal tooth based band saw (refer to "Processing Toughness of GMET" p. 37) and both the tensile (Tensile Yield Test Results, p.55) as well as four-point bend data (Four-Point Bend Testing p.80), provides overwhelming evidence that the glass phase in these GMETs is extraordinarily tough and exhibits behavior that is more consistent with metal rather than by an amorphous oxide glass structure.

GMET Tensile Test Samples

Room temperature composite strength tests conducted on "dog bone" shaped, glass-encapsulated laminates (see fig. 24) have experimentally shown that the glass (more than 75% by cross-sectional area in the neck region of the sample) and metal (less than 25% by cross-sectional area) composite can routinely exhibit *tensile* yield strengths of 80 – 120 MN/m^2 (these *tensile* strengths are on a par with many aluminum alloys.)
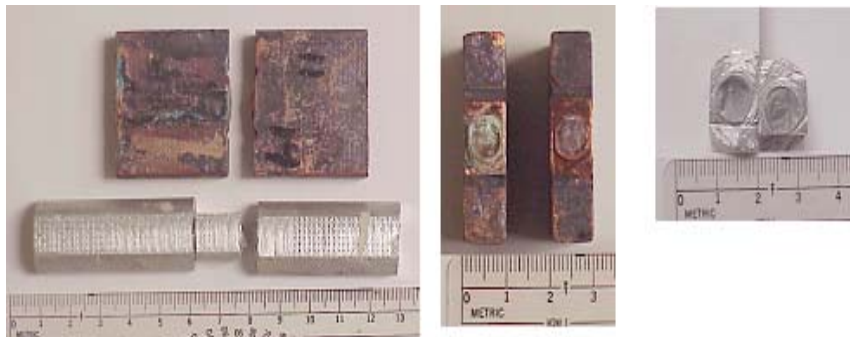

Fig. 24: Cermet "Dog Bone" Cermet Test Samples; Left: Cu and, Al samples after testing; Middle: Cu/glass cylinder (glass 7 mm wide; 0.5 mm copper wall thickness in neck region); Right: Cross-section of Al based composite and glass cylinder shape test composite (glass 7.0 mm wide; 0.5 mm Al wall thickness in neck region)

54

Tensile Yield Test Results

A number of glass cored aluminum composite dog-bone samples were tensile tested on an Instron hydraulic drive system that had an elongation sensor mounted across the center of the neck region of the dog bone samples. The gauge length for the sensor (placed at the neck region of the test samples) was 1.0 cm, all elongation results match the system's actual strain.

The cross-sectional areas of all the cermet glass cores were 38.5 mm^2 (glass core diameter of 7.0 mm). The outer aluminum envelope was about 0.5 mm or less in thickness resulting in a maximum area of about 5 mm^2 for the metal phase at the neck. The tensile load was derived using these combined areas and data is normalized relative to the total load for either material (guaranteeing lower bound yields for the glass phase.)

A tensile test of a glass based laminate sample is displayed in fig. 25 along with an identical aluminum sample. This plot of the yield curve displays how a GMET (over 88% glass by cross-sectional area at the neck region) test specimen responded to deformation under tensile load. System strain rate was set at: 0.002cm/sec.

Unlike the normal failure modes that pure ceramic or glass samples exhibit, the GMET displayed in fig. 25 did not show any obvious sign of abrupt failure while undergoing tensile elongation.

As seen from the glass's laminate tensile deformation curve, the sample exhibited a classic metal-like rollover until complete GMET failure finally occurs. After the rollover point on the graph is reached, the glass must still be carrying a significant amount of the tensile load since the metal phase alone could never support such a large load alone while still exhibiting this type of load to elongation curve (a load value that would cause even

ten times the area of metal to exhibit an identical failure curve; hence, if the glass had already completely failed, the metal phase in the sample would undergo failure at load values far lower.)
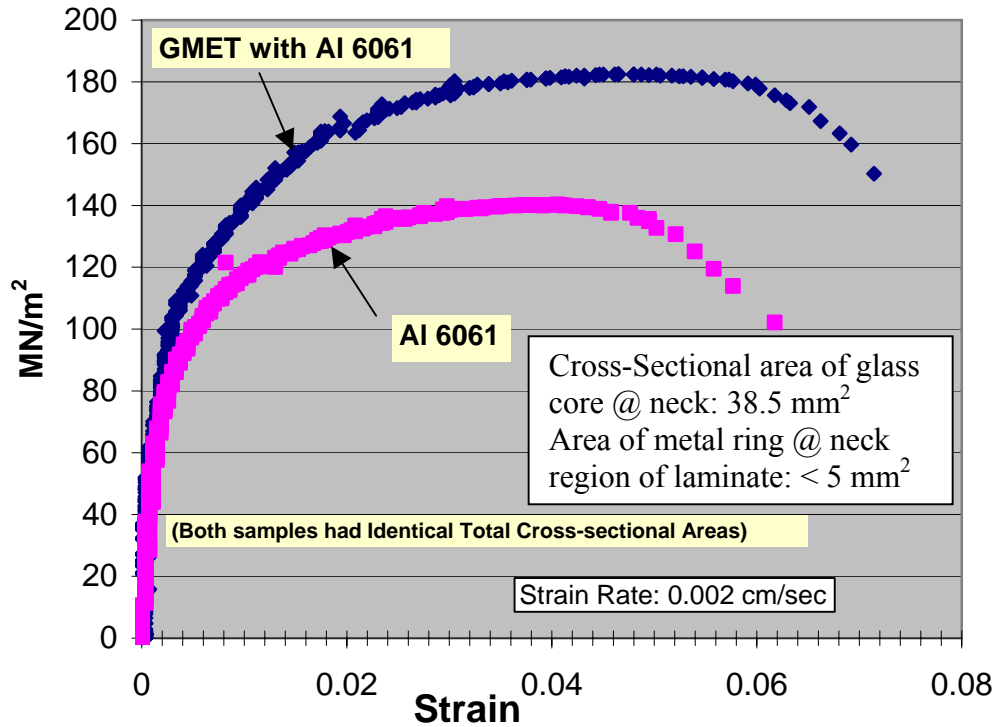
Fig. 25: Tensile elongation curves for an aluminum and higher yield glass-metal "Dog-Bone" samples (composite over 75% glass by cross-sectional at the neck region; see fig. 24 for sample images; tensile elongation was measured at the neck region.) Gauge length for the elongation sensor at the neck region was 1.0 cm

The yields for a number of GMET were tested and their yields ranged from 80 – 100 MN/m^2 with ultimate yields of 120 to nearly 250 MN/m^2.

A total of nine aluminum samples were tested under tensile loading with nearly identical results (four with elongations sensors, five using drive displacements.)

Aside: twenty copper/glass core samples were tested previously with near identical results as these aluminum based glass cermets (the ultimate yield values of the Cu/glass

samples were between $180 - 250$ MN/m^2) but no elongation sensor was mounted; only screw drive readouts were obtained.

While the elongation to load failure profile for the copper based glass laminates was identical to the aluminum alloy dog bone samples, most of these original results are not available since the data was discarded because the extreme plastic flow properties was originally discounted as not physical. Only later, after torsion testing, four-point bending of copper based specimens followed by tensile testing of aluminum based GMET confirmed these older results as valid did the author realized that the glass was acting in a manner that explained the previous plastic deformation/elongation similar to that of a metal. While a number of the Cu-glass cermets tensile curves were printed and saved, the original raw data files were permanently deleted and as a result, these original data graphs results are not being reproduced.

The GMET that was used to create the graph displayed fig. 25 had most the metal at the neck region cut away in a narrow band (about 1.5 mm wide) so that a small scratch could be made to the surface of the glass core at the neck region. Interestingly, this sample still had tensile yield strength and failure morphologies similar to that of a pure aluminum test sample (see fig. 26) even through the glass layer was both exposed by cutting away the metal in a narrow band/ring section at the center point of the neck and damaged (scratched with an approximately 1 mm long by 0.5 mm wide and deep using a diamond scribe) before loading.

The tensile yield for this mostly glass cored cermet is impressive for an amorphous oxide glass. The elongation to failure morphology is extraordinary (area ratio over 88%:

38.5 mm^2 for the glass and much less than 5 mm^2 for the aluminum phase across the neck region tested) and absolutely inexplicable.

All the GMETs behaved almost identically to that of a metal in tensile loading – similar initial elastic, and 'plastic-like' response along the yield to elongation curve and most critically, progressive failure morphology almost identical to that of the aluminum throughout the curve.

Relative to these tensile test results, it does not appear, after an extensive literature search, that any researcher has ever reporting a laminate that is a majority glass by volume or cross-sectional area, with substantial internal flaws such as large bubbles, intrusions and significant surface scratches, sustaining such enormous tensile strains much less exhibiting such enormous elongations.

Aluminum and GMET Tensile Yield Tests Results (Elongation Sensor)

The aluminum sample (6061 alloy) in fig. 26 exhibits an initial proportional yield of between 60 - 80 MN/m^2 and an ultimate yield of about 140 MN/m^2. This graph's overall shape and yield value appear typical for aluminum alloys (cross-sectional total area of 43.5 mm^2).

As can be seen from the elongation curves for the Al/glass composite (fig. 27), this tensile elongation curve is nearly identical in shape/performance to the Al test sample.

The aluminum/glass sample's tensile curve displayed in fig. 27 had a higher ultimate yield of 181 MN/m^2 and an impressively high elongation displacement even though it had an identical total cross-sectional area of 43.5 mm^2 (glass core: 38.5 mm^2) as the aluminum test sample (area: 43.5 m^2). The total elongation before failure of the GMET

composite in fig. 27 was 0.11 cm, which is somewhat greater than that of the Al metal's (0.095 cm) total displacement (see fig. 26.)

**Tensile Elongation of an Aluminum Sample
(Al080501)**
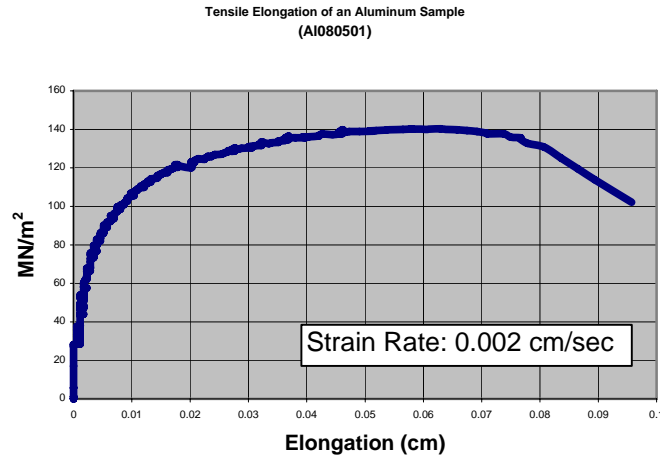
Fig. 26: Tensile versus strain of a solid aluminum 'Dog-bone' sample

**Al-Glass Cermet Tensile Data
(Al080502)**
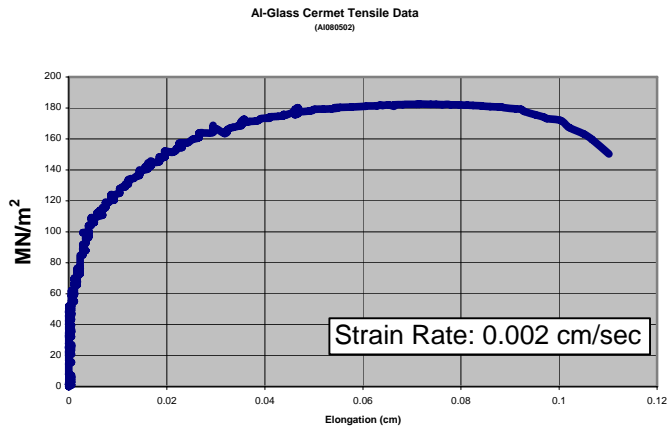
Fig. 27: Tensile versus strain of an aluminum-glass composite 'Dog-bone' sample

Gauge lengths for the sensors at both these samples neck regions were 1.0 cm. The cross-sectional area of the solid aluminum alloy dog bone sample was 43.5 mm^2 so as to closely match the total cross-sectional area of the GMET samples. This allows the tensile yield of the glass cermets to be related to the metal sample in a one-to-one manner.

A number of glass cored aluminum composite dog-bone samples were tensile tested.

Just as for the previously tested glass cermets, the cross-sectional area of the glass cores were also 38.5 mm^2 and the aluminum cross-sectional area of the outer skin was about 5 mm^2 or less at the neck. The tensile force was derived using these combined areas and data is normalized relative to the total load for either material (guaranteeing lower bound yields for the glass phase.)

The Al-Glass sample displayed in fig. 28 has an initial proportional yield of between 60 and 95 MN/m^2. The ultimate yield of the glass cermet was an impressive 246 MN/m^2.

This tensile yield data appears to demonstrate that under the correct processing conditions, the yield for these mostly glass laminates can be extremely large even compared to 6061 aluminum alloy. The elongation displacement for this sample is somewhat smaller compared to the previous specimens (fig. 25, and 27), which might indicate that the glass phase in this cermet was more brittle. Considering the elongation performance, the failure morphology still must be highly plastic in nature.

Al-Glass Cermet Tensile Data
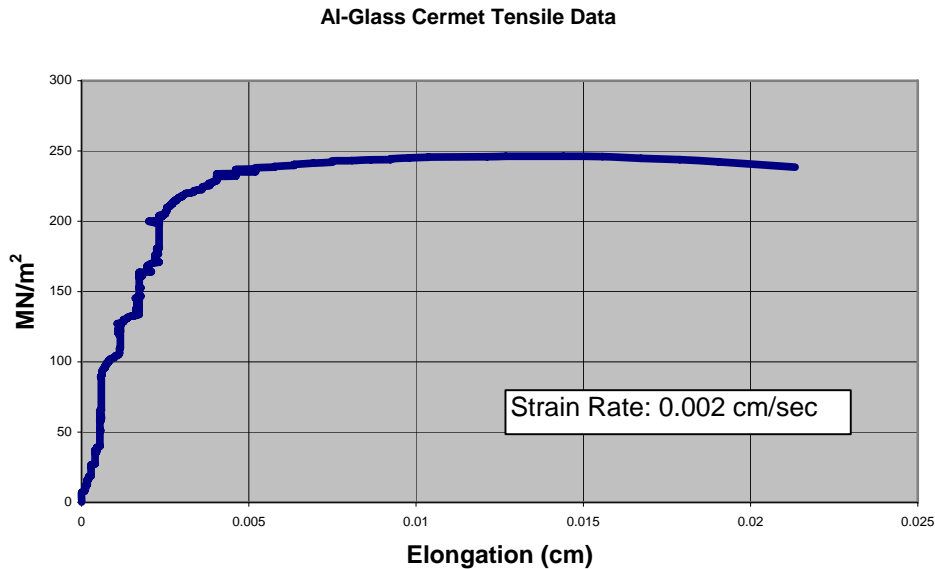
Fig. 28: Tensile graph of an Aluminum-Glass composite 'Dog-Bone' sample

The graph for this GMET (fig. 28) does not display a simple relationship to the load. At a number of points, the load rises with no measured elongation by the composite. This rapid increase of the load by the GMET is most likely due to the resistance of the glass phase to easily yield in a plastic manner. As mentioned, this glass may have been more brittle and displayed less metallic character compared to the other cermets samples.

The Al/glass tensile test shown in fig. 29 is similar to all previous tests but had a slightly higher ultimate yield but a smaller initial yield.

This laminate appears to exhibit a more gradual but significant series of minor failures (progressive small cracks being created?) but this did not appear to significantly affect the ultimate yield (151.7 MN/m^2).

Al-Glass Cermet Tensile Data

Fig. 29: Tensile graph of an Aluminum-Glass composite 'Dog-Bone' sample

Analysis of the GMET Elongation Sensor Tensile Tests

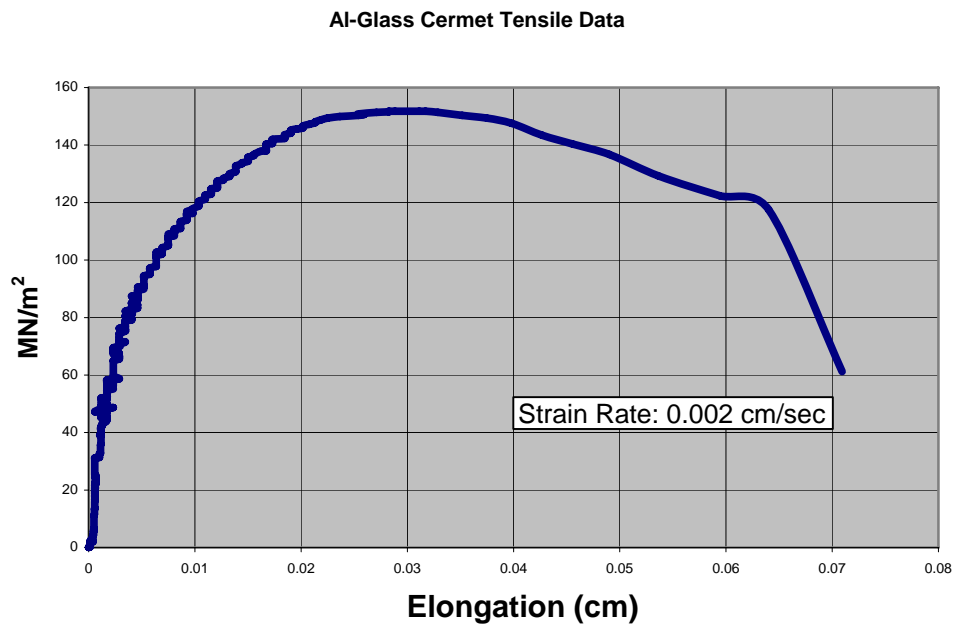From the data graphs of the glass cored aluminum dog bone samples the glass phase's overall effect on the tensile performance in the composite exhibits no significant difference from that of solid aluminum alloy; otherwise, the Al tensile curve and the GMET tensile plots would fundamentally differ in overall shape and especially in their load/extension values, which is not the case.

The GMET displayed in fig. 25 has an initial proportional yield of between 80 to 100 MN/m^2. The proportional yield continues to at least 140 MN/ m^2 before the slope begins to fall rapidly. The total strain system was 0.062 (or 0.062 cm over a gauge length of 1.0 cm). The failure morphology is nearly identical in response to load to elongation as the nearly identical 6061 Al alloy dog bone sample displayed in fig. 26.

The GMET displayed in fig. 27 had yield performance also similar to the aluminum test sample. The GMET composite had a slightly higher ultimate yield of about 182 MN/m^2 compared to some of the other laminates produced.

An unexpected difference between the two tensile plots displayed in fig. 26 and 27 is the ultimate yields – the composite sample exhibited a substantially higher ultimate tensile as well as a higher proportional yield: 180 and 70 MN/m^2 respectively, compared to the 6061 solid Al alloy: 140 and 60 MN/m^2 respectively. Since these samples had equal cross-sectional areas at the necks, the differences in yield between the two specimens can only be attributed to the glass phase in the composite sample.

The glass cermet load to extension curve displayed in fig. 28 had a very high ultimate yield (246 MN/m^2), and while the brittle nature of this composite partly explains its shorter elongation compared to the other GMETs, the ultimate yield does not necessarily

follow this logic. More than likely the increased yield is a convolution of both the increased brittleness combined with a still substantial plastic response. Relative to its plastic response, the glass modification may play a significant role.

The load to elongation curve for the GMET in fig. 29 displays very pronounced plastic flow, and still a slightly greater ultimate yield compared to the aluminum test sample.

While GMET are not fully plastic in a manner identical to aluminum, these laminates still support enormous elongations before failure unlike anything ever reported previously for an oxide glass composite. Significantly for engineering applications, none of the cermets displayed sudden cataclysmic failure but rather, smooth predicable progressive yield to failure.

Al/Glass composite Tensile Tests (Displacement Data Graphs)

The following tensile test data graphs are all based on the tensile screw drive displacement to track deformation along the entire sample – so the long tails are not physical. Only the load response is reliable. All these samples where tested at a strain rate of 0.002 cm/sec.

The sample displayed in fig. 30 shows a very slow and linear progressive failure up to about 100 MN/m^2 and then a slow rollover up to the ultimate yield point. Elongation performance after the ultimate yield down to the zero load point is not indicative of the composite's real performance (see previous tensile loading graphs for the Al/glass composites more representative failure mode.) The displacement for the composite was recorded only indirectly by measuring the drive motion, which does not really provide any direct measurement of the neck region of the 'dog bone' samples but rather, only the

composite's deformation as a whole. The gross tensile properties of the neck region are mapped.

Tensile Data Al/Glass Cermet
(MF2066)
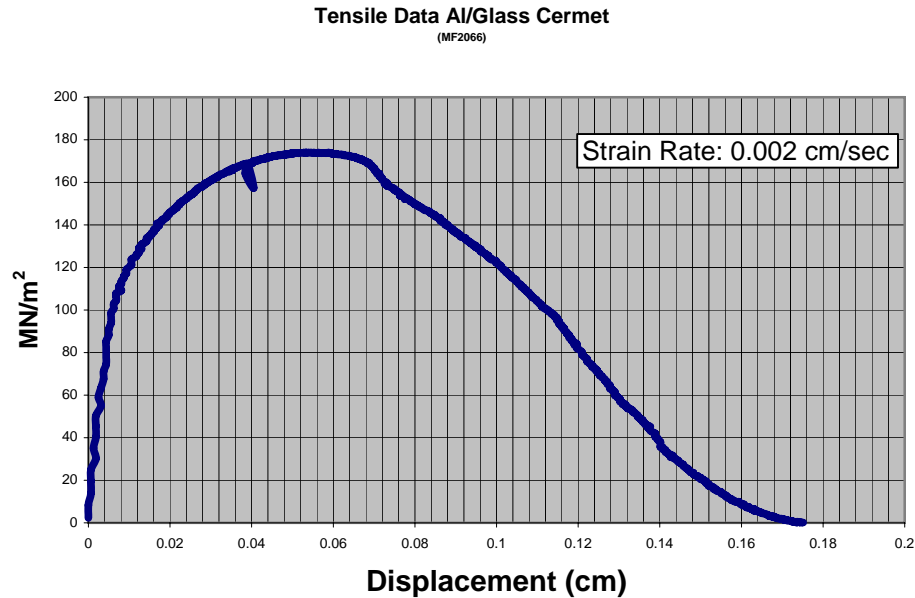
Fig. 30: Tensile graph of an Aluminum-Glass composite 'Dog-Bone' sample without elongation sensor readout

This sample, as well as the others, all had glass core diameters larger then the previous tensile curve samples (8.5 mm) displayed in this thesis (the others all had only a 7.0 mm diameter.)

One point to note is that the total elongation displacement for this sample is rather large compared to all curves that were measured using an elongation sensor directly attached to the neck. This difference could be caused by a number of reasons – the entire sample's elongation (from the metal section clamped between the jaws and leading up to the neck portion) heavily influenced the resulting curve, or the neck region did in fact exhibit enhanced elongation due to the performance of the glass, or the curve is a convolution of the two in varying, but unknown degree's.

64
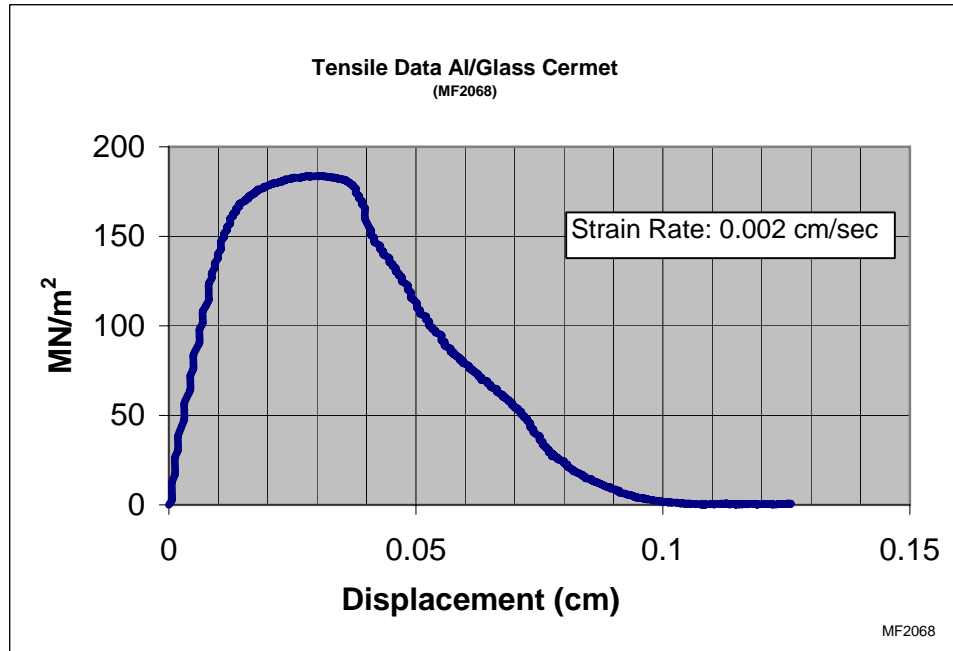
Fig. 31: Tensile graph of an Aluminum-Glass composite 'Dog-Bone' sample without elongation sensor readout
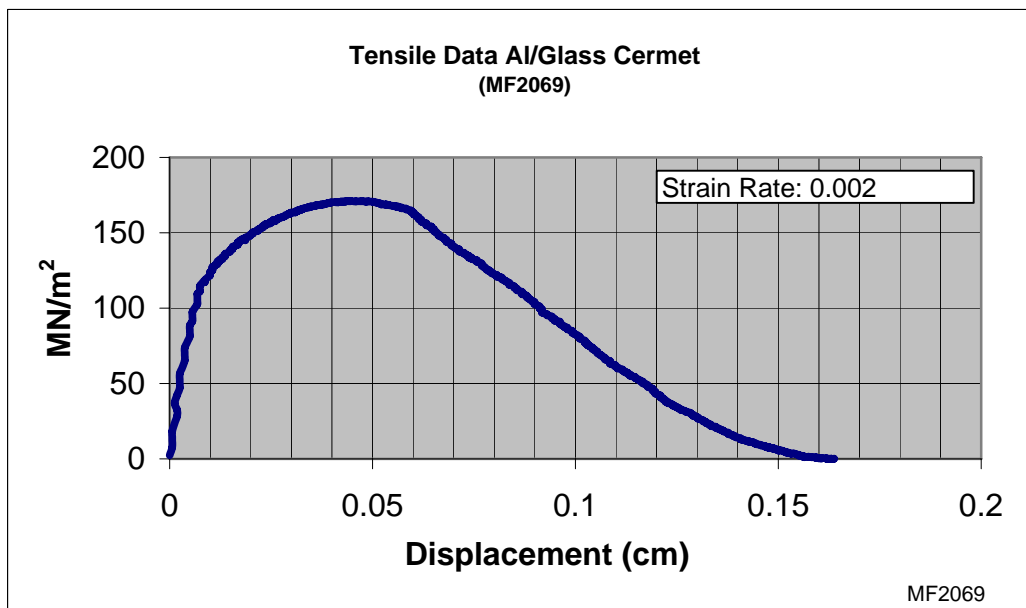
Fig. 32: Tensile graph of an Aluminum-Glass composite 'Dog-Bone' sample without elongation sensor readout
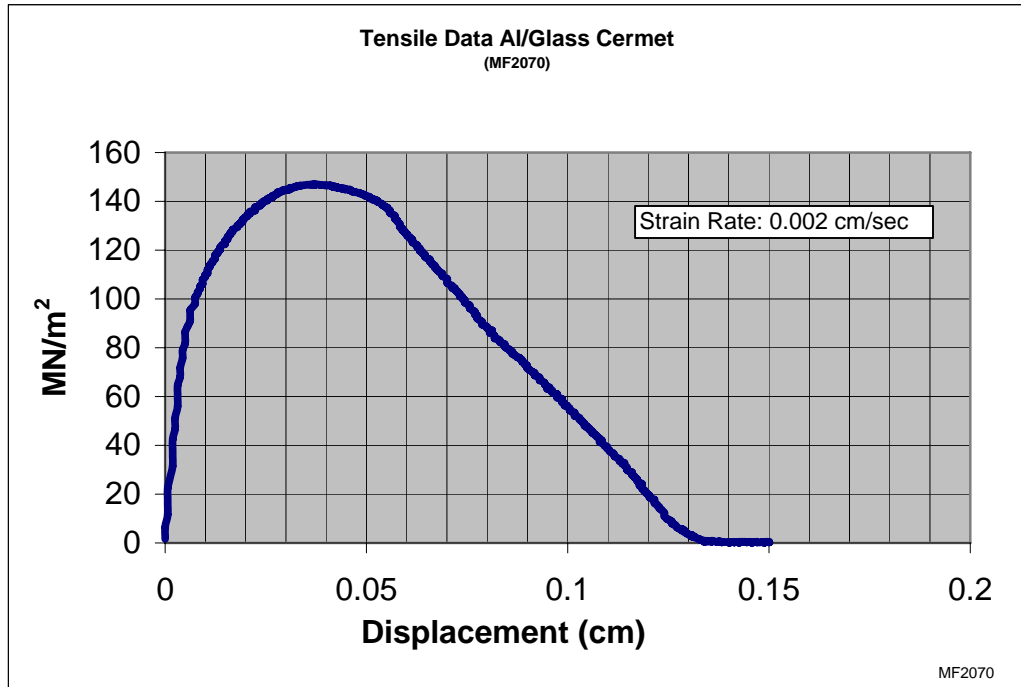
Fig. 33: Tensile graph of an Aluminum-Glass Composite 'Dog-Bone' sample without elongation sensor readout
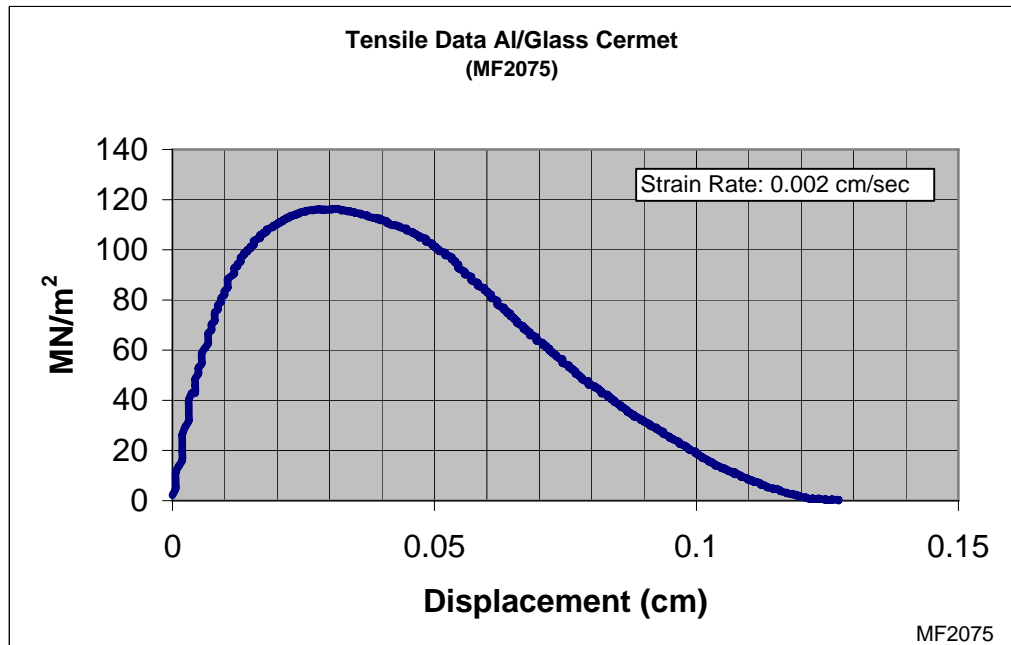
Fig. 34: Tensile graph of an Aluminum-Glass composite 'Dog-Bone' sample without elongation sensor readout

All these aluminum based GMETs (fig. 30 through fig. 34) display significant plastic deformation performance in their ability to carry load. While no direct strain to load results are available, these elongations to load turnover morphologies are very impressive for a composite that has an even greater glass to metal cross-sectional area (over 90 %).

All the tensile results, combined with the torsional data give extremely strong experimental proof that the glass phase has some plastic flow allowing for the extraordinary elongations/deformations properties under either tensile or torsional loads to failure.

Chapter 4

Testing of the Glass & Metal Laminate Interfaces

Adhesion Testing of Metal/Glass Interfaces

The peel test for adhesive films is a well-established methodology to determine the surface bond strength between various materials. This test is performed by first bonding then pulling a tape like material (a metal foil of either Al or Cu) from a surface (our specially modified glass) so that a critical force is reached at which point a crack is initiated at the foil/binder interface, and the tape starts to peel off from the surface. From simple geometry, the critical energy needed to cause failure can be derived. This is a direct measure of the interface toughness since the creation of the failure point occurs at the onset of fast fracture.

This type of setup can be used to measure the toughness of a metal/glass interface. A calibrated strain gauge is used to anchor one end of a metal foil, and the other end is bonded to the special glass. The glass has been bonded to a copper plate that is affixed to a slide. This moving slide allows the foil to constantly be pulled off the glass surface at 90 degree's (see fig. 35.)
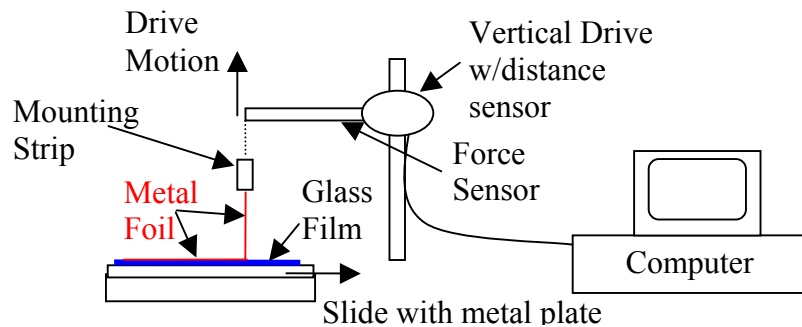
Fig. 35: Schematic of metal foil puller and computer recording system

To start the process, a force is slowly applied until it is large enough for the foil to begin to peel. The peeling force is recorded until the foil sample reaches its end point. As the metal foil is peeled from the glass, a new surface area is created that is a direct measure of the interface energy or the glass toughness.

In the case of measuring the toughness, the peel test is a simple methodology, albeit a limited one due to sample preparation issues such as poor bonding, incorrect pull angles, and peel area control issues. The procedure is more likely to produce lower bound measurement values of glass/metal interface toughness but it does provide a rough value.

A picture of the actual system is displayed in fig. 36. Experimental tensile pull data results using this system are displayed in fig. 37 and 38.
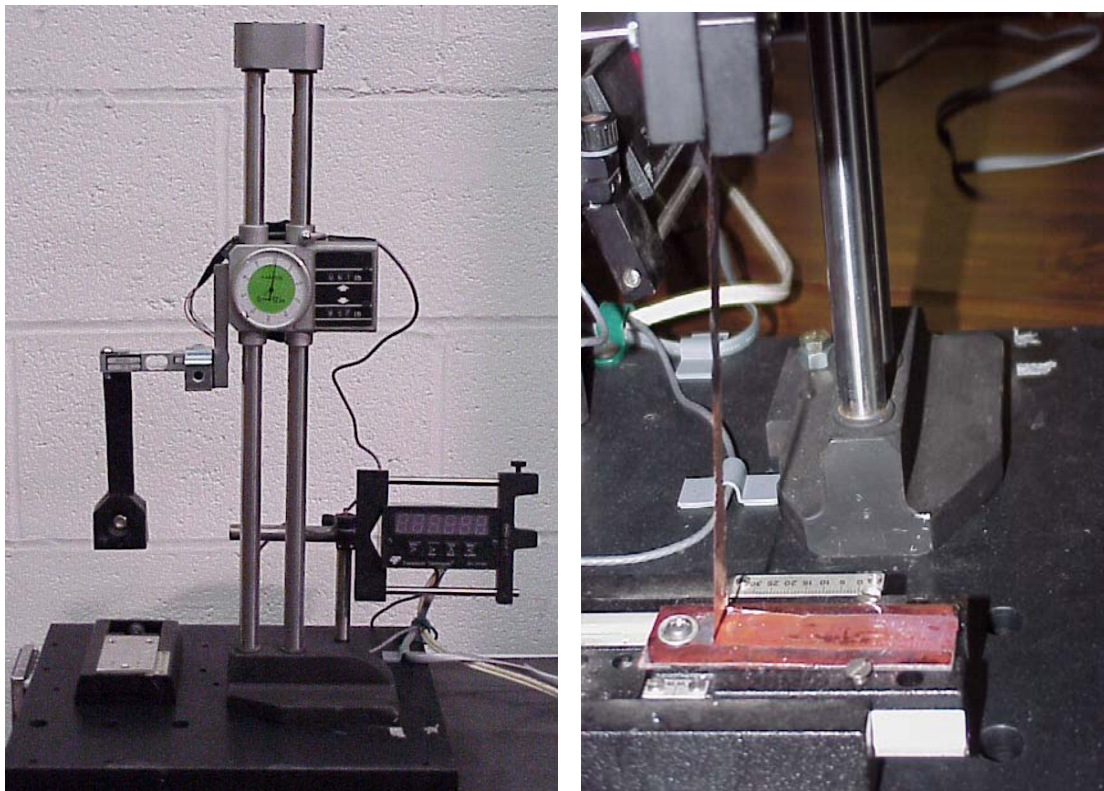
Fig. 36: Left: Computer interfaced peel tester assembled by the author. Right, Mounted Sample: Copper foil bonded to glass being peeled
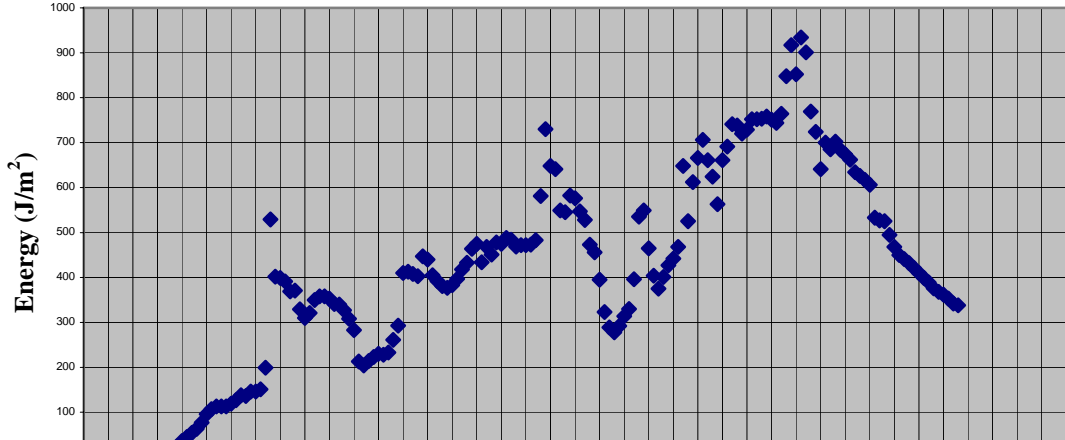
Fig. 37: Interface Peel Energy a Cu foil from glass under constant acceleration (peak value 950 J/m^2.) Variation in bonding values is due to a number of factures: poor oxide growth, and/or foil tearing (manual foil removal causes much of the variation)

Al Foil Adhension on Glass
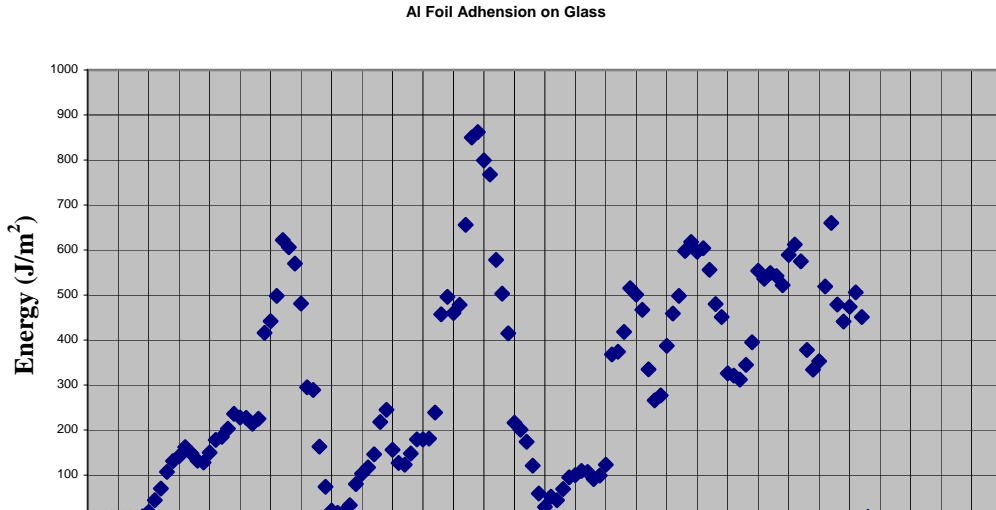
Fig. 38: Energy needed to peel an Al foil (10 mil) from the glass surface. Maximum delaminating value was 880 J/m^2 (jumps were caused by removing the load and reapplying due to system design parameters. Manual foil removal)

Using this peel testing system, five copper and five aluminum foils were pulled from the sealing glass. The resulting peel energies were all similar for the successful specimens.

The peel test samples were prepared by heating some glass to 820 C in a crucible. A copper plate was placed in the furnace (also at 820 C) for 45 - 60 seconds, than removed and placed on an insulating pad. Immediately, about one cm^3 of liquid glass was poured onto the hot copper plate and spread flat also using a small glass plate. A partly copper foil (foil heated to 500 C for two – three minutes) was then aligned and laid onto the surface of the cooling glass.

Due to problems of uncontrolled rates of oxide growth and/or etching of the metal foils by the liquid glass, poor bonding between the foil and glass occurred for some samples. As a result, the foils did not always adhere to the molten glass surface uniformly, and in the case of the aluminum foils, had a tendency to dissolve into the molten glass. The foils did not really provide the best possible bond to the glass and the pull data is rarely uniform or consistent and is more likely a lower bound. Occasionally a small amount of liquid glass would adhere to the top of the foil and as a result, cause the foil to tear and change its width. No attempt was made to optimize this test since only a rough lower bound was being sought to qualify the previous toughness estimates made using the tensile and bend testing data results.

Despite these problems, a few of the best-made foils did provide useful data on the interface bond energy.

From these tests, some of the interface bonds showed rather high energy in order to break them. Ignoring the first few seconds of data, the average energy to remove the foil was still rather impressive considering this is just a glass/metal oxide interface that is being subjected to the tearing force. The critical crack energy gives the system's toughness using the simple relation:

$$K_c = \text{Measured Force (J) / Foil Width (m}^2)$$

(This relation does not include plastic effects but for a glass film and metal foil at room temperature this issue is not important for first order measurements.)

The copper/glass interface, the peel energy was measured as: **0.95 kJ/m²**. And for the aluminum/glass interface, the peel energy was: **0.88 kJ/m²**.

These results are impressive for a glass/metal interface and correspond well with the tensile and four point bend tests results that were calculated based on the bulk samples that had cracks created with poorly controlled depths.

Fracture toughness of these peel samples is obtained using the energy needed to start fast fracture, and Young's modulus of the glass. The general equation for fracture toughness is given by:

$$K_f = (E * K_c)^{\frac{1}{2}}$$ where E is the systems Young's modulus and K_c is the

fracture energy

The following toughness values were derived for the copper and aluminum systems (the Young's modulus for the glass and Al are about the same: 69 GN/m²):

$$\text{Cu/Glass: } K_f = \textbf{8.1 MN m}^{\textbf{-3/2}}$$

and

$$\text{Al/Glass } K_f = \textbf{7.8 MN m}^{\textbf{-3/2}}$$

These results are very high compared to the fracture, and fracture toughness of simple glass (K_c of only 0.01 kJ/m² and K_f of 0.75 MN/m$^{-3/2}$.) The interface glass and metal-oxide interface is not unlike the bulk glass composition used to form the glass cores in the tensile dog bone test samples and the glass layers in the four-point bend samples. These

values are consistent with the results obtained in the four-point bend and tensile tests using the larger metal and glass plate samples.

Using an Instron tensile system, a series of copper and aluminum foils were pulled off a glass coated copper plate. The samples were made using better parameter control and slightly different process conditions (glass @ 820 C pored onto a pre-oxidized 1.8 cm x 8 cm x 0.16 cm copper plates (Cu plates pre-oxidized at 820 C for one minute, and the glass was coated while still in the furnace.) Glass layers were about half a millimeter (0.5 mm) thick. The Cu foils were pre-oxidized at 820 C but only for five seconds (Al foils at 550 C.) The results of two of the copper foil tests are displayed in fig. 39 and 40.

Tensile Adhesion Cu Foil to Glass
(MF2063)Foil Width: 1.0 cm
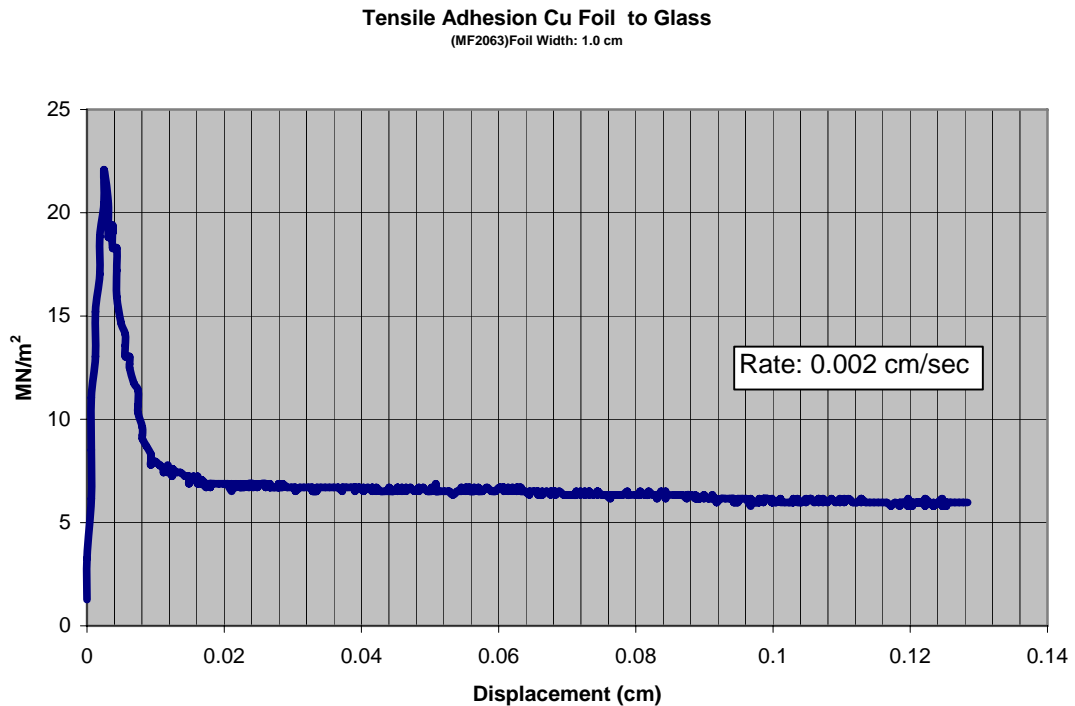
Fig. 39: Force needed to break the copper foil/glass interface bond: average 6.70 MN/m^2. Measured using an Instron tensile tester (@0.002 cm/sec)

Tensile Adhesion Interface Test (Cu Foil)
(MF2058)
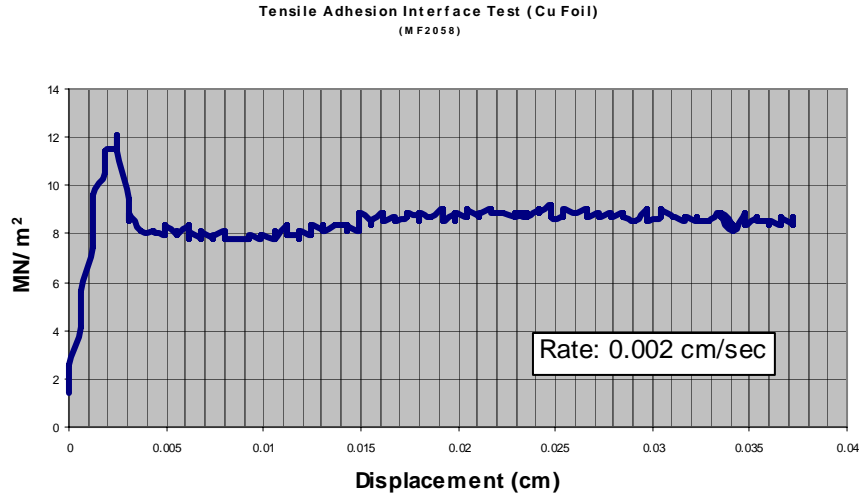
Fig. 40: Force needed to 'peel' or break the copper foil to the glass; average force to break the interface: $8.0 - 9.0$ MN/m^2

The yielded results for the two-aluminum foil peel tests (see fig. 41 & 42) are about 5 - 6$^+$ MN/m^2 and are similar in magnitude to the previously displayed values for the Copper foil tests (fig. 39 & 40) with the glass.

Aluminum Tensile Adhesion
(MF2061)
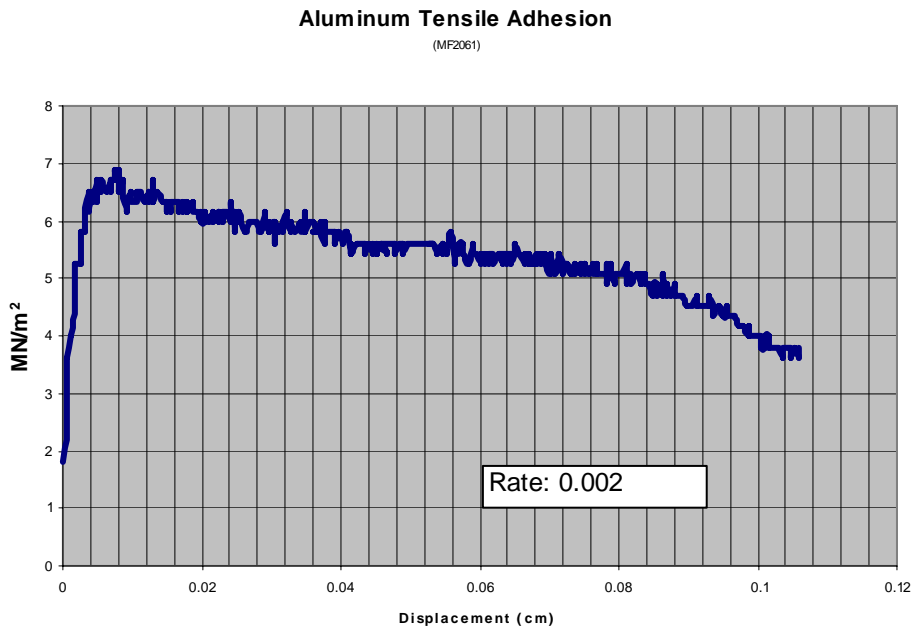
Fig. 41: Tensile adhesions pull test of an Al foil bonded to glass

74

Tensile Adhesion data Al Foil
(MF2064)
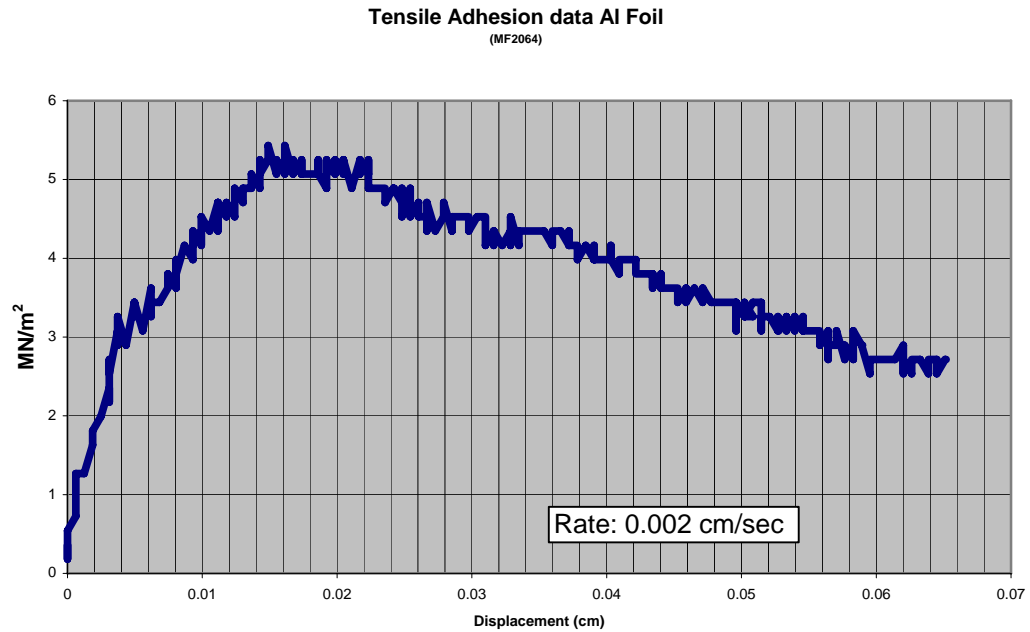
Fig. 42: Tensile adhesion pull test of another Al foil bonded to glass

All these results show that the interface energy needed to break the glass/oxide bond with either copper or aluminum at a steady rate is 670 Nt/cm^2 and 860 Nt/cm^2 or in terms of interface energy required: 0.67 kJ/m^2 and 0.86 kJ/m^2 for Cu and Al, respectively. These results using an Instron tensile tester closely agree with the previously obtained peak measurement values using a much more simple laboratory peel tester and poorly manufactured test samples.

Interface Results for the Cermet

A SEM map of the composition across the interface of one of the copper/glass samples is displayed in fig. 41. As can be seen from the compositional map for the copper (top image, 'Copper Concentration SEM Map', see fig. 43), the copper has indeed diffused/created a copper oxide intermediary film more than 75 microns into the glass phase. The aluminum signal across this interface is due to the aluminum within the glass

phase that is bound to oxygen as Al_2O_3 (See fig. 43 for magnified images of the metal/Cu-oxide/glass interface region.) Both these SEM results indicate that the glass and copper has reacted in such a manner so as to create a significant, and chemically complex common oxide region across the interface between the glass and metal.
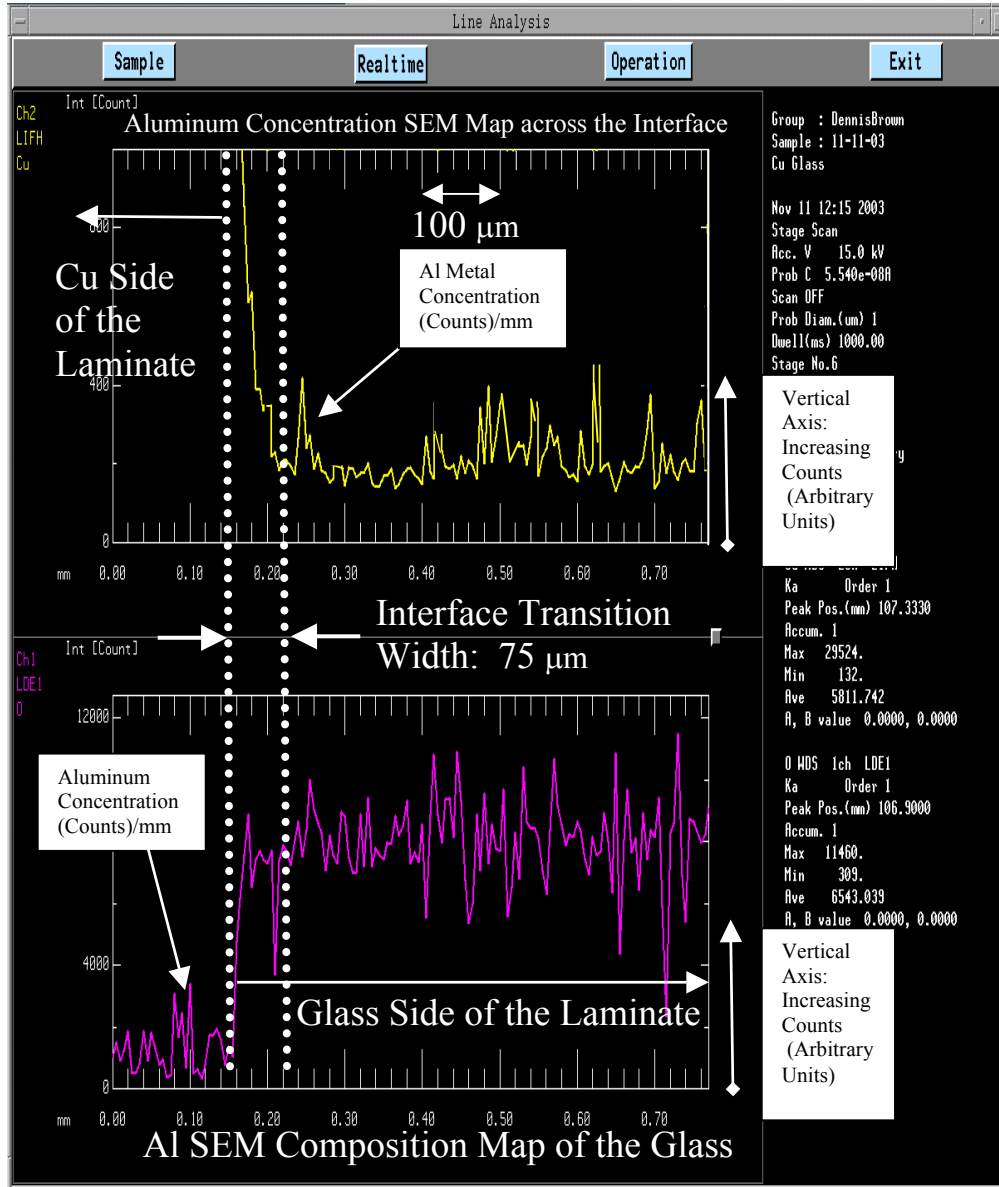
Fig. 43: SEM composition map for Cu (upper map) and for Al (lower map) across the metal/glass interface region. Note the change in the Cu concentration across the interface, while the Al concentration (as Al_2O_3) is fairly uniform across this region.

Copper Plate

Glass region is transparent so the oxide growth zone extends down and outward into the glass zone in a complex 3-D shape

Flat Upper Surface of Interface Region
Cu Oxide with the upper surface borderline drawn in for clarity

Glass Phase

Glass Phase

Glass region is transparent and the interface 3-D Cu oxide growth zone is readily visible in the matrix

Planar Crack in the Glass Layer

Oxide Layer 50 – 75⁺ um

Copper Plate

Cu oxide dendrite crystals that have grown into the glass phase

75 mm

Fig. 44: Polished, and magnified polarized white light image (top) of a deformed glass-copper interface area displaying oxide interface region (white light, bottom image)

While an initial Cu oxide layer was grown on the copper plate (one minute @ 820 C), this layer is inconsequential considering that it requires 25 hours (1500 min.) to grow a 100 μm thick layer on copper heated to 950 C in air (ref. 17.) Rather, the massive interface layer between the glass and metal phase for these samples could only have been created by a chemical reaction between the glass phase and copper plate during cool down (resulting in the dendrite crystals that grew in the glass phase displayed in fig. 44.)

Adhesion peel tests conducted for both aluminum and copper foils bonded to the glass strongly indicate that the bond strength is mostly due to oxide that grew due to presence of the liquid glass phase as can be seen from the images displayed in fig. 44. As previously discussed, the bond interface energies were found to be very high: between 670 Nt/cm^2 and 860 Nt/cm^2 or 0.67 kJ/m^2 and 0.86 kJ/m^2, values far too large to be obtained by a hundred Ångstroms or less of Cu oxide created by such a short exposure to air.

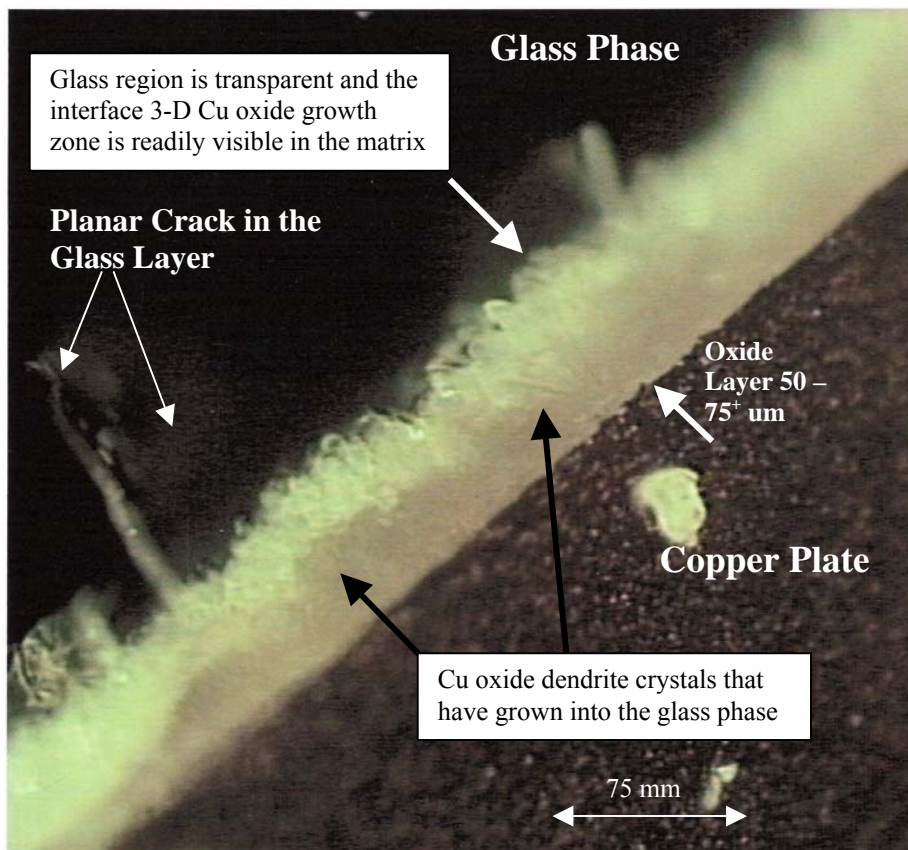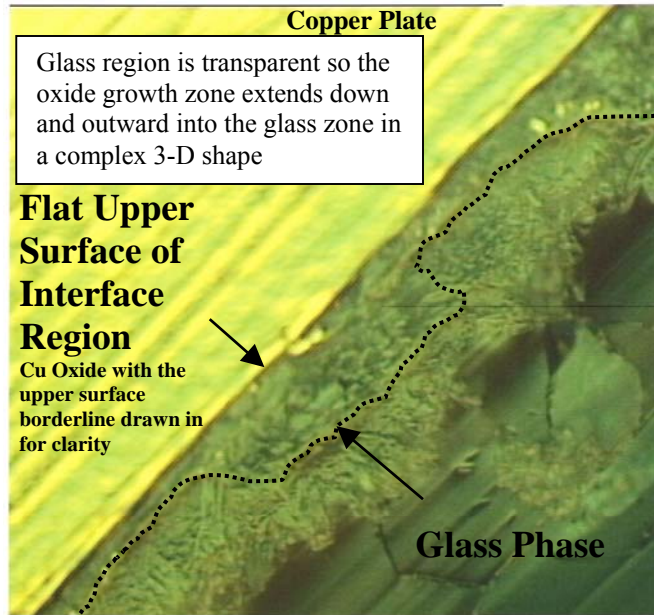This Cu/glass bonding strength has also been partly confirmed by the fact that the Cu/glass laminate system has routinely withstood very high cooling rates of 200 C/sec without failing or even significant cracking at the interface or within the bulk glass – as determined by examining a glass layers on copper plates that were rapidly cooled. In fact, the copper/glass laminate was shocked cooled by water quenching a 550 C preheated sample – see Fig 45 for images of three different metal/glass cermet laminates and the cooling rates that they successfully supported.

In rapid thermal cycling tests using even greater rates than those previously stated in fig. 45, failure always occurred within the glass phase and *never* at the interface

boundary. Aluminum alloy bonding with the glass also appears to be chemical and strong as indicated by tensile pull interface adhesion bond energy results for this type of metal.

Copper cermet withstood a 200 C/sec cool down rate without failure to room temperature from 550 C to room temperature

Aluminum cermet withstood a 1.0 C/sec cool down rate from 450 C to RT

The steel cermet withstood a 5 - 10 C/sec cool down rate from 1100 C to RT

Fig. 45: Laminated metal/glass cermets and cooling rates that did not lead to failure

Lattice Mismatch Issues

The question of lattice mismatch between amorphous or ceramic materials, and metals on an atomic scale has also been studied in the literature. Due to a metal's unidirectional bonding, mismatch problems generally do not appear to compromise the bond strength between the layers. This is believed to be due to the metal phase, at the interface, readily forming dislocations in order to relieve any residual stresses created by improper bonding between the atoms across the interface between the metal and the glass phases (ref. 18).

Such a process has no significant effect on a macro-property such as the compressive/tensile loading along the metal and glass interface due to CTE mis-matching. Relative to long-term creep effects of the metal phase, the process could have some influence in preventing rapid material flow due to compressive forces within the various phases.

As mentioned previously, the purpose of laminating a ceramic with a metal is to create a series of metal layers within the composite to allow the ceramic phase to be made tougher. Various models proposed by researchers indicate that as the number of layers are increased, the overall bulk toughness of the laminate will improve rapidly.

The primary mechanism allowing for this increased toughening involves the stopping of cracks propagating within the ceramic phase by blunting of the crack tip when reaching a nearby metal interface (refs. 18, 19, 20, and 21.) At the interface, the metal will fully stop the crack propagation if the metallic layer is at least ten microns thick. Another, but less important mechanism is crack arresting by way of new area creation. When a crack reaches an interface, energy must be used in order for the crack to continue to propagate, which slows or even stops the crack from propagating.

When CTE mismatching is exploited by using a metal that has a CTE greater than the ceramic phase (but not significantly greater than 15% or the structure will usually fail), cracks can be 'pinched off' by the compressive loads sustained by the glass phase. This mechanism can have a very strong influence on increasing the 'apparent' toughness of a ceramic laminate (first cited by this author.)

Four-Point Bend Testing

Due to the exciting results found for the tensile test specimens, the overall toughness of these GMET composites four-point bend tests were performed on a number bonded and non-bonded copper/glass laminates.

The assemblies were compression tested in a four-point bending rig (see fig. 46.)

This testing apparatus, with samples, was use in conjunction with an Instron tensile/compressive system with computer data recording. The screw drive feed out

sensor was used for measuring the deformation of the composite sandwich. Unlike the tensile test specimens, this measurement for the laminate's deformation does not account for mounting rig geometries. The plot of the drive displacement on the lower axes of the graph is not a direct measure of the laminate's actual bend defection (but they are in a one-to-one relationship.)
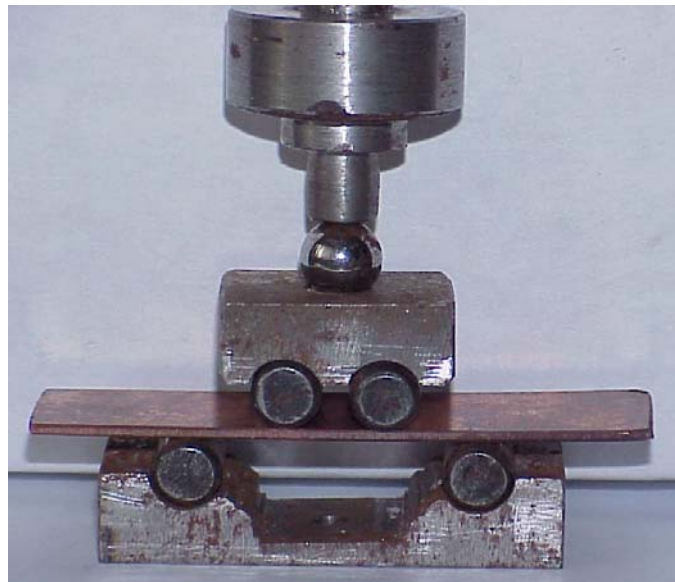
Fig. 46: Image of four-point compressive tester with Cu plate

The laminated samples were based on copper plates that were 82 mm long, 18 mm wide, and 1.5 mm thick.

Samples were created by first heating the copper plates and growing a thin oxide layer (thickness not measured) at 820 C for one minute. Then pouring liquefied glass onto one of the Cu plates (glass & Cu @ 820 C.) No attempt was made to obtain a specific glass thickness (but all were measured to be between 0.45 to 0.5 mm thick.) Another oxidized Cu plate was placed onto the copper/glass sandwich and the whole assembly aligned. The samples were sandwiches of glass bonded to a lower and upper

copper plate. The laminate system was cooled at a moderate rate to room temperature (allowed to cool down in a furnace for two hours at a starting temperature of 550 C.)

For more layers, this process was just repeated. Due to melting point issues with aluminum at this glass processing temperature, only copper/glass laminates were constructed.
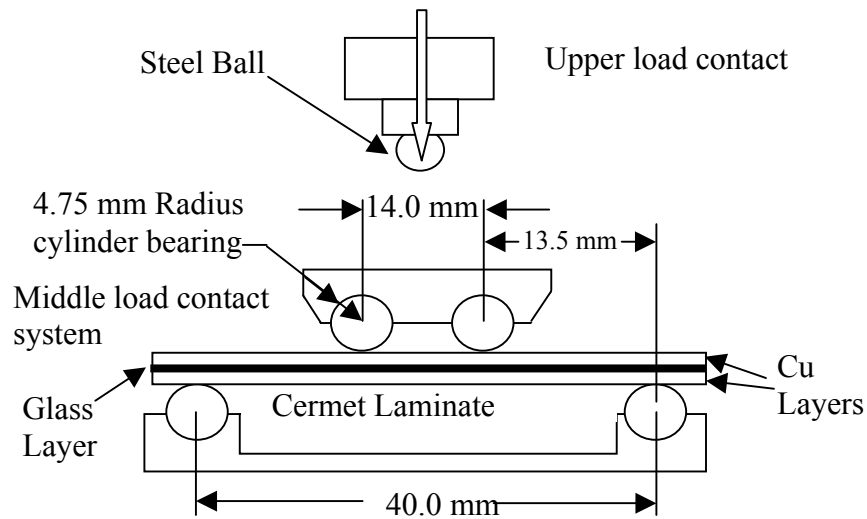
Fig. 47: Four-point tester dimensions – unit is made of steel. Roller bearings and ball are case hardened steel. Cu/Glass/Cu laminate sample shown mounted between cylinders

Due to the high temperature needed for rapid oxide growth, the copper was very soft (ductile) after cooling and could easily be bent four to five millimeters simply by using hand pressure.

The four-point bend tests were conducted, at room temperature, on laminates constructed from copper plates that had single and double glass layers bonded between them (i.e. a Cu-glass-Cu or Cu-glass-Cu-glass-Cu laminates.) The instrument used for testing was an Instron compressive/tensile testing system using a four-point compressive

testing rig (see fig. 46 & 47.) All the samples were compressed at a strain rate of 0.002 cm/sec and at room temperature.

Samples were both visually and audibly observed for failure features during testing. The results for all the glass based laminates were remarkable in that all of the tests stop limits of the machine were reached **before any of the samples could achieve an obvious failure point** in their resistance to the bending force, or exhibit any apparent major failure by the glass layer (i.e. extensive glass cracking or crumbling leading to copper plate separation.)

Besides bonded glass/metal laminates (three total layers), singular glass plates, glass and copper plate assemblies (not bonded) as well, were bend tested. Also, five layer glass/metal bonded laminates were tested (these consisted of two glass layers that were separated by a single copper plate and then, this assembly was, in turn, mounted/bonded between two more outer copper plates.

Four-point Bend Data

A simple unbonded copper/glass/copper sandwich assembly was tested in the four-point rig. The glass plate was 1.0 millimeter thick and heat-treated copper plates (two) were used. See fig. 48 for the test results of this unbonded Cu/glass/Cu sandwich.

In this test of a non-bonded Cu/glass/Cu sandwich, the system demonstrates all the classic characteristics of brittle ceramic failure – that is, the load very rapidly builds up until the point at which the system energy reaches a critical value and fast facture occurs leading to glass layer fail (initial slope: 1930 MN/cm.) This can be seen in the plot by the sudden drop in load when the Instron drive extension reaches 0.07 cm.

At this point the copper plates take most all the load and the force buildup begins to rise at a much slower rate (after failure slope: 121 MN/cm.) Glass fragments, between the plates, are still resisting extension as they continue to fail by being crushed.
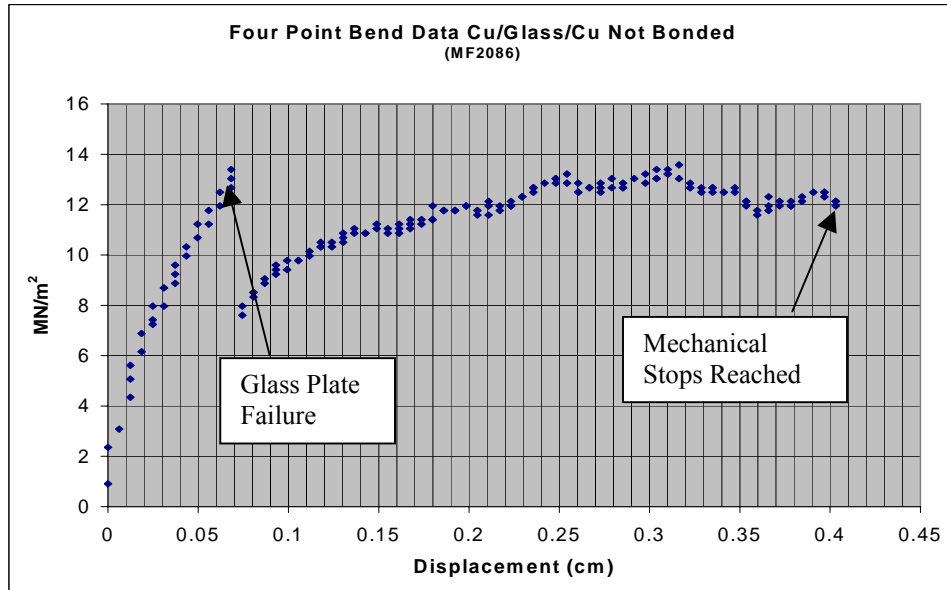
Fig. 48: Cu/glass/Cu sandwich – plates not bonded
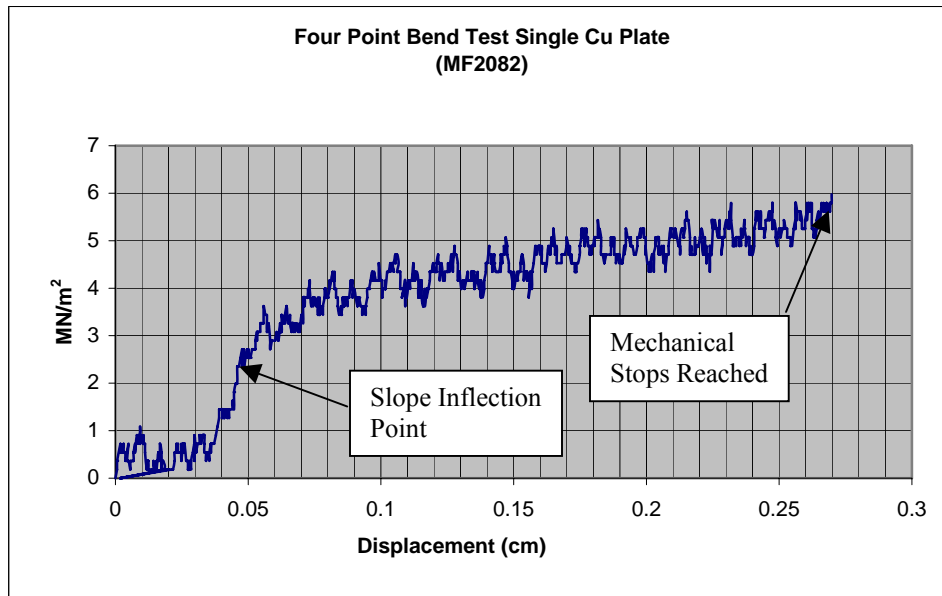
Fig. 49: Four-point loading single copper plate (heat treated; typical of cermets)

In fig. 49 is a plot of the load to extension of a heat-treated copper plate. This system shows, after an initial rapid loading period, a very slow load buildup to 6 MN/m^2.

From the plot for the graph with a bonded Cu/Glass/Cu displayed in fig. 50 (from now on, all bonded three layer Cu/glass laminate's will be referred to simply as Cu/glass samples), the sandwich exhibits a possible inflection point (start of glass failure) around 0.8 cm extension at a load of 27 MN/m^2. The overall slope for this composite is about 174 MN/cm.

The effects of the loading on the copper plates, as well as the glass layer is a complex convolution, but from observing a series of test samples, under different conditions, some general observations can be drawn. All the bonded Cu/glass samples supported large loads and very large extensions without signs of obvious cracking or mechanical failure of the glass phase between the plates. Some of the bonded laminates had very clear slope changes around 30 – 40 MN/m^2 (five layer), and some between 20 – 25 MN/m^2 (three layer.)
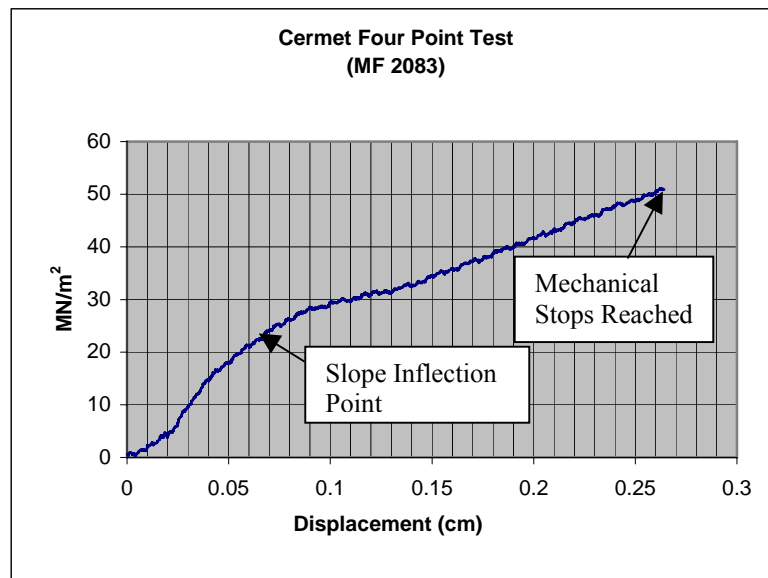
Fig. 50: Copper/glass sandwich deformed until sample geometry stop limit

While it is not clear whether the glass is carrying most of the load during the remaining extension after any inflection points are reached/passed (but the slope data tends to indicate that it is, to some extent, since the copper plates are so ductile and offer a much lower yield value – 6 to 7 MN/m^2), none-the-less, the laminate's glass layer(s) are exhibiting tremendous resistance to complete laminate structure failure/glass breakage and release since the glass/metal systems did not debond during the testing.

One valid conclusion relative to the load/extension plots of the bonded laminates is that the composites continued to show good resistance to load, unlike the non-bonded system or simple copper plates after the inflection points where pasted.

Some of this behavior may be due to work hardening effects in the copper, but this mechanism could only account for a small percentage of the load bearing behavior change of the laminate since the non-bonded laminate did not clearly demonstrate this type of behavior.

This can be seen by looking at the slope of the load to extension for the copper plate bonded to glass (five layer) after failure (fig. 51.) The slope was, after the inflection point, 121 MN/cm. This is possibly due to the glass phase still offering considerable resistance to the bending load even as cracks form within the matrix.

Some Cu/glass laminates exhibited a very pronounced inflection point. The four-point load extension displayed in fig. 51 shows a fairly abrupt change in slope after the load reaches 30 MN/m^2. This is most likely caused by sudden, partial failure of part of the glass layer (onset of initial, massive crack generation within the laminate.)

Four-Point: Three Cu/Two Glass Layers
(MF2089)
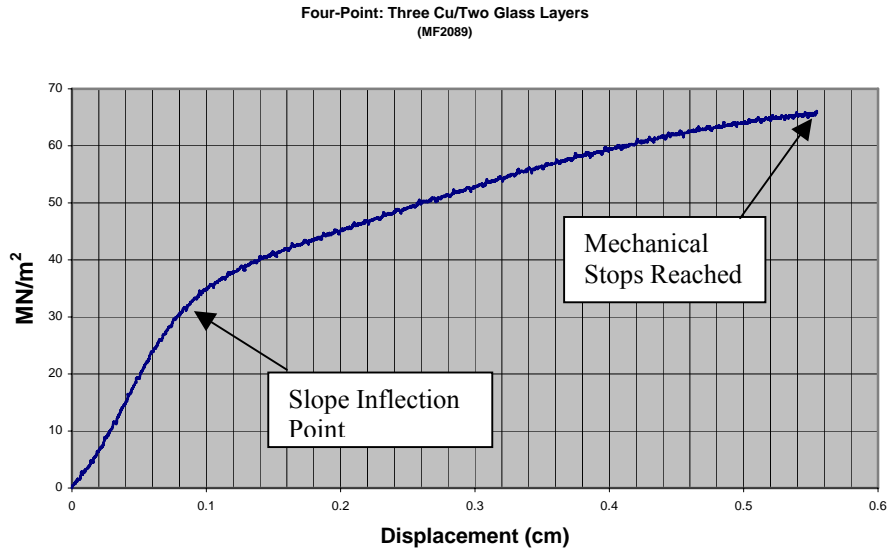
Fig. 51: A Cu/Glass/Cu bonded laminate; note inflection point near 30 MN/m^2

Four Point Cu/Glass Data
(MF2094)
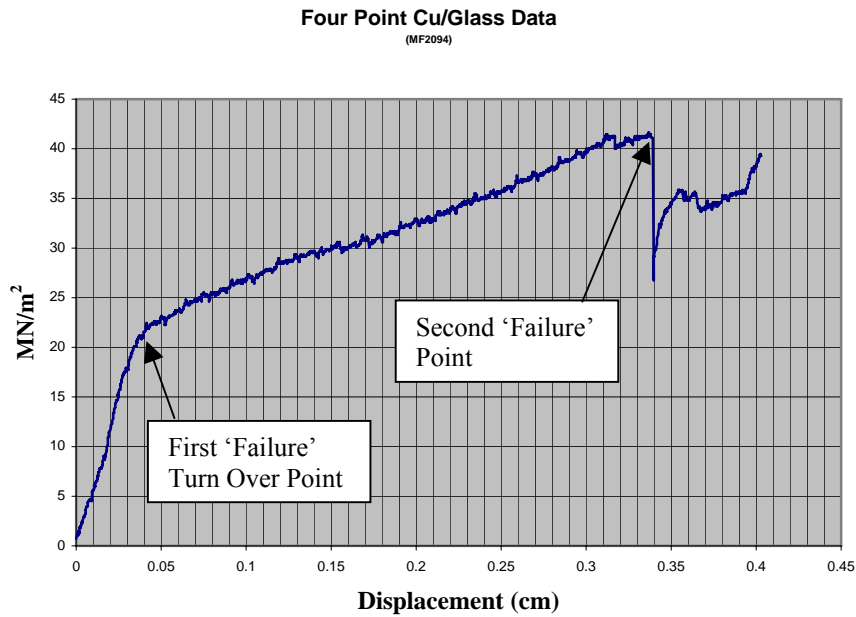
Fig. 52: Cu/glass/Cu bonded laminate

Both the plots in Figs. 50, and 51 have an inflection point occurring between 20 – 25MN/m^2. The laminate in fig. 52 exhibits another clear failure point after reaching a

load of 41 MN/m^2 with an extension of 0.34 cm. Again, a significant failure in the glass layer has occurred. From visible inspection of the glass layer at the time of testing, the glass layer appeared to have moderate edge cracking but upon removal from the four-point bend jig, the laminate remained bonded together and no significant glass fragments fell from the assembly.

Four Point Bend Test Cu/Glass/Cu
(MF2095)

Failure Point

Mechanical Stops Reached

MN/m^2

Displacement (cm)
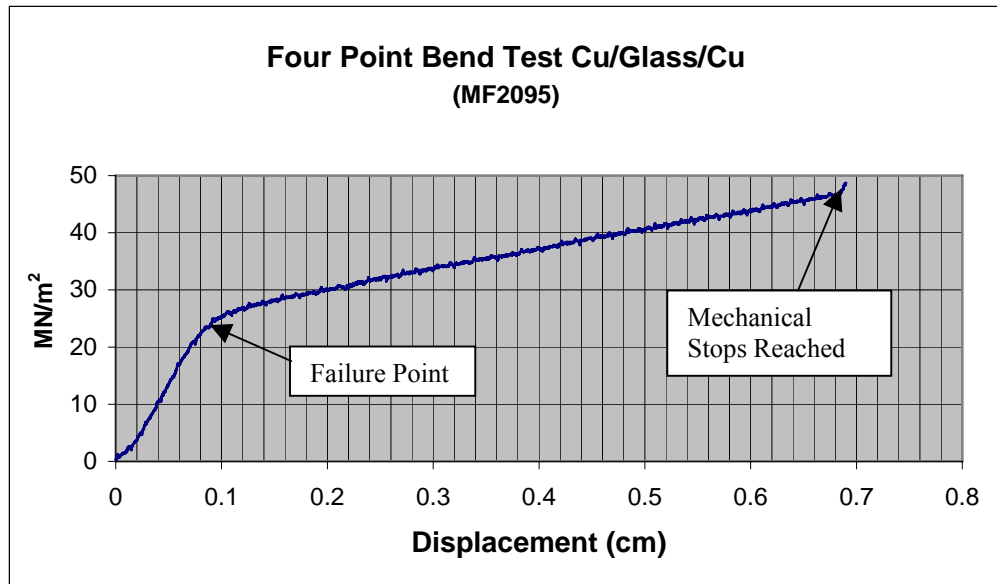
Fig. 53: Cu/glass/Cu bonded laminates: measured deformation 18 mm

The initial slope for the laminate in fig. 53 is 550 MN/cm, and after the inflection, only 62 MN/cm. The initial slope for the laminate in fig.53 is about 277 MN/cm, and after the inflection point, only 36 MN/cm. The lesser slopes are more metal-like in their response and the large slopes, more glass or brittle like. For the second failure event in the laminate displayed in fig. 52, a major glass failure within the ceramic layer appears to occur. The failure by the laminate was followed by another smaller but very steep load rise/change that once more acted as if a glass region was reloading. Unfortunately, the four-point rig/sample reached its limit stops and the test was terminated. As stated

previously, the sample was then dismounted and the metal plates were still strongly bonded together by the glass phase. Cracking existed but glass was not breaking free nor did the metal plates separate.

The laminate deformation response in fig. 52 gives strong direct evidence that even after major failure occurs for the laminate just under 25 MN/m^2 the glass layer is still contributing to the laminate's overall strength/resistance to load (by the second failure event) until equipment stop-limits are reached.

Laminate Flexure Strength

The flexure strength for the laminates that had obvious slope changes (initial glass layer failure) and for the metal and glass plates were derived from the four point test results - see table 3 for a list of the data.

Sample	Type	ε_c (cm)	σ_f (MN/m^2)	F_c (MN/m^2)
MF 2086	Cu/Glass/Cu Not Bonded	0.07	13.8	124
MF 2082	Copper Plate	0.05	2.7	24
MF 2083	**Cu/Glass/Cu**	**0.07**	**25.0**	**225**
MF 2089	**Cu/Glass/Cu**	**0.09**	**34.0**	**306**
MF 2094	**Cu/Glass/Cu**	**0.04 & 0.34**	**23.0 & 41.7**	**207 & 375**
MF 2095	**Cu/Glass/Cu**	**0.08**	**23.0**	**207**

Table 3: Flexure Strength of glass/Cu laminates using four-point bend data: ε_c is the bend deformation at 'failure' extension value, σ_f was the yield load at 'failure'; F_c is the calculated flexure strength

The flexure strength for a rectangular plate is given by:

$$F_c = (3e\ \sigma_f) / (w\ h^2)$$

Where 'e' is the lateral separation distance between the upper and lower loading points for the laminate (e = 13.5 mm; see fig. 45), 'w' is the laminates width (18.0 mm), and 'h' is the laminate layer thickness (for slope change or obvious glass phase failure, the glass thickness: 0.5 mm, is used.)

From table 3, the flexural strength of the bonded glass based laminates is generally almost twice the strength of the unbonded glass/metal stack (MF2086). These flexure values are based on the initial yield points in the bonded laminates graphs (where the slope suddenly changes in the load versus displacement graphs, not the machine stop points which would be far larger.) Note that sample MF2094 has two distinct flexure strengths due to the pronounced change in slope at the two points in the graph.

These flexure strengths are certainly lower bound limits since the bonded glass laminates do not exhibit classic failure at any time due to the machine stop limits and continued to resist bending until that point.   While the copper plates yield strengths are convoluted into the results, this effect is only a small fraction of the laminates total flexure strength as shown by the rather small copper plate 'flexure' failure value.

These flexure values for the cermet are very similar to high performance ceramics such as Al_2O_3 (340 MN/m^2) and high quality SiC (550 MN/m^2.)

Details of Glass/Metal Interface after Deformation

These bend test results do not really demonstrate the extraordinary performance of these laminates since they endured bend deformations - the absolute extension that these laminates endured without failure, or before any turnover in their resistant to bend deformation occurred, is huge for a glass: up to 18 mm for a 8.2 cm long plate – see fig. 54.

Two multi-layer sandwiches sample (three copper and two glass layer all bonded together) endured an extension of over 18 mm without any sign of failure (see fig. 54, glass/Cu samples 'd & f'.)

The glass layers in the sample displayed in fig. 54, laminate 'd', did show cracks and glass loss near the edges, but still maintained good bonding between all the copper plates (as did all the four-point bend Cu/glass samples.)

These impressive toughness and fracture toughness values obtained for the entire set of bend and tensile test samples are difficult to understand using only standard ceramic/metal laminate crack stopping theory (ref. 9.)
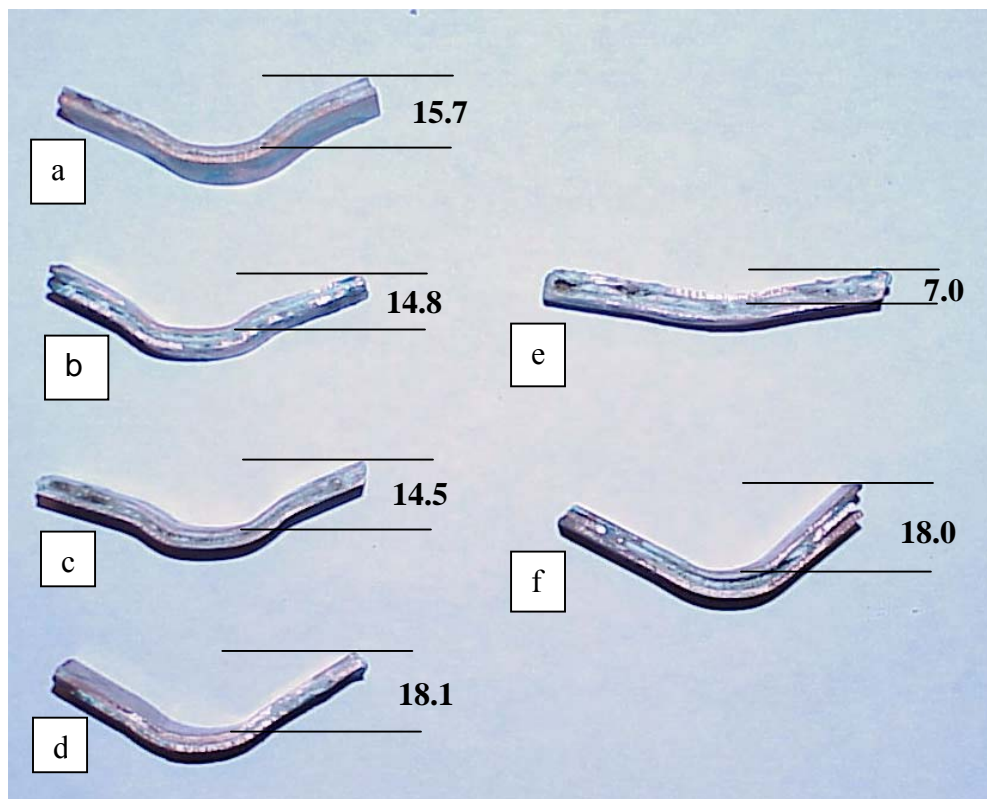
Fig. 54: Various four-point deformed copper/glass bonded laminates (all displacements of the copper/glass laminates are in given in millimeters; no samples debonded nor suffered cataclysmic failure despite these extreme bend deformations)

In fig. 55, an image of three multi-layer copper/glass laminates that were bent in four-point testing is displayed. The glass layer in these samples was about 0.5 mm thick. The copper layers where each 1.6 mm thick and annealed to a very soft temper. None of the four-point bend samples failed during the test. That is, the copper and glass layer assemblies remained strongly bonded together even after massive deformations.

From magnified white light imaging of some of the bulk glass regions from a number of four-point bend specimens (see fig. 55, 56, 57, and 58), a few interesting features relative to the performance of the GMET can be observed.
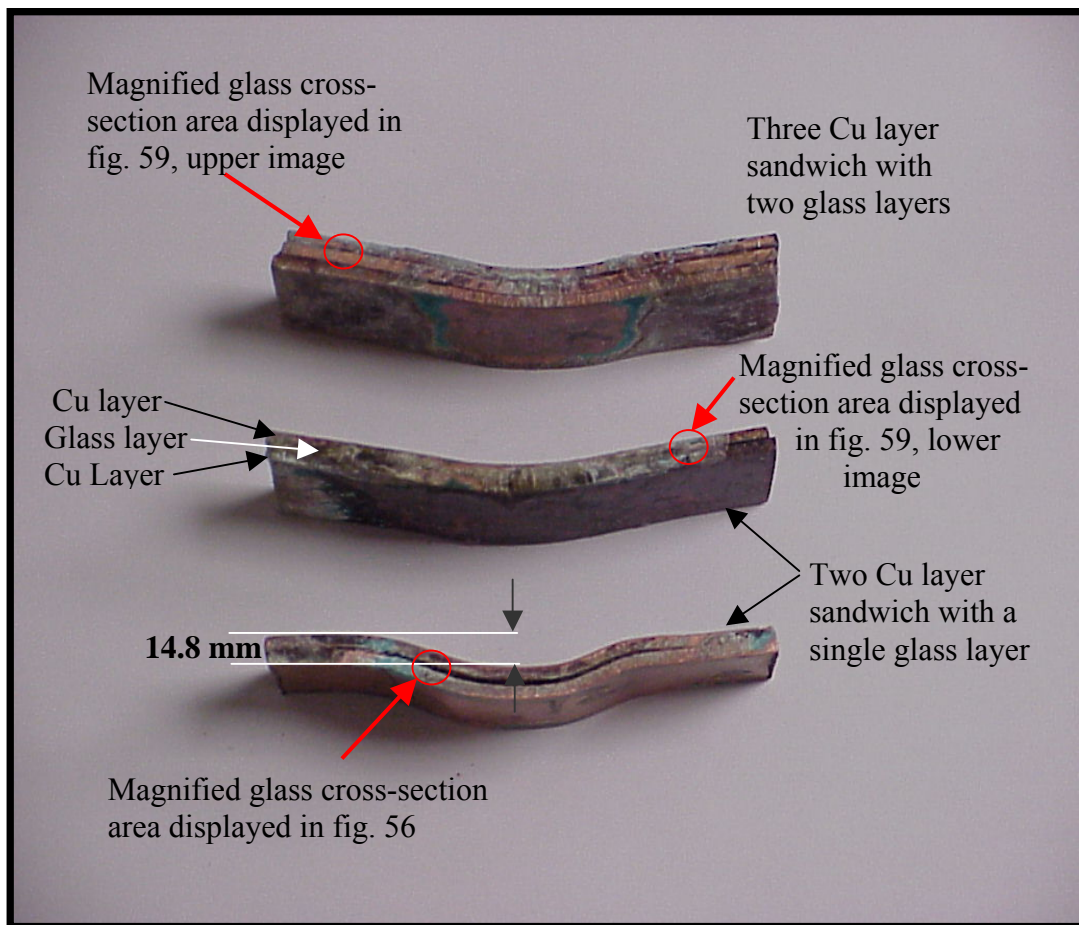
Fig. 55: Deformed copper/glass laminated cermets from four-point bend tests

In the four-point bend samples that endured extreme deformation, cracking within the glass phase generally did not follow typical random direction morphology or random size assortment (see fig. 56 and 57.)
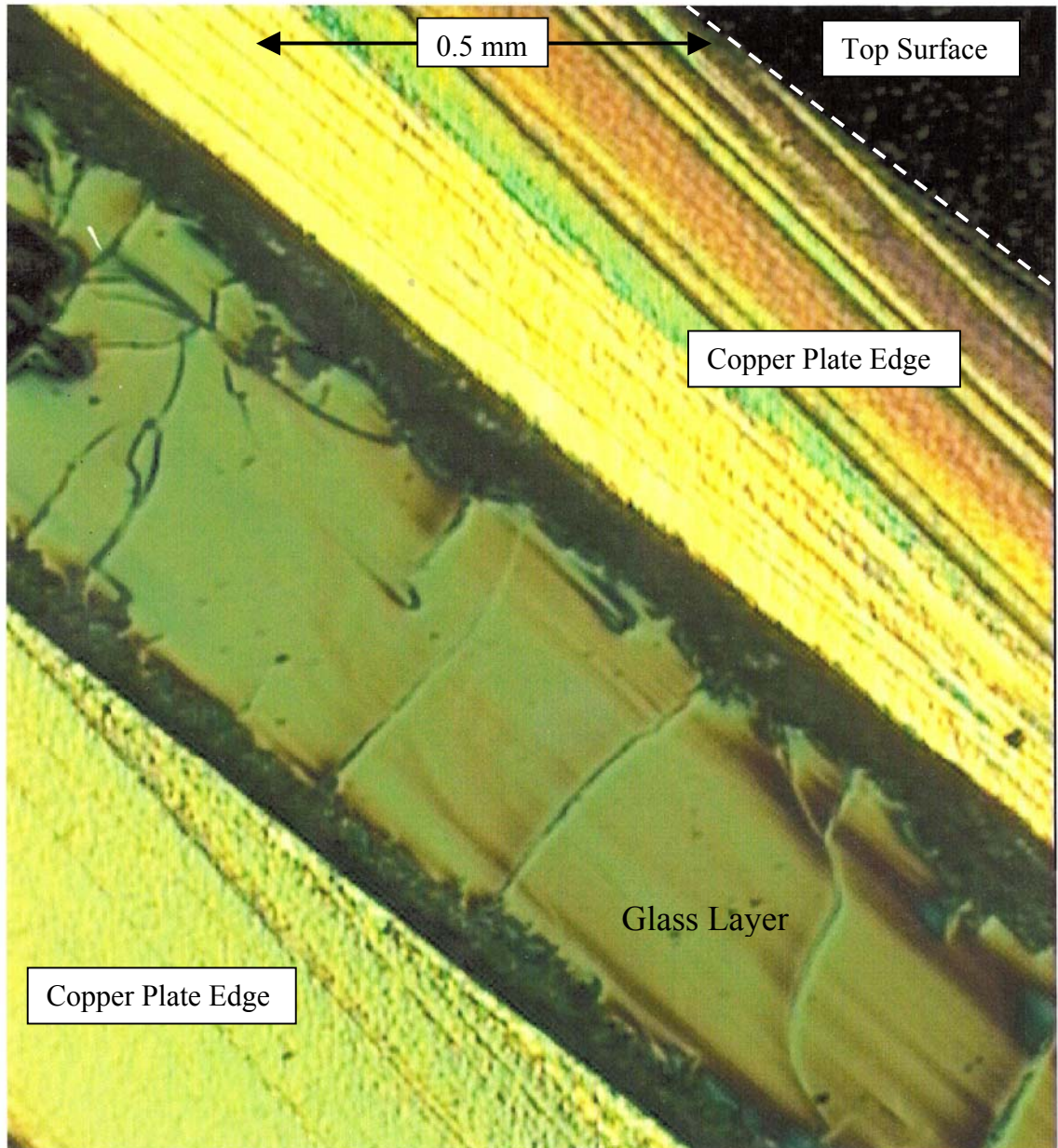
Fig. 56: Polarized white light magnified image of a four-point bend laminate glass layer after undergoing major deformation (note columns of relatively damage free glass)

In the laminate samples that endured the largest bend defections, only a limited number of larger cracks formed in the glass phase, mostly oriented perpendicular to the metal plates. These cracks apparently relieved the extremely large stress fields that were generated by the large bending deformations, yet the glass did not debond (see fig. 55, 56, and 57) nor more importantly, did the visible cracking lead to any significant crumbling/continuity failure within/across the glass phase between the copper plates (fig. 56, and 57 upper or lower image.)
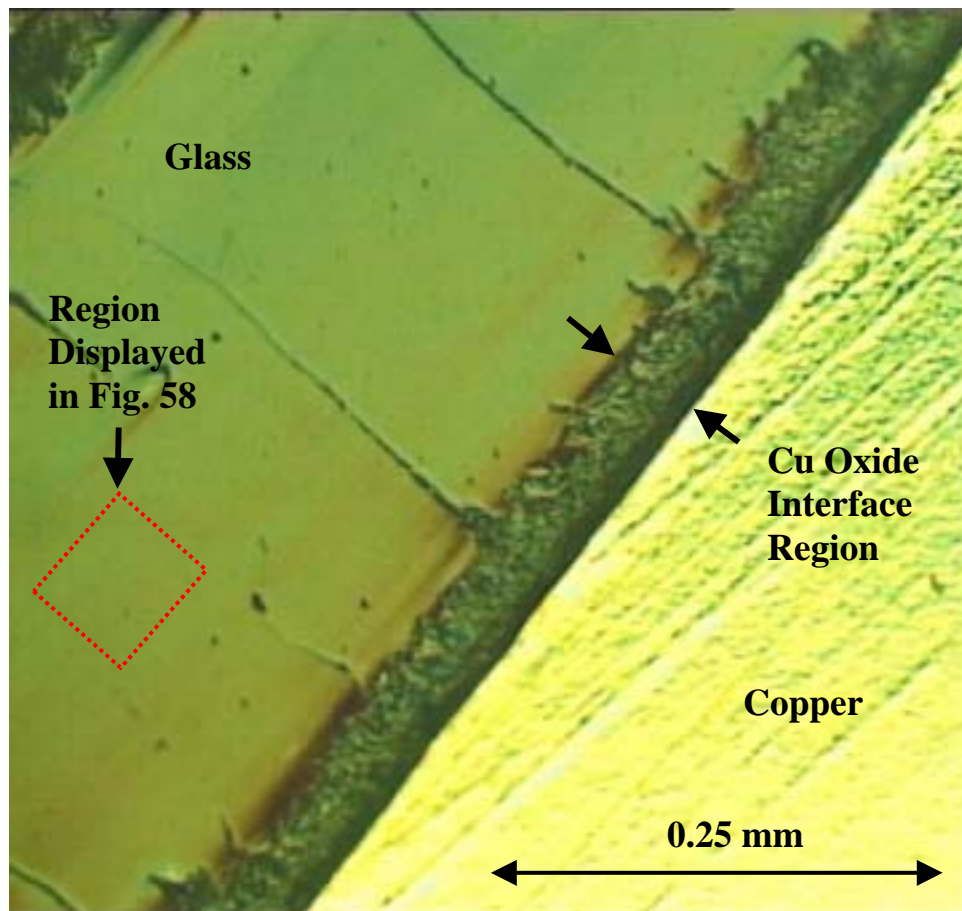
Fig. 57: Polished, magnified and polarized light image of glass and metal layer after undergoing four-point bend testing after major deformation. Red box is magnified image displayed in fig. 58. Note columns of relatively damage free glass

Significantly, the large cracks within the glass phase of the laminate structure created isolated areas of completely damage-free glass 'columns' (fig. 56 & 57) that do not appear to contain any micro-cracks (see fig. 58.)
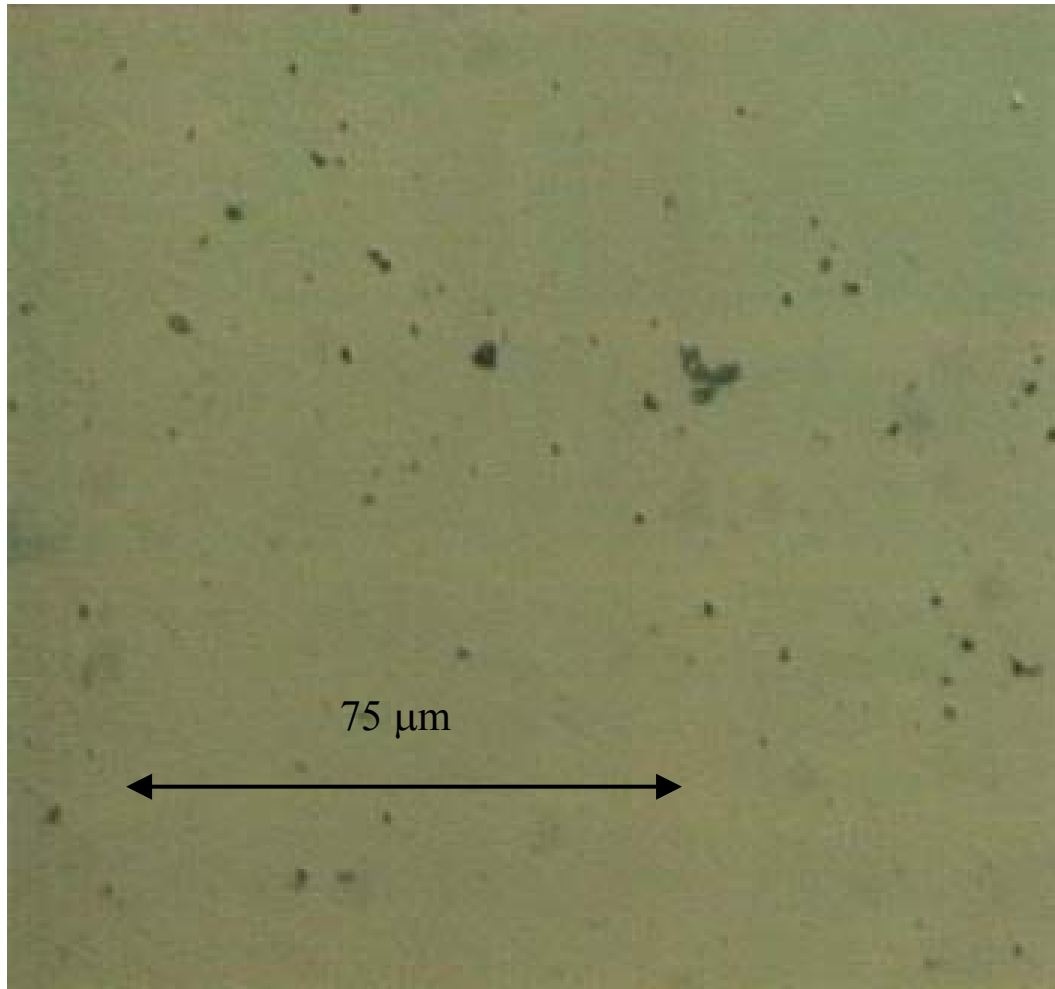
Fig. 58: Polished, magnified and polarized light image of glass (Crack free region.) Speckles/dark areas are debris created by polishing the surface for better imaging

These four-point bend samples indicate that the glass phase appears to resist random (non-perpendicular to the metal plates) crack formation within the glass matrix by relieving critical point stress fields by opening singular large cracks that maximize strain relief in a manner that appears to prevent total laminate failure.

This data is consistent and partly explains the unusually high fracture toughness that this glass phase has demonstrated in the four-point bend testing. The tensile test data – specifically the metal like elongation curves are very difficult to explain merely by using crack growth/blunting - especially since most of the glass volume is not in contact with the metal, or for that matter, very close to any metallic surface in those samples.

Rather, the glass in the tensile testing appears to tolerate extremely large deformations before failure and then, when failure does occur, it is progressive and gradual like a metal – for a glass based laminate, this is unusual and probably occurs either by inhibiting/tolerating crack growth in such a manner that the glass accommodates these very large elongations or else by some currently unknown mechanism.
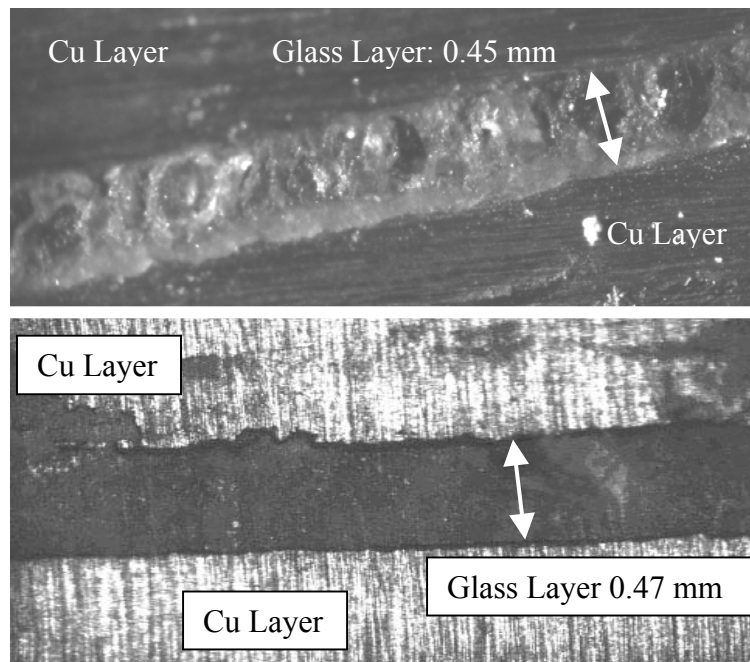
Fig. 59: Top Image: Detail of glass layer in Cu/Glass/Cu laminate after moderate bend deformation of 14.5 mm - no apparent cracking but some stress induced chip pitting on the surface (partly due to rough polishing.) Bottom Image: Glass layer from multi-copper/glass laminate (after moderate bend deformation of 14.8 mm; no visible cracking)

Summary of Four-point Bend Results and Bulk Laminate Toughness

These four-point bend test results for the GMETs show how these composites offer remarkable resistance to total glass failure (i.e. Cu plates remain bonded together, while the glass layer show's no signs of significant breakage much less crushing) despite exhibiting extraordinary total bend extensions (up to 1.8 cm for a sample only 8.2 cm long and 1.8 cm wide.)

These bend deformation tests, combine with the tensile elongation results indicate that these glass/Cu laminates offer remarkable resistance to failure under tremendous deformations or elongations – a performance that has never previously been reported by any other researcher for an oxide based glass system.

Two primary factors probably have contributed to this strange behavior in both the tensile and bend test samples. First, the proprietary glass (very approximate composition: 45% Al_2O_2, 43 % SiO_2, and the remaining composition is both common and special modifiers) has resulted in an amorphous ceramic that has very different chemical and, very possibly, physical properties compared to most oxide glasses. This is partly due to the fact that the proprietary glass melt has been specially modified with unique chemical additions, may help suppress crack propagation and/or growth and increase the plastic response of the amorphous network.

Secondly, processing the glass into a laminate structure that includes metal plates appears to have improved the system's overall bulk toughness. As indicated by other researcher's (that cermet laminates need metal plates within tens of microns of the ceramic phase in order to achieve maximum ability to arrest cracks), it would appear highly unlikely that the metal phase in the laminate structure alone could completely

account for such a large improvement in bulk toughness or sustain such large elongations considering the wide separation between the metal plates. The fact that the glass phase is mostly encapsulated probably reduces the number of surface defeats since the glass is strongly bonded to the metal plates; hence, the atomic glass network does not have a free surface, so these normally free bonds are now satisfied. Also, the glass surface is protected from both mechanical and chemical degradation effects that can lead to the creation of micro cracks.

Many of the metal/glass four-point bend samples showed similar resistance to major cracking that should lead to complete failure – that is, vertical cracks do developed within the glass layer but only after very heavy deformations (over 10 mm displacement from center by the laminate) by the metal plates. Yet this cracking within the glass phase never led to overall laminate failure – that is, the copper plates separating during or after testing. This non-failing behavior might be understood by comparing similar bend data for metals. In four-point bend testing of metal plates, when the outer radius of curve for the plate is large, the metal's outer surface/region will be in extreme state of tension.

As this tension reaches the metal's ultimate yield strength, vertical cracks tend to develop along this outer radius and relieve the tensile loads.

In a glass plate, with the upper (inner radius) region in compression, only the glass volume in the outer radius will quickly reach a tensile state that nucleates a crack (that surface is in the greatest tension.) Because these samples are laminated between metal plates, as a vertical crack propagates within the glass phase is quickly arrested when it reaches an upper or lower metal plate and is blunted. Such a crack will not then propagate or grown any further.

Any horizontal cracks in the glass phase that is in tension would still not be stopped until they changed direction (see fig. 55 & 59.) These results tend to support the hypothesis about the tendency of the sealing glass to exhibit greater tolerance to cracking by better accommodation with the metal plates via plastic relief. The fact that neither of the glass layers in fig. 55, and 59 showed any sign of extensive macroscopic cracking within the surface volumes, much less the massive cracking expected of a glass layer so heavily deformed with deflections of almost 15 mm (at the center) over a 80 mm long sandwich, is very interesting and strongly indicates that not just crack arrestment is at work in these cermet samples.

Of course, extensive cracking could be occurring deep within the laminate glass layer that is not close enough to an edge for visual inspection. This question was better addressed after a GMET was constructed that had only one metal plate with a glass layer bonded to it that was deformed in the four-point loading system (see fig. 60.)
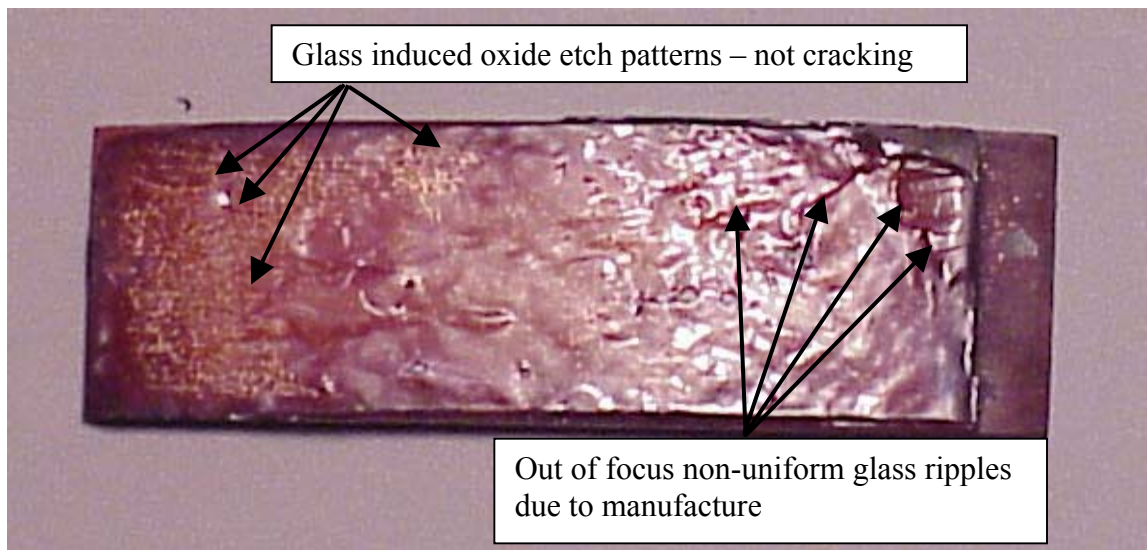
Fig. 60: Surface/volume image of a moderately bent glass layer (0.8 mm thick) that is bonded to a single copper plate (82 mm L, 25 mm W, 1.8 mm thick, with center deformation of 5.0 mm.) Top surface was not bonded to a metal plate during melting/cooling and is randomly rippled. Notice that there are no visible cracks in the glass phase for this slightly enlarged view of the glass phase bonded to a single Cu plate. Inspection with a 10x ocular did not reveal any surface or volume cracking.

This sample was moderately bent (5.0 mm total bend displacement from level at the center region) at room temperature. Yet upon close examination (10x ocular), no cracks could be discerned within the glass volume – just etching by the original liquid glass on the copper oxide surface at the interface. From the image it can clearly be seen that the glass in the laminate is still transparent. This proves that the glass phase is still amorphous and that even if micro-cracks did exist, they must be on the order of a quarter wavelength of light or less and can not be very extensive within the matrix.

The glass layer on the cermet sample that was bent (fig. 60) clearly demonstrates that the glass phase can readily accommodates fairly large deformations without cracking in order to relieve stress fields – that is, plastic flow is most likely occurring within the glass phase at room temperature (this glass that has a softening point near 500 C.) This aspect of the research is more fully discussed in the next section.

In contrast, a normal glass undergoing any moderate bend testing would quickly nucleate cracks, and these would then rapidly spread leading to extremely rapid failure; also, any large crack-free glass volumes would quickly be crush from forces within the deformed laminate sandwich due to the brittle nature of the glass phase. The deformation testing results of these GMETs, the sandwiches do not exhibit this type of behavior; but rather, similar to the tensile results, the glass phase appears to readily accommodate the increased stresses caused by the strains within the laminate structure without undergoing major failure via extensive or even any significant cracking.

This non-standard behavior of this glass may be due to enhancement of the plastic response – leading to a true amorphous oxide glass that exhibits extraordinary toughness and will support some significant plastic flow for slow (0.002 cm/sec) deformation rates.

Plastic Flow in Glass (oxide)

In the work of D.M. Marsh (see Proc. Royal Soc., London, series A, vol. 279, No. 1378, pp. 420-435) he has shown that typical oxide glasses do exhibit limited but still significant a *macro* plastic flow component when deformed by diamond 'hardness' indenters. Marsh proposed that modifiers used in oxide glasses (such as those used in soda glass) create breaks in the normally near continuous atomic linking found in amorphous, non-modified, glass structures. This more open network containing additional free bonds appears to allow for moderate plastic flow by the material when placed under the stress of an indenter.

Further, the model he proposed is also supported by experimental work performed by other researchers. For instance, measured crack velocity in glass is significantly lower then what brittle crack theory in glass would predict; also, tensile yield of 'flaw-free' glass fibers differ from that predicted by theory based on a fully brittle amorphous structure.

Marsh proposed that plastic deformation by the glass accounts for these variances and his predicted values using his model for yield does in fact closely agrees with actual experimental values. These results indicate that glass does exhibit moderate plastic behavior (for such an extremely brittle material) to a rather nonqualified extent. The 'plastic' yield effect does significantly reduce crack propagation velocity in the brittle matrix but under tension, cracks in glass are still extremely unstable and will readily cause bulk failure. All other amorphous oxide glasses whether with or without structure modifiers remain extremely brittle relative to impacts and offer very poor bulk toughness/fracture toughness.

Under Marsh's proposed model, the glass remains extremely brittle but also exhibits limited true plastic flow and as Marsh notes, modifiers in glass can cause the amorphous structure to become more open and possibly, allows the covalent bonding within the oxide structure to act slightly more plastic when deformed.

I believe that the special propriety modifier developed for this glass not only further enhances this effect, but also enhances the ability of the amorphous structure to re-establish bonds after heavy induced flow. This improved modifier results in an amorphous structure that can support very plastic-like deformation to relieve stress fields without massive cracking even under tension.

The experimental results strongly support the contention, that existing cracks that do form are readily stopped (see the tensile and four point bend data graphs.) This stopping power cannot be simply due to crack arrestment by the metal phase (ref. 19, 20, 21 and 22) since the metal phase is often many millimeters away from the bulk glass.

Rather, crack arrestment by plastic relief at the crack tip more accurately accounts for the tensile, the extreme four point bend, and torsional experimental results in relation to the high power white light imaging of the glass matrix after heavy deformation. In the bulk glass volume and interface images the glass phase is highly transparent (still amorphous so the modifier is not creating a cermized or crystalline phase) but no micro cracks are visible nor is the glass phase seen to be scattering light by cracks that are on the order of a quarter wavelength of light (between 1000 – 1500 A) or larger.

The tensile and torsional data strongly tends to support the premise that the glass is somehow supporting large tensile (for a ceramic or glass) deformations, thus allowing the laminates to exhibit extremely high tolerance to bending or elongation. The glass phase

does exhibit some typical crack morphology under significant tension/rotation/bending but these cracks are limited and stable; further, and very significantly, the overall bulk glass maintains its load bearing integrity without developing massive minor cracking between the large cracks allowing the damaged free column regions within the glass layer to remain intact and maintain the sandwich's integrity (fig. 55, 56, and 57.)

The extent and magnitude of these deformations within the glass matrix for the tensile samples cannot be directly measured nor can precise pre-cracks be made for these tensile samples as of yet (this issue will be addressed in a future paper, where R-Curves will be developed for the glass matrix.)

The extraordinary deformations and elongations supported by the glass matrix indicates that the linear displacement for any given glass volume, while small in absolute terms compared to very ductile metals is, relative to normal bulk oxide glass, extremely large; especially compared to what singular glass rods or plates of similar dimensions could possibly endure. The model proposed in this thesis would also readily account for the large toughness and fracture toughness the GMETs exhibit.

Toughness and Strength to Weight Ratio's

The toughness and fracture toughness values calculated from these tests are **impressively high: 2 - 3 kJ/m^2 and 5 - 7 MN/m$^{3/2}$** respectively: values based on an arbitrarily selected "initial" crack size that leads to fast failure by the glass phase. These calculated values are in very close agreement with the adhesion test data for the actual metal foils bonded together by the modified glass.

By comparison, non-toughened glass has toughness/fracture toughness values of only 0.01 kJ/m^2 and 0.7 – 0.8 MN/m$^{3/2}$ respectively.)

These toughness and fracture toughness results, including the tensile ultimate yield values, are displayed in the following table. As can be seen, the GMETs strength to density ratio performance is nearly as good as 6061 light Al alloy.

Material	Fracture Toughness $(MN/m^{3/2})$	Toughness (kJ/m^2)	Strength -Density Ratio
Glass	0.7	0.01	0.8
Toughen Alumina	3 - 5	0.02	1.3
Al Alloy*	10 - 50	8 - 30	52
Aluminum Cermet	**7.8**	**0.88**	**72**
Copper Cermet	**8.1**	**0.95**	**78**

* Based on 6061 Al alloy experimentally measured for this thesis

Table 4: List of some of the physical properties of a few common materials and the laminated cermets (based on the one of better yield values: 180 MN/m^2 @ 2.5 gm/cm^3 for glass/Al, and 250 MN/m^2 @ 3.2 gm/cm^3 for the best glass/Cu sample)

Chapter 5

Light-weight, High Performance, Multi-Impact Ballistic Armor

The Hidden Threat: RPG-7 (Rocket-Propelled-Grenade) and 7.62 mm assault rifle using ball/armor-piercing (AP)

Armor plates based on carbide ceramics are very light for a given stopping power (75 kg/m^2 versus 7.62 mm) and these composites can, depending on the manufacture's ability to make flaw free plates, offer excellent protection; however, all existing ceramic based ballistic insert plates fail after a single impact or even when simply dropped on a concrete surface or onto rocks from a standing height.

In the 1980's, the U.S. Army Ballistic Research Laboratory (ABL) began a study of the ballistic performance of glass armor. The results, especially when their effectiveness is measured against the tremendous penetration power of shaped charged warheads (RPG's: **R**ocket **P**ropelled **G**renade" a misnomer for the weapon) were impressive (see Appendix: "Ballistic Research Laboratories Observations" and for the full report, ref. 23).

Numerous researchers have studied the ballistic resistance properties of glass (refs. 10, 11, 12, 23, 24, 25, and 26.) These researchers have determined that glass armors are superior in stopping power versus shaped charged jets then any existing armor on a weight bases and that glass armor has equivalent stopping power against kinetic ball and armor piercing rounds, on a weight bases, as do ceramic armors. Yet, this type of armor suffers one overwhelming problem: brittleness.

As discussed in the Army Ballistic Laboratory (ABL) report, powerful supersonic glass dust jets created by the impacting round defeat ballistic ball rounds. Yet, due to the brittle nature of simple glass, after a single kinetic impact by a 7.62 mm round, typical glass armor readily fails and cannot withstand any subsequent kinetic impacts/rounds.

Since this glass based cermet laminate is so extraordinary tough, a small research effort into determining whether this type of laminate could be used as a possible ballistic armor was initiated – that is, a ballistic study was conducted to determine whether this type of material could defeat typical 7.62 mm military rounds at a performance to weight ratio's that was compatible to existing ballistic grade ceramics/light metal armors.

Typical man portable military ballistic rounds exceed 850 m/s and are based on 5.56 mm and 7.62mm diameter copper jacketed lead ball or even titanium metal slugs (AP rounds) that can typically punch through 1.25 cm of case hardened steel plate. Because laminate cermets sacrifice glass volume for metal volume in order to improve overall toughness, issues of thickness and overall laminate density becomes paramount relative to stopping power performance. For this and other reasons, a program to more thoroughly investigate all these issues was started.

GMET In-house Ballistic Testing

In tests using very simple three layer glass/metal laminate armor inserts (a 15 – 20 mm thick glass layer bonded to a 3.5 millimeter thick front and back metal plates) this glass and aluminum GMET composite demonstrated that it is fully capable of defeating 7.62 mm military rounds (a standard ball round with an impact velocity of 825 m/sec) at an area weight of 13.8 lbs/ft^2 (78.4 kg/m^2).

The laminate structure was an aluminum box with front and rear walls filled with the proprietary glass, and had two internal copper witness foils (0.2 mm thick) buried in the glass which were equidistant apart with the first foil about 5 mm from the front glass/Al internal surface within the case (see fig. 61 for schematic of the insert design.)
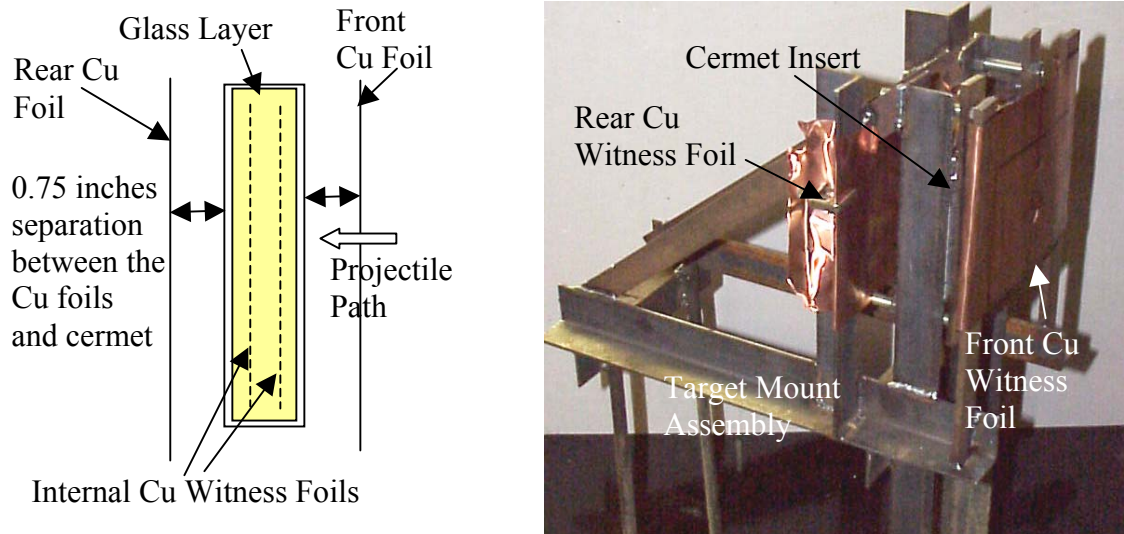
Fig. 61: (Left) Schematic of cermet plate & Cu witness foils; **(right)** Target mount
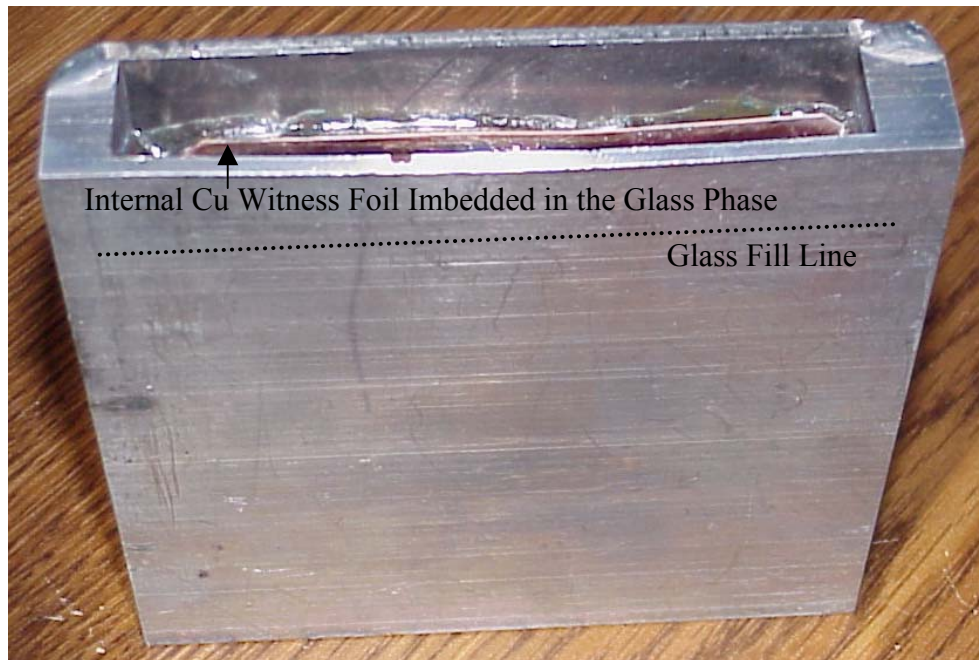
Fig. 62: A Three Layer (Al/Glass/Al) Laminate with internal Cu witness foils

The overall insert size was: 12.5 cm tall by 11.3 cm wide, with the free volume of the case filled with the proprietary toughened glass and depending on the insert tested, this glass layer varied from 15 mm to 20 mm thick (see fig. 62 for a 2.0 cm thick sample.)

The resulting inserts had a total weight of 1.6 kg or less.

A total of five laminates were tested versus standard military projectiles: 7.62 mm ball round @ 2700 ft/sec (approx. 825 m/s), zero oblique angle trajectory, three meter stand off distance.
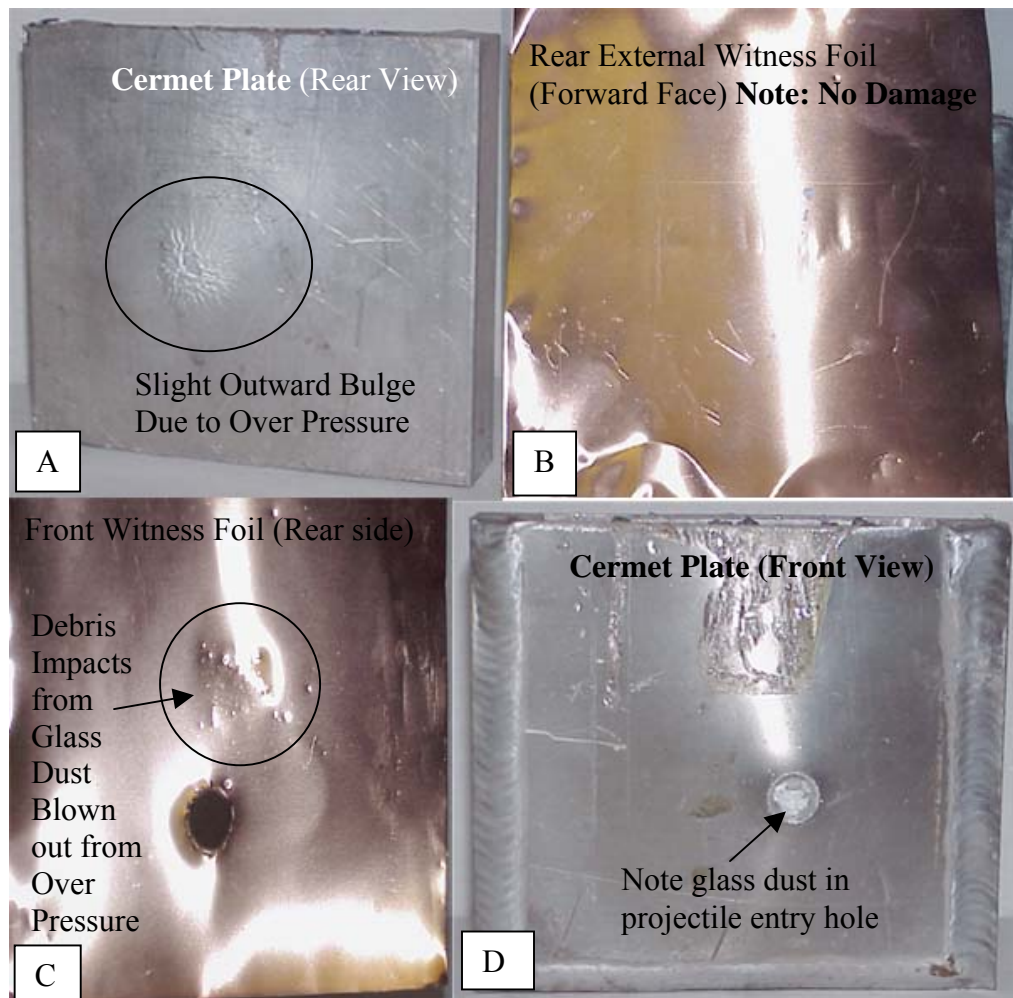
Fig. 63: Cermet Insert after Ballistic Impact and External Cu Witness Foils

As can be clearly seen for this particular insert, the front of the plate bowed outward (fig. 63, image 'D') towards the bullet's initial flight path due to over-pressure within the case. Five millimeters into the laminate, the bullet's diameter increased to over 10 millimeters as determined by the hole in the first internal copper witness foil. After 12 millimeters of penetration travel from the impact surface, the bullet's diameter and/or fragments increased to over 20 millimeters in cross-sectional area (as determined from the second internal copper foil (neither internal foil shown.)

The kinetic ball round did not defeat the glass cermet insert as can be seen by the rear side of the aluminum case is deformed, not punched through (see fig. 63, image 'A'.)

The cavity of the laminate contained mostly glass dust and fragments. No bullets fragments large enough to be identified were found. Only a chemical analysis could distinguish between glass and bullet powder or fragments.

While the glass within the plate around the entry point was destroyed - this was expected - the GMET only contained two internal test foils, and was not a true multi-layer, fully dense laminate nor did this GMET exploit the special modifier. This test does fully demonstrate the physics/process by which ultra-light cermet armor can fully defeat a 7.62 mm projectile.

These ballistic test results demonstrate that a metal-glass laminate readily defeats a military bullet round by completely pulverizing the projectile by glass fragment production that converts the bullet round into near microscopic fragments. This was proven since **no bullet/fragment even reached the back wall on the inside of the cermet aluminum box as demonstrated by the fact that the interior wall did not**

exhibit any damage or impact marks. During impact, within the laminate case near the impact site, much of the broken glass had been converted into an aggressive hypersonic powder that instantly eroded the bullet into fine dust and converted the round into a simple overpressure.

This physics is also relevant to projectiles that strike the plate at higher angles – the bullet will easily 'dig' into the soft aluminum surface and make contact with the glass phase where it will be broken up and destroyed. Hence, higher angle attacking projectiles will generally be destroyed, not just dangerously deflected.

This insert performance compares very favorably with many other common armor materials (area weights are based on a thickness that yields 100% stopping power against normal velocity military 7.62 mm ball rounds): the GMET insert: 13.8 lbs/ft^2 (78.4 kg/m^2); titanium: 11.8 lbs/ft^2 (67.0 kg/m^2); silicon nitride: 9.2 lbs/ft^2 (52.3 kg/m^2); silicon carbide: 6.2 lbs/ft^2 (35.2 kg/m^2); alumina: 14.6 lbs/ft^2 (83.0 kg/m^2); and steel: 16.5 lbs/ft^2 (94.0 kg/m^2).

Summary of Three Layer Cermet Ballistic Testing

In these tests conducted using three layer aluminum/glass inserts versus 7.62 mm rounds at zero oblique angle of impact, and a three-meter standoff distance, a critical layer thickness and laminate density and a superior metal/glass combination were determined.

Tests were performed on various combinations of materials and glass thicknesses, and the results are displayed in Table 5.

These ballistic impact results with the glass laminates in the form of an aluminum box encapsulating a different layer thicknesses of glass offer various performance results. The laminate with a 1.8 cm layer of glass can just barely defeat a 7.62 mm military round.

Material and Wall Thickness (Front/Rear)	Glass Thickness	Ballistic Result
Aluminum 2.5 mm/2.5 mm	1.5 cm	Bullet not defeated (round punched through) and glass entirely destroyed
Copper 3.0 mm / 3.0 mm	1.5 cm	Bullet not defeated (round punched through) and glass partly destroyed
Copper 3.0 mm / 3.0 mm	1.8 cm	Bullet not defeated (round punched through) and glass mostly destroyed
Aluminum 2.5 mm / 2.5 mm	1.8 cm	Bullet barely defeated; rear wall breeched by glass fragments and glass in the box destroyed
Aluminum 2.5 mm / 4.0 mm	2.0 cm	Bullet fully defeated; rear wall fully intact; glass mostly destroyed

Table 5: Ballistic test results of Al/glass filled boxes versus 7.62 mm military kinetic round

An interesting and important result from these ballistic tests was the discovery that while the all the copper targets failed, the damaged propagated by the bullet did not entirely destroy the glass. Moreover, the thicker glass samples bonded to the copper plate had more shock damage – glass destroyed – than the thinner copper/glass samples.

See fig. 64 for an image of a single Cu/glass laminate after ballistic impact. As can be seen from the image, while the bullet cut completely through (as expected), the glass

layer was not destroyed except within roughly one-bullet radii. This result confirmed that the copper/glass laminate samples exhibited superior toughness and ability to withstand ballistic impact when compared with the aluminum cermet samples.
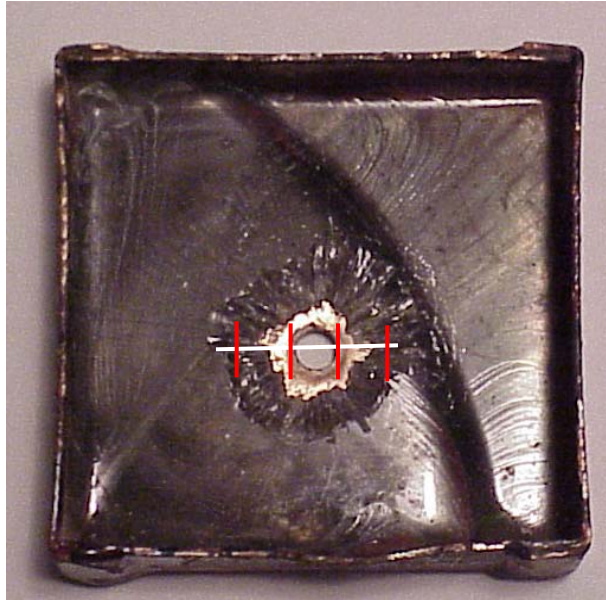
Fig. 64: Single layer Cu/glass laminate (8.5 cm x 8.5 cm box): Interior glass layer (3.0 mm thick) bonded to a copper plate (2.5 mm thick). Red lines: bullet diameters

Furthermore, the thinnest glass layer on the copper suffered significantly less damage than any other sample tested. This leads to the conclusion that for ballistic impacts, thinner but higher layer density metal/glass assemblies should prove superior in overall toughness (but not stopping power to weight) to a near solid block of glass encapsulated by a single metal jacket (ref. 23, 24, and 25).

The Cu/glass laminate displayed in fig. 64 shows a number of important details. First, and foremost, the glass layer survived nearly intact after ballistic impact. Second, cracks from the impact site did not propagate outward into the remaining glass layer; and the cataclysmic damaged extended only about 12 – 15 mm beyond the center point of the impact site.

112

This result clearly demonstrates that thinner glass layers strongly bonded to a metal (especially copper) offers superior resistance to fracture. As a consequence, a larger glass/copper laminate, both thicker and containing more layers, was constructed (fig. 65.)

.
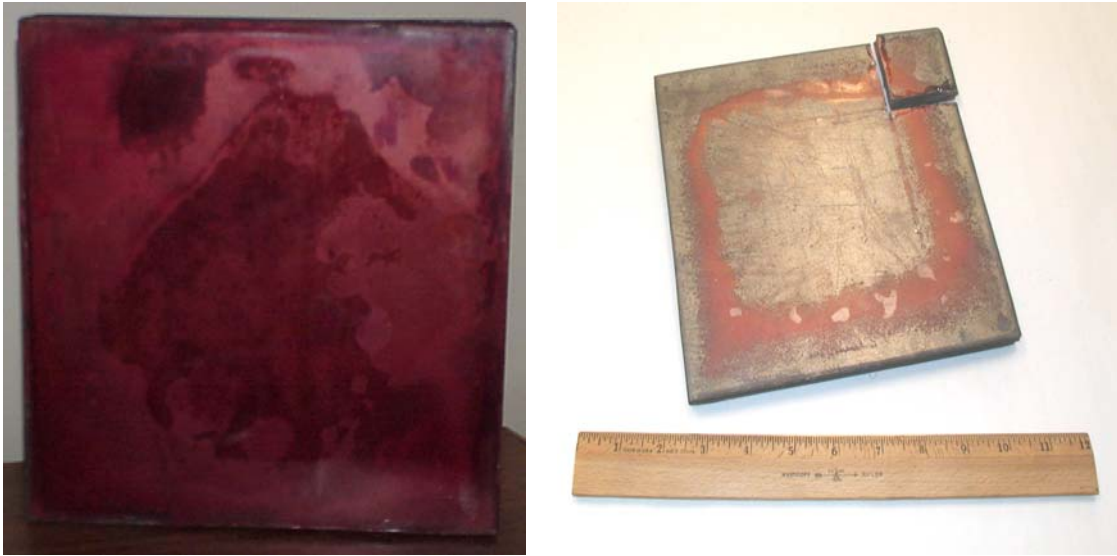
Fig. 65: Left Image: A twenty-four layer copper and twenty-four layer glass hot pressed laminate. **Right Image:** Twelve-copper and twelve-glass layer composite

Due to these laminate's much larger dimensions - 21 cm by 21 cm and 3 cm thick, these composite structures had to be hot pressed from a stack of glass and copper plates (800 C, 10 Kg/m^2 for three hours.) The glass layers were 1.2 mm thick each, the copper plates were 0.5 mm thick and each was stacked in an alternating pattern. As can be seen by the fairly uniform red copper oxide color of the top glass layer, in fig. 65, and was true for all the hot pressed laminates upon closer examination, the bonding was excellent despite the CTE mismatch between the glass and copper phases.

In fig. 66, the copper/glass stack's edge is displayed in greater detail. An interesting aspect of this copper/glass laminate is that normal plate glass was used in place of the sealing glass (as a cost-savings measure.)
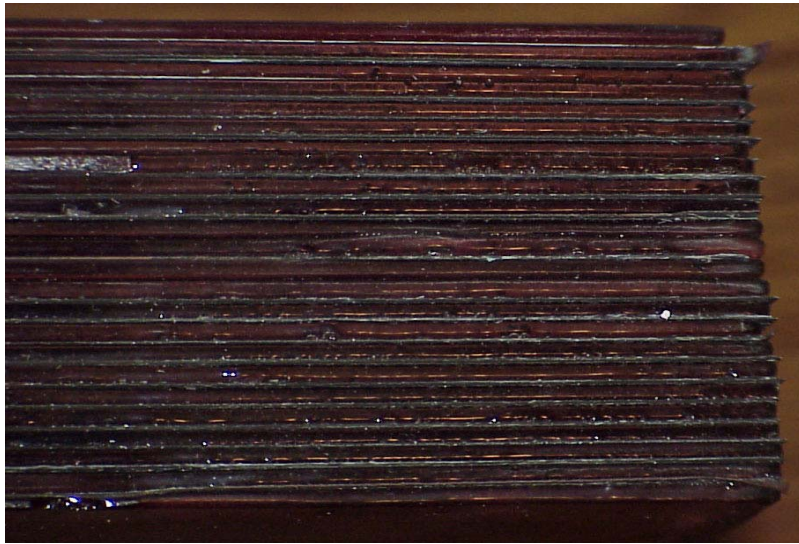
Fig. 66: Close-up of laminate structure: Glass/copper plates bonded [24 glass (each 1.2 mm thick) and copper (0.2 mm thick) layers.] This large area multi-layer laminate was created by hot pressing (@800 C, one hour with 10 kg/m² force.

A full size glass/metal laminate was tested versus multiple impact 7.62 mm military rounds under the same conditions as the previous single glass layer targets. (The laminate withstood and fully defeated three impacts without cataclysmic failure of the laminate structure - see fig. 67.)

This Cu/glass laminate contained only fifteen layers of glass (1.2 mm thick each) and fourteen layers of copper sheet (each 0.2 mm thick.)

The military has a major need for light armor that, like normal metal armor, can endure two or more ballistic strikes per continuous plate. To date, no such ceramic armor has ever demonstrated this property.

This glass based cermet laminate (over 17% glass by volume but not weight) has impressive ballistic stopping power. But until the manufacture of this toughened laminate and a search of the literature tends to confirm, that such a hard ceramic composite has never before been shown to defeat multiple-impacts for the same continuous plate.

114
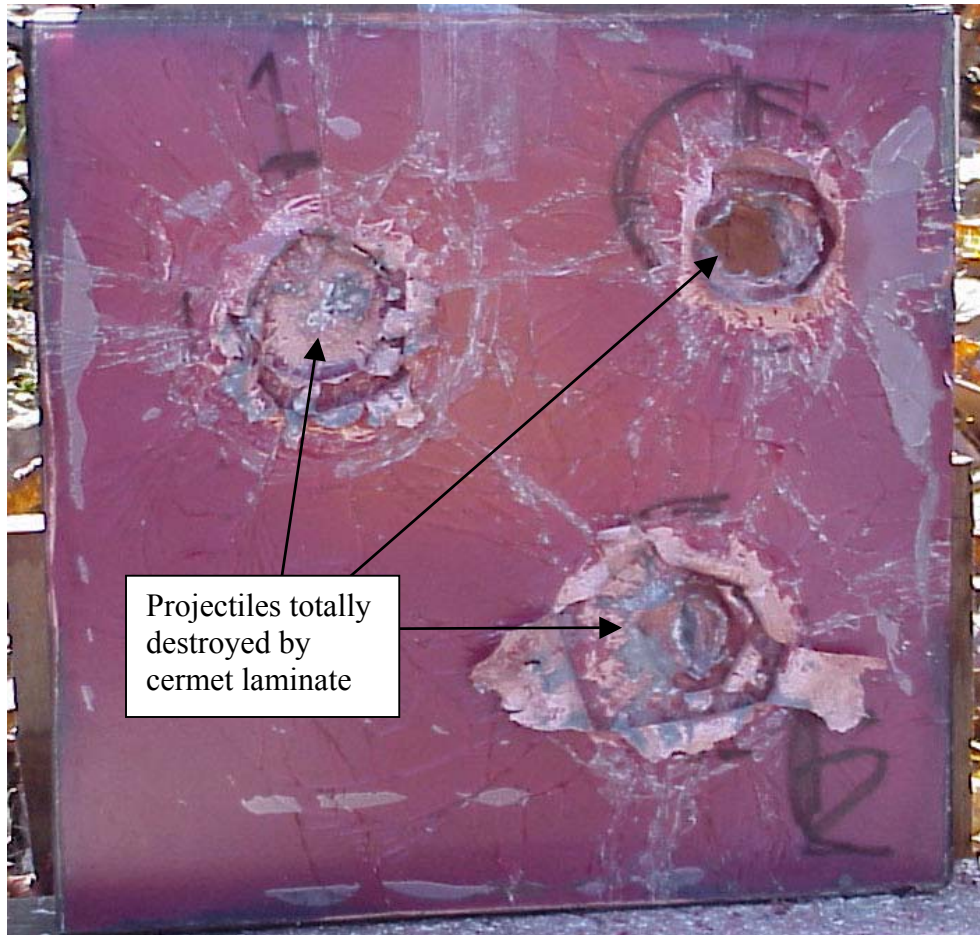
Fig. 67: Multi-layer Cu/glass laminate after multi-impact using 7.62 mm ball rounds. All projectiles were fully defeated. Laminate structure, due to high toughness, did not exhibit cataclysmic total structural failure in defeating multi-impacts as would a solid ceramic ballistic insert or glass plate of similar dimensions

The rounds did not penetrate more than a centimeter into the Cu/glass plate system. As a consequence, the bullet fragments created a much larger impact area then compared to the case when the bullet fully enters into the laminate (as is evident from the thinner Al/glass laminates: see fig. 63 D) and is destroyed by hypersonic glass particles. The large hot pressed Cu/glass laminate, more than the previous single layer glass/copper target, clearly demonstrates the advantages of using higher-layer densities with thinner glass layers. This ballistic test validates the need for multiple-impact resistant laminates

to be made with layer densities at least on this order (10 - 12 Cu layers per cm.) The thickness ratio for the glass to copper has not been qualified but the current four to one ratio appears very robust in defeating 7.64 mm rounds.

In Table 6, a list of important ballistic and physical properties for the most common types of armors in use by U.S. military and police forces are displayed along with those of the Al/glass laminated cermet developed from this research.

Material	Density (Mg/m^3)	Toughness (kJ/m^2)	Multi-Hit Capable	Stopping Power For 7.62 mm Min. Thickness (in) /Area Weight (lbs/ft^2)
Silicon Carbide*	3.2	0.05	**No**	0.25* / 3.3
Aluminum Alloy	2.7	8 - 30	Yes	1.3 / 18.2
Titanium Alloy	4.5	26 - 50	Yes	0.65 / 14.6
Steel (all grades)	7.9	15 - 65	Yes	0.5 / 20.5
Al/Glass Laminate	**2.5**	**5 – 10**	**Yes**	**0.75 / 6.75**

*Requires Kevlar backing for full defeat
 Ti ballistic data based on: Ti-6Al-4V or MIL-A-46077
'Stopping Power': material defeats 7.62mm ball round @2700ft/s; reference for Ti, Al, steel: JOM 49(5)(1997) pp.45-47

Table 6: Properties of various armor materials including proposed new aluminum based laminated cermet armor (stopping power; bullet barely defeated)

The primary objective of this experiment was to demonstrate that a light GMET armor will erode and destroy/defeat a typical military ball projectile. This erosion process should defeat AP rounds just as effectively as ball rounds since the hypersonic glass 'dust' is orders of magnitude harder than most metals used for AP rounds (Ti, W.)

Summary of the Ballistic Section

Metal/glass laminates based on aluminum offer outstanding prospects for use as light, true multiple-impact ballistic protection armor. Also, due to their special physics of interaction relative to shaped charged jets, these metal/glass laminates offer outstanding stopping power, for their weight, against these types of attacks. Due to these GMETs high toughness, and ready formability this armor material would be ideal for use as personnel body armor – that is, these laminates have the ability to endure rough handling, and due to the metal and glass phases, could easily be hot pressed with complex concurs that would follow normal body shapes, offering better all around protection and comfort to the user.

While hot rolling is not required to create these high performance laminates, the ability to create larger area plates with very high layer densities would necessitate such a process.

Due to this thesis work, and directly as a result of the Navy SBIR, a major defense company (Foster-Miller) has agreed to develop, with CCI, a glass/Cu laminate backup armor for experimental testing with their active anti-RPG defensive system – thus providing a possible system to defeat any remaining metal jets that partly defeat their active armor (explosive based.)

Navy SBIR performed during this Thesis

The use of glass armor to defeat attacks by shaped charged warheads that creates a super-hot, hyper-velocity jet of metal has been exploited previously by many researchers (ref. 12, 13, 23, and 26, et. al.) Glass has previously been shown to effectively stop these attacking jets three times better (on a weight basis) than steel and has also been shown to

be significantly superior in performance to many ceramics (ref. 23). Despite this property, due to innate brittle nature of glass, the use of this material as a lightweight RPG defensive armor has never been seriously considered, at least, until now.
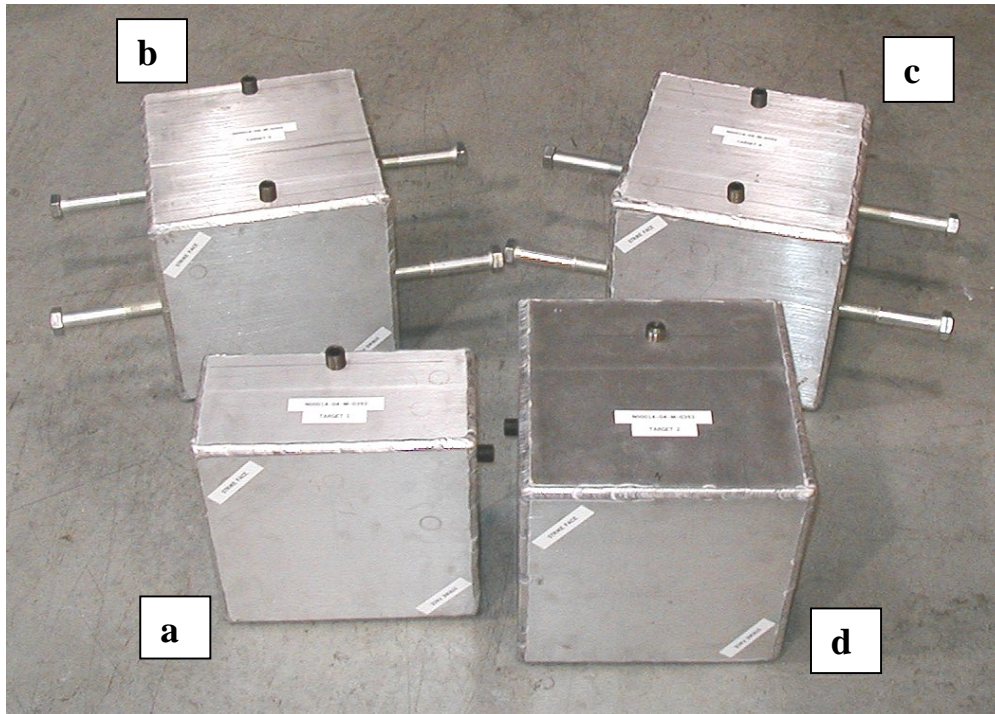
Fig. 68: Basic Cermet Laminate RPG test targets (all based on 10 inch by 10 inch glass/metal laminates structures within a steel box); smallest test target, 40 lbs total weight; largest, 100lbs w/two sets of laminate plates); **a**) Single laminate sandwich plate (24 glass layers); **b & c**) Two laminate sandwich plates (12 glass layers each); one mounted to the interior of the steel facing plate and one mounted to the interior of the rear steel plate; **d**) Two 24 glass layer laminate sandwich plates mounted in the same configuration as a & b

In the summer/fall of 2003, the Navy SBIR office issued a request for proposals for a light vehicle armor system that could defeat standard handheld RPG's. A small defense company (with twenty employees) took the lead role in an effort to win a Navy SBIR request (No. 51-023) by using this armor concept.

A company scientist – Mr. Christopher Duston of CCI, a subsidiary of Technology Assessment & Transfer, in Millersville, MD, and I co-wrote a proposal for the Navy

SBIR that we won. The author's responsibilities were to develop the principle optimized armor design using the basic copper based GMET concept and offer rolling facilities for development of any test laminates for the Navy. The company manufactured the various large area targets (See fig. 68 for before images of the targets) and arranged as well as co-supervised target testing by the Army Ballistic Laboratory, Aberdeen, Md.

The live fire tests were conducted using U.S. Army Viper shaped charged warheads. The metal jet that this warhead creates can cut through fifteen inches of steel. In comparison, a Russian made RPG - 7 (standard hand held RPG weapon used by Third World soldiers and insurgents) can burn through nine inches of steel[7].

The summary is reproduced in the 'Appendix' section. See fig. 69 for an image of one of the Cu/glass laminates after impact by the Viper shaped charged warhead (A total of four laminated cermets were live fire tested.)

The key point to note from the Army's original conclusion for this RPG testing against GMET design is that the glass/Cu laminate performed as well as an equal thickness of glass (excluding the front/rear Al facing plates which were factored out). This does not appear, at first, to be a surprising result – the laminate is glass-based. But it is important to note that almost one-fifth of the laminate is metal, by volume.

This is a major reduction in total glass volume, yet the RPG's hyper velocity jet attacks were being defeated as if the target composite was made of 100% glass. As previously mentioned, RPG's have the ability to cut through steel three times more effectively than that of glass, and while this has not been demonstrated, are probably even more efficient in cutting through copper (the ability of a shape charged jet to cut through

---

[7] Private discussion with Army scientist at the U.S. Ballistic Research Lab., Aberdeen, MD

a metal is directly dependent on the metal's melting point.) The hyper-velocity molten jet, in all testing against glass based cermet laminates constructed on this author's design, were defeated at a rate normally found only for a structure containing 100% glass. The reasons for this are numerous and most prominently include the fact that the primary defeat mechanism by which any glass material defeats an attacking metal jet is to develop glass based 'counter' jets (fig. 70.)
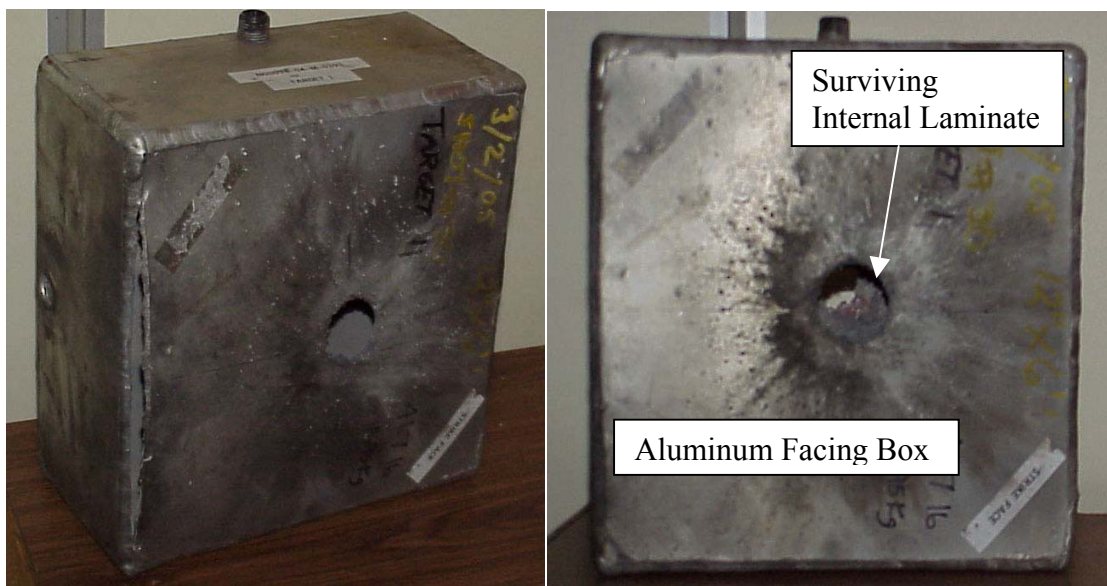
Fig. 69: Copper – Glass laminate after a US Army Viper shape charged warhead impact. While the jet was not fully defeated (as expected), the laminate did not fail outside of the burn through hole (The Viper will fully penetrate '15 inches' of steel. This laminate had only 4 cm of metal/glass.) Note reduction in jet diameter within the laminate case, image to the right

Unlike metals and ceramics, which use their high melting temperatures to dissipate energy and cool the attacking jet (see ref. 12), glass uses two different mechanisms: first, a "pinch-off" effect and, most importantly, counter jets (refs. 13 and 23.) While these mechanisms explain why glass is so effective, they do not account for how the copper based glass laminates, which are 17 percent metal by volume, would also be just as effective.

The use of metal plates to toughen ceramics is well documented (ref. 4); however, results from this thesis strongly indicate that metal plates in a laminate structure could serve other functions besides their physical protection of the ceramic phase. Primarily, the two metal plates that sandwich any given glass layer could act as focusing structures that would direct and better contain the glass jets that would be created by the heat of the attacking charge. Such a focusing mechanism, because it would be directed perpendicular to the attacking jet, would vastly increase the efficiency of the glass jets to "cut" or disrupt the metal jet - see fig. 70.

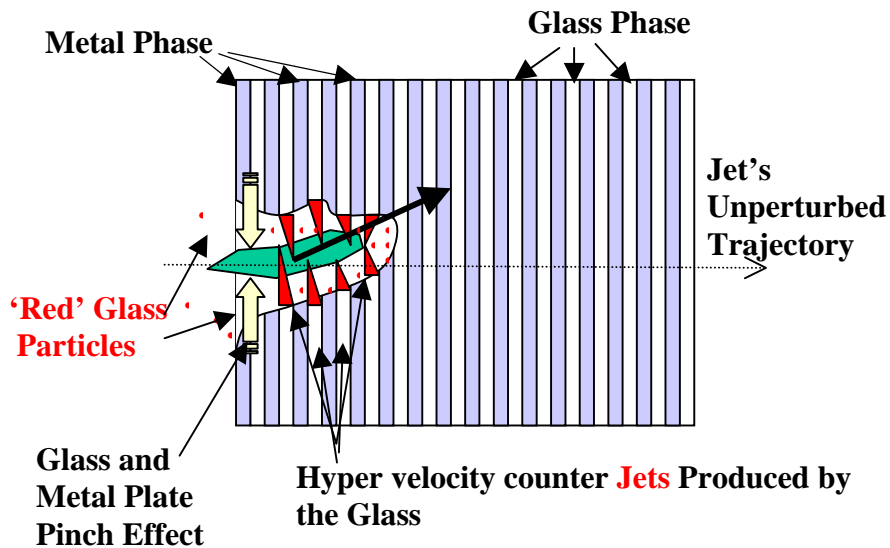**Fig. 70:** Defeat mechanisms of RPG produced jets by glass/metal laminates

Also, the glass jets create an extreme overpressure (or shock wave) that will cause the metal plates to "ring" at hypersonic velocity. This will cause these metal plates to make rapid contact with the attacking jet. Such a mechanism is the same methodology used by 'active' RPG defensive systems – namely, they use a chemical charge to accelerate a

metal plate to over 1 km/s to impact the attacking jet. This partly cools, and breaks up the attacking jet.

Since red glass production (see BRL Observations report in the Appendix), jet development, and the glass 'spring back' mechanisms sited in the references as effective defeat mechanisms are significantly reduced as glass is replaced by metal in the laminate structure, a laminate with more metal, less glass should exhibit significant reductions in the ability of the GMET to defeat the attacking hyper-velocity metal jet. For this reason, only the afore-mentioned "focused" counter jet and "metal ringing" mechanisms can account for a glass laminate with a 17 percent metal phase by volume defeating a jet at the same efficiency as an identically sized target made solely of glass.

This discovery has major implications in the study of defeating shape charged warheads by passive armor. If these mechanisms can be quantified and refined, the weight of a laminate fully capable of defeating a shape charged jet could be significantly reduced by optimizing these processes.

The ARL ballistic scientist indicated during a private conversation that if a passive system's weight could be reduced from its current stopping power weight of 485 kg/m^2 to 295 kg/m^2 (roughly a 40% reduction), then this would achieve a revolutionary improvement in passive armor performance.

With the tragic toll these man-portable weapons are inflicting upon American troops, such improved armor would be an invaluable addition to the U.S. war fighter and could, if successful, save many lives and dramatically reduce severe injuries.

Thesis Summary

This thesis research into the "DEVELOPMENT OF A NEW TYPE OF COMPOSITE MATERIAL: A GLASS BASED LAMINATED CERMET" has far exceeded original goals and has been extremely successful.

One primary objective – developing a tougher laminate cermet - has been far more successful than initially predicted; further, in this thesis a composite based on metal and glass has demonstrated that a "semi-liquid" glass can be co-rolled, when partly encapsulated by a metal phase, in a manner that allows the shear induced deformation flow of the glass to closely match that of the metal phase has been confirmed. This rolling experiment has also validated the primary claim in patent (U.S. # 5,900,097.)

Matching the shear flow of a glass and metal simultaneously has major implications in possibly allowing the mass production of high layer density laminated cermets – a composite that, until now, has never had a viable production methodology.

In examining the toughness of various larger volume GMETs used in this thesis, it has been determined that these samples exhibit extraordinary high toughness and enhanced fracture toughness despite being mostly glass. These GMETs have demonstrated deformation tolerances in tensile and torsion as well as toughness values much higher than any previously documented ceramic laminate.

These GMETs have exhibited an overall toughness of 0.95 kJ/m^2 and fracture toughness of 8.1 $MN/m^{3/2}$ as calculated from peel interface experiments. Similar values were obtained from tensile failure data based on approximate initial crack length measurements. Compared to simple glasses, these results are two orders, and one order of magnitude higher relative to fracture toughness and bulk toughness, respectively.

Four-point bend samples, which have 0.4 – 0.5 mm thick glass layers, endured levels of deformation that, normally, are usually only tolerated by metals and similar ductile materials – certainly not ceramics, much less glass. Two metal/glass laminates successfully endured a 1.8 cm bend deformation deflection for an eight cm long sample, without failure (that is, the glass maintained bonding between the two metal layers.)

In tensile experiments, the over eighty-eight percent glass by cross-sectional area GMETs withstood elongations, without failures that are nearly identical to that found for aluminum alloy. In fact, the initial yield/extension curves behave exactly like this type of metal up to and more amazingly, well past the ultimate yield point. Relative to yield strength, these cermets performed as well as aluminum alloys (6061) but might, as indicated by one glass laminate sample (with a ultimate yield of nearly 250 MN/m^2), offer even higher yield values with no increase in weight.

Significantly, these new glass based composite laminates have exhibited an even more important characteristic than mere toughness or tolerance to tensile loading – these laminates have, under tension, exhibited failure morphologies identical to that of aluminum. This property, more than the bulk toughness, offers the most unique feature of this new type of composite – a glass based material that provides progressive, metal-like failure rather than sudden, cataclysmic failure normally observed/associated with most glasses or ceramic materials. This characteristic, more than any other, would allow this new class of glass based composite to be used in real world load bearing applications.

The torsion results are equally surprising for a cermet rod that is over 95% glass by volume. The room temperature angle of twist sustained by the cermet was over 45 degree's with an ultimate shear yield half that of an identical copper rod experiencing

124

torque forces under the same conditions. The shear yield values obtained in the torsion tests of the GMETs agree very closely to the tensile yield data (being 0.57 as large – a scaling facture more *expected of a material that acts like a metal in its deformation response than a brittle glass*.)

Extensive experimental data obtained in this research confirms that the glass phase is not only excellent at arresting cracks but appears to supports extremely large metal-like plastic flow. Apparently, the new glass modifier has created an amorphous glass system that more closely resembles a metal in its plastic flow characteristics to stress and deformation – even under very high tensile or torsional strain.

Relative to armor applications, this thesis work has reconfirmed that glass based armor is viable against all common man portable weapons. Further, the GMET developed in this thesis is the first time a low-density very high performance and *super tough multi-hit tolerate ceramic-based armor* has been created.

In this research it has been demonstrated for the first time that a mostly glass based armor could withstand multiple 7.62 mm military ball round impacts and not cataclysmically fail (much less the three impacts these laminates survived while still fully defeating the rounds.) Results from this thesis have regenerated interest in glass armors for use against shaped charged warheads and have shown, for the first time, that a metal/glass laminate is as good or even superior to simple glass in its ability to defeat this type of attack (simple glass is the gold standard armor versus this type of weapon.)

Relative to shaped charged warhead defeat, this work was the first instance that previously well known materials properties/physics have been used in a manner that significantly allows this tough armor to be manufactured with not just any lost in

protection levels due to the presence of a large proportion of metal (17%) but actually a net increase in defeat. These lamination results indicate that it might be possible to improve the performance of glass based cermet armor even further and make the material significantly lighter.

Thesis Conclusions

This self financed thesis research into developing a new, and revolutionary glass based laminated cermet composite has demonstrated that this type of material not only offers many process advantages over conventional ceramic based laminates but has demonstrated that a majority glass, by volume, cermet can exhibit toughness/fracture toughness values that are extraordinarily high – similar to that of a metal. In fact, this new amorphous glass has plastic flow characteristics more similar to a metal than what is normally associated with such brittle oxide based amorphous ceramics.

Also, the mechanical processing of this GMET such as cutting with a band saw is nearly identical in performance/damage profile to that found in cutting a true metal like aluminum.

These results have strongly demonstrated that a GMET can be made so tough and resistant to tensile failure that it has metal-like bulk mechanical deformation properties and would be a viable candidate for use in many engineering applications that, until now, only metal materials have exploited.

Deep Space Applications

The use of a glass-based composite in an aerospace vehicle is not just speculation but is currently being done. The new Airbus A380 super jumbo jetliner is using a number of

glass fiber reinforced aluminum composite panels instead of simple aluminum alloy. This composite is know as a GLARE Laminate and has a woven set of glass fibers mated to aluminum panels. This arrangement has reduced structural panel weights by 10% and improved both fire resistance and bending fatigue (ref. 27.)

In a high cost, highly harsh environments like manned space flight, this material offer's many advantages over any existing aerospace metal, polymer or ceramic materials.

For projected GMET composites the glass phase can have lead or boron (depending on the radiation threat profile) added to increase the hard or soft radiation performance of the glass phase. With these additives, it is possible to create a fully load bearing, non-parasitic aerospace grade material that can be designed for spacecraft that is significantly superior to aluminum, on a weight bases.

Material	Density* (Mg/m^3)	Tensile Yield[+] Strength (MN/m^2)	Fracture Toughness $(MN/m^{3/2})$	Toughness (kJ/m^2)	Strength - Density Ratio
Al Alloy(6061)	2.7	140	25	18	52
Aluminum Cermet	2.5	180	7.8	0.88	72
Copper Cermet	3.2	250	8.1	0.95	78

* Cermet densities displayed are based on laminates developed for this thesis (88[+]% glass by volume)
[+] Yield values of the metals and GMET both experimentally measured

Table 7: Load bearing physical properties of GMETs and 6061 Al alloy

For instance, versus proton/neutron/solar event radiation and secondary cascade radiation threats, this composite can be used in constructing the load-bearing spaceship structures/skins with densities 10% to even 25% lower (for a B & Li based oxide glass)

than 6061 aluminum alloys but have proton/neutron absorption/reflection properties similar to plastic (ref 28.)

For the gamma, or x-ray threat spectrum lead glass will offer the design engineer the opportunity to create a fully load bearing structure that has no added parasitic weight costs compared to current designs that require this extra shielding material to be added on top of the existing structural components in critical areas such as sleeping or emergency shield rooms.

Electronics Equipment Racks

Sleeping Crew Chamber

Laboratory and Station Support Equipment

Orion Moon Orbiter

Space Station Destiny Laboratory module
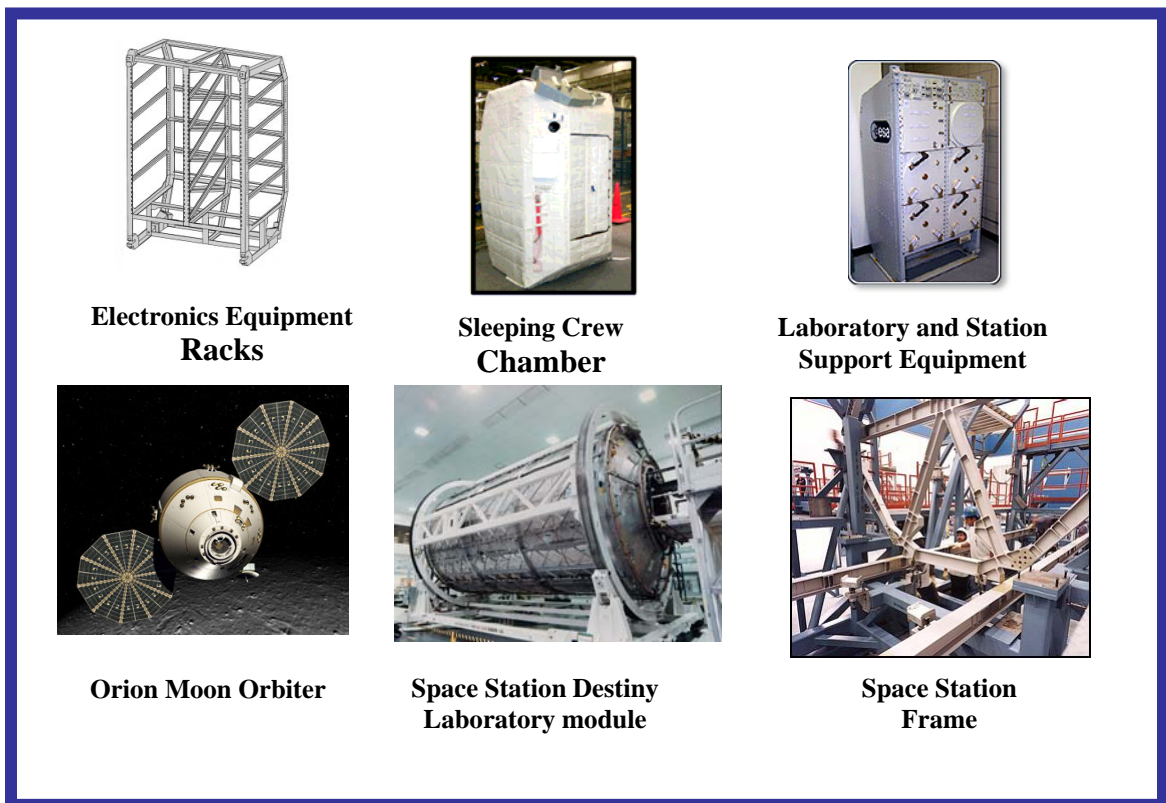
Space Station Frame

Fig. 71: Aerospace examples of items GMETs could work towards

An added benefit for this GMET laminate in space craft construction is that these composites (based on the proven shaped charged warhead stopping power of these GMETs) offers excellent micro-meteor, and especially for low earth orbit, debris

protection that is superior to any existing material – armor grade metal or ceramic - on a weight bases.

Relative to crew safety this glass based composite, unlike currently proposed polymers, is highly tolerant to heat/UV radiation and will not readily support combustion.

In regards to assembly/manufacture of components/structures this new glass based cermet laminate offers many advantages over any existing ceramic or fiber based composites – many standard metal working/processing methodologies can be exploited. Relative to cutting and drilling, the glass phase tolerates being cut using standard tooth metal blades and drilled by simple metal bits. The laminate is based on metal and glass, allowing hot forming complex curves to readily be performed. Even some limited bending at room temperature is fully tolerated by the glass phase in the GMET.

Due to the glass phase's superior bulk toughness compared to any existing glass, riveting and bolting can be used for assembly of components. Since the laminate is encased in metal, edge welding could be used.

Relative to mass manufacture of large area plates, this work has demonstrated that encapsulated hot rolling can be exploited, via shear-induced flow matching between a glass and a metal, to enable the rapid creation of glass-metal layers for these laminate structures. For a complex laminate composite requiring a high layer density for thick laminates, it should be possible to use hot roll forming to create these laminated structures – a process that could readily lend its self to lower cost, mass production.

I have also demonstrated that this new composite is not just a viable armor but also a superior one. Compared to most ceramic armors, the glass based laminates are the only armors that can offer true multiple ballistic impact protection. Relative to metal armors,

glass based laminates are significantly lower in weight for similar ballistic protection but can also offer superior stopping power against shaped charged warhead jets compared to any other existing armor material.

While the study of glass based laminated cermets has only just been done, none-the-less, many firsts have been achieved:

1) Development of a completely new, and revolutionary type of glass based laminate composite or GMET that is has a glass phase that is both tough and fracture tough as many common light alloy metals and appears to readily arrest cracks like a metal.

2) This composite shows great promise as a load bearing material since its failure morphology is very similar, in tensile loading, rotation, and bend test deformations to that of aluminum alloy – that is, it appears that this glass using the special modifiers allows the amorphous oxide glass to support significant plastic flow at room temperature.

3) The demonstration that under specific conditions of strain rate, and temperature that metal and glass phases can be made to simultaneously match their three-dimensional shear induce flow when processed using hot rolling.

This research thesis has led to the first publish account of a glass based laminate cermet which we refer to as GMETs. More significantly, the research has led to the development of a revolutionary oxide glass that offers extraordinary toughness/fracture toughness and plastic flow-like properties similar to that of a metal – in fact, an oxide glass that in tension acts nearly identical to 6061 alloy aluminum in both yield and failure morphology.

Relative to critical applications, a glass based laminate that has outstanding armor qualities and stopping power versus shaped charged hyper-velocity molten metal jets that is superior to any other existing armor. Importantly, the creation of hard ceramic armor systems that are truly multi-hit capable.

In conclusion, this thesis research funded entry by the author has achieved a number of significant firsts: the simultaneous flow matching of metal and glass phases within a laminate structure under hot rolling; the creation of a new type of laminated composite – a GMET; and most important of all, a revolutionary advance in glass related composite science by the creation of a new type of glass system that is both extraordinarily tough/fracture tough but deforms, even under massive tensile elongation, identically to that of a metal.

Appendix

Ballistic Research Laboratories 's (ARL @Aberdeen, MD) Observations

During the late 1980s, the Ballistic Research Laboratory, ARL, Aberdeen Proving Ground, MD evaluated the ability of glass to stop the penetration of a copper jet (shaped charge surrogate) in comparison to a ceramic. The materials selected for evaluation were fused quartz (FQ) and crystalline quartz (CQ). The net conclusion of the Army Ballistic Laboratory was '***The ability of the glass to better stop the jet is clearly illustrated with a 25% reduction in the depth of penetration.***'

(Editors note: In the following sub-sections, a summary of the BRL test results are presented along with relevant excerpts from the summary and observations by the experimenter.)

(a) The force of the jet's impact will compact the glass to form a permanently higher density material about 1-mm thick around the penetration path.

(b) *"Particles ejected from a fused quartz target were found to be densified by up to 10%". (p.1)*

- *"The impacting jet permanently densified (the) volume surrounding the penetration path"(p.16) (*Ed Note: Similar results would be seen for AP rounds*)*

(b) The glass will then shatter, spewing densified particles back into the jet (Ed. note: or kinetic round), similar to the mechanism of composite armor.

- *"...and the fracture initiated at a bonded interface between glass plates." (p.16)*

- *"Surrounding target material fails into particles which are dispersed by the blast while material in the penetration path is highly mobile and escapes as the target fails." (p.16)*

(c) The densified particles will react with the copper particles, disrupting the stream

- *"Earlier studies showed that reflected debris particles can disrupt a jet (Ed. note: will hold for kinetic rounds) as it passes through a tubular opening" (p.22)*

(d) Form a red (copper) glass, which proceeds to pinch off of the jet.

- *"Since closure occurs before the surrounding glass undergoes brittle fracture, it is concluded that closure is primarily associated with recovery from high pressures near the penetration front." (p.16)*
- *"Evidence indicates that there is a significant interaction between the jet and red glass which fills the penetration path." (p.41)*

(e) The jet is broken into smaller elements, which are easier to stop by the glass itself, the rear steel shell, or the vehicles base armor.

- *"These two particles are tapered, which gives evidence of erosion as the penetrated the red glass." (p. 41)*
- *"Figures 20, 22 and 24 (of the BRL report) suggest that a glass target may interact more strongly with a jet broken into discrete particles." (p. 44)*

With applicable summary comments including:

- *"It is apparent that fused quartz, early in the penetration, becomes a more resistant target material than crystalline quartz." (p. 14)*
- *"Interaction with the red glass was strong enough to arrest the forward motion of the entire sequence of jet particles." (p. 41)*

"Layering dissimilar target materials should also produce irregular penetration paths which may be disruptive." (p. 49)

Live Fire RPG Program Results

Summary: The Army Ballistic Laboratory test results for the GMET Armor

CONTRACT: N00014-04-M-0393

TITLE: Fluidic Counter-Jet Armor

REPORT: SUPPLEMENT TO THE FINAL REPORT

BY: Chris Duston, Principal Investigator for SBIR

DATE: 07 March 2005

PERIOD: 8/30/04 -2/28/05

FUNDING: $99,978

Technical: Jeff Bradel, ONR353

Executive Summary

The targets produced during this program were tested at the Army Research Laboratory on 02 March 2005 against the VIPER, a shaped charge warhead, which is capable of penetrating 15 inches of steel. The test results demonstrated that copper/glass laminates performed better than solid glass, and display far greater durability.

RPG Range Testing

Each target was set with the VIPER (US Army shaped charged warhead) placed two cone diameters from the strike face (the glass based laminated cermet). Behind the target was placed a two-inch standoff air gap and a series of one-inch thick steel witness plates.

RPG Impact Data Results

The shaped charge jet impact results are summarized in Table 8.

TARGET	NOMINAL AREAL WEIGHT (PSF)	STYLE	NUMBER OF ¼" ALUMINUM PLATES	PENETRATION REDUCTION (inches)
1	40	Solid	3	3"
2	80	Solid	3	3.16"
3	80	Split	4	4.16"
4	120	Split	4	9"

Table 8: Following the tests, the majority of each target remained with the penetration path clearly visible through the center

Analysis

The VIPER (a US Army shaped charged warhead) is capable of penetrating 15 inches of steel plate. From the work previously performed at the Ballistic Research Laboratory (BRL; ARL, Aberdeen, MD), the performance of glass targets was similar to steel on a thickness basis but significantly superior on a weight basis. When the lower density of glass is accounted for (0.094 vs. 0.283 lb/in^3), the weight efficiency of glass is 3.0 times that of steel. It was hypothesized by BRL and shown by this work that laminates of metal and glass would further improved efficiency performance.

Using regression analysis (see results, fig. 72), three similar performance predictions were obtained for the laminates. To perform the analysis, the weight of the aluminum plates holding the laminates was removed. Considering only the laminate weight, the regression calculated a weight efficiency of 2.9 (R-squared = 74%). When the style of the target with either a solid laminate block or a split laminate front and back, was included

in the analysis, the estimated weight efficiencies were 2.5 and 2.7 (R-squared = 77%), respectively. The chart displayed in fig. 72 illustrates this data.
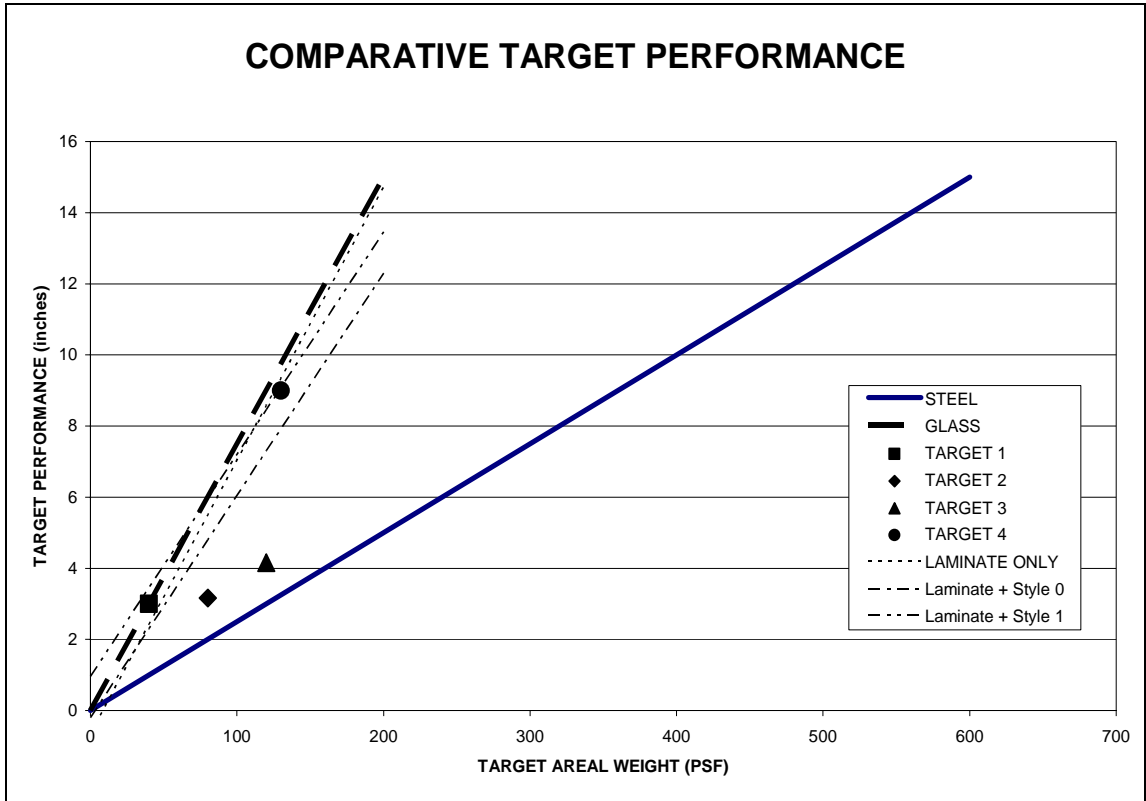

Fig. 72: Test Results analyzed for RPG Jet attack on glass based cermets

Summary of RPG Test Results

The weight to stopping power of these glass based laminated cermet armors were 10% better than solid glass - a significant improvement over the previously best performing material in defeating shape charged hyper-velocity metal jets. These test results also demonstrate the tremendous weight efficiency of glass laminate targets compared to steel for a given required thickness. The durability of glass based laminates have been previously demonstrated by Mr. Brown in his thesis research and from these RPG test results to be far greater than that of simple glass as well.
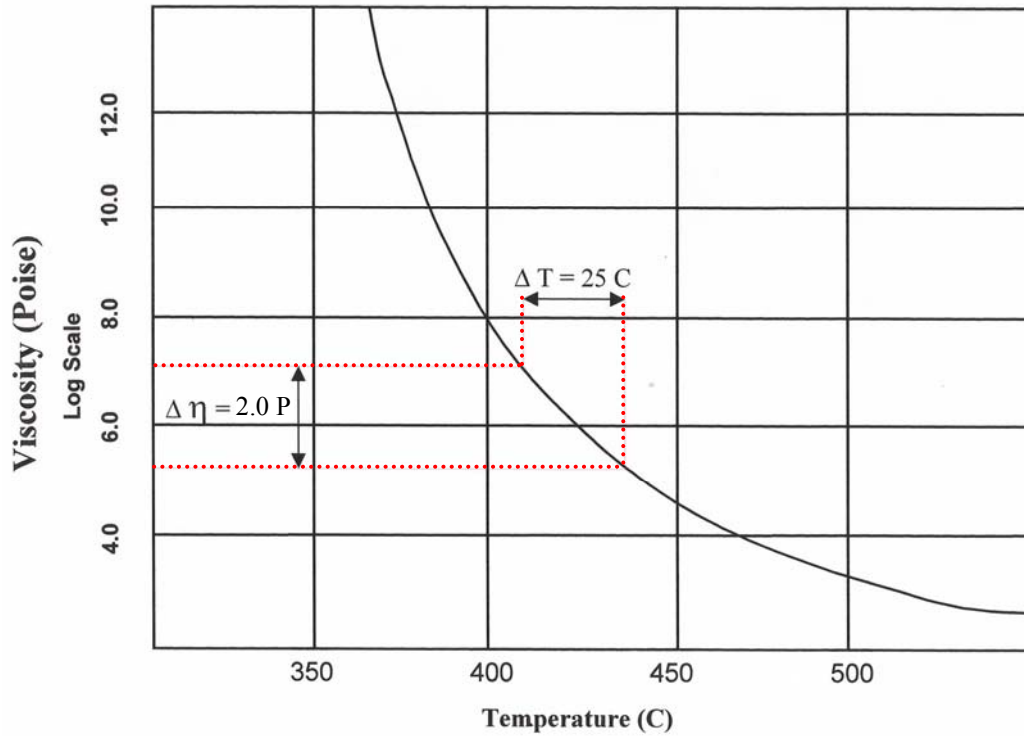
Fig. 73: A Sealing glass (Schott ALGS-32) viscosity/temperature curve (Not the special Glass created by the author but what this glass is based on)
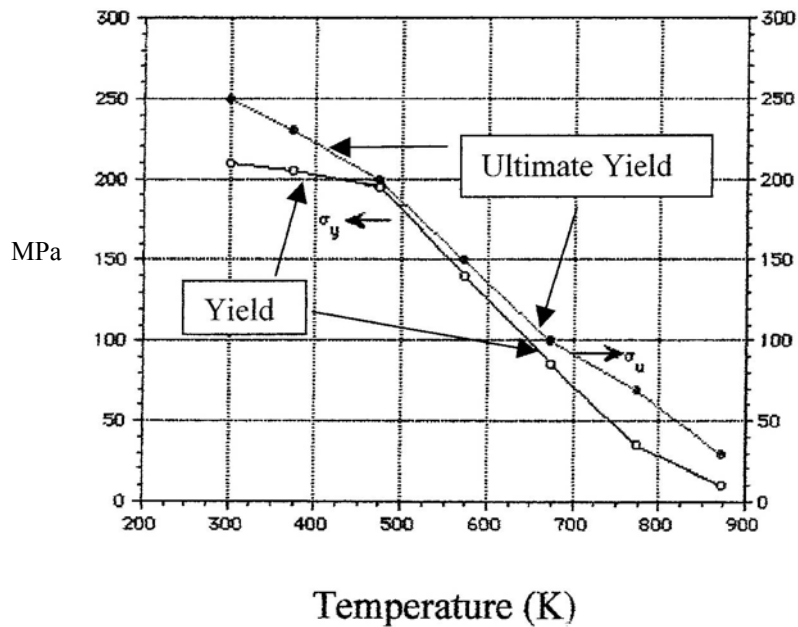

Fig. 74: Yield of copper versus temperature (Hand Book Chem/Phys, 1st Ed, CRC Press, pg 12 – 108) Yield: 50 MPa @ 750 K: Shear yield is then about 28 MPa

Misc. Data Graphs

Curve Fitted Cu Rod Torque Data

In fig. 75 the initial graph segment for the solid copper rod torque data from rise to major roll over is displayed. Using the raw torque data, a power law-fitted curve has been overlaid on the torque graph and the inflection point located (point C at the tangent to the fitted line).
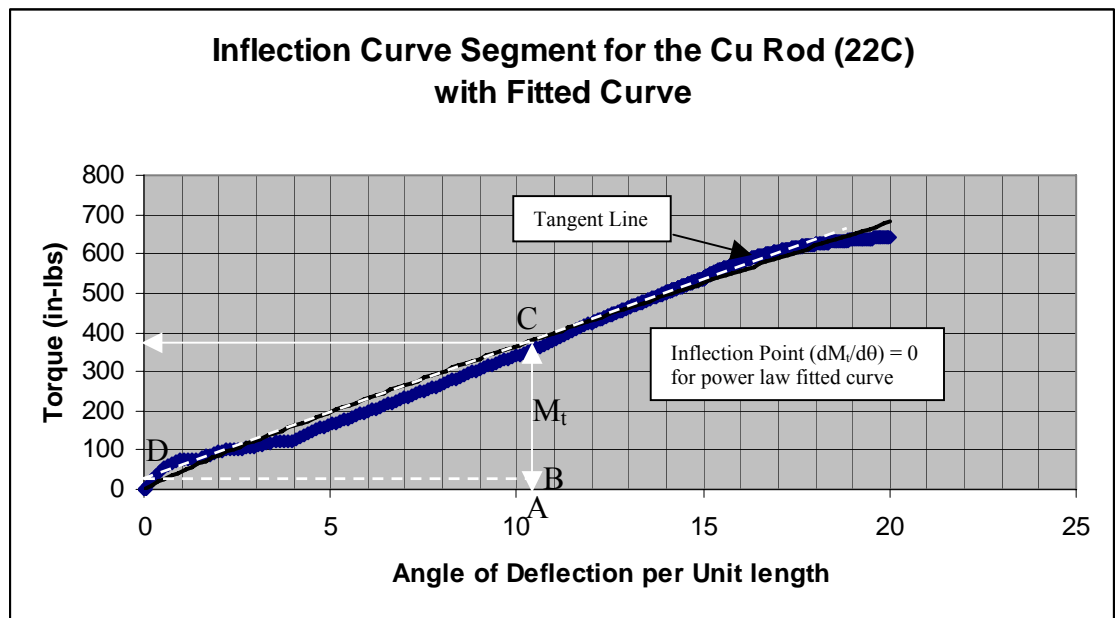

Fig. 75: Torque data segment from room temperature solid copper rod torque graph. Angle of twist data has been normalized for the gauge length (10 cm)

Using the geometric method the maximum surface shear stress is given by:

$$\tau_{Surface} = [1/(2\pi a^3)][(BC + 3AC)] \text{ where } a = 0.5 \text{ in}$$

By inspection of the graph: BC = 345 in-lbs, AC =387 in-lbs so these values the maximum surface torque to be calculated as:

$$\tau_{Surface} = [1/(2\pi a^3)][(387 - 42) + 3(387)] = 1912 \text{ lbs/in}^2 = 13.2 \text{ MN/m}^2$$

References

1) "Damascus Steels " O., J. Wadsworth; Scientific American, Feb. 1985

2) "Welded Damascus Steels and a New Breed of Laminated Composites" J. Wadsworth, D. Wha Kum, O. Sherby; Metal Progress, Feb. 15, 1987

3) "Compound Plastic Deformation of Layers of Different Metals" G. E. Arkulis. Daniel Davey, and Company Inc. Israel Program for Scientific Translations, Jerusalem, 1965. pp.178-212 and, esp. pp. 192 and also, pp.198-204.

4) "Development of Failure Tolerant Multi-Layer Silicon Nitride Ceramics: Review from Macro to Micro Layer Structures", W. J. Clegg, K. Kendall, N. Alford, T. W. Button, and J. D. Birchall, Nature, 347 (1990), p.455.

5) "Design of Si_3N_4-based Ceramic Laminates by the Residual Stresses" N. Orlovskaya, J. Kuebler, V. Subbotin, and M. Lugovy; J. Mat. Sci., 40 (2005) pp. 5443-5450

6) "Stress Redistribution in Ceramic/metal Multilayers containing Cracks." Q. Ma, M. C. Shaw, M. Y. He, B.J. Dalgleish, D.R. Clarke, and A. G. Evans. Acta Metall. Mater. Vol. 43, No. 6, pp. 2137-2142 and "The Physical Properties of Glass" D. G. Holloway; pp. 45-47; Wykeham Science Press London, 1973

7) "The Fracture Resistance of Metal-Ceramic Interfaces"; A.G. Evans and B.J. Dalgleish, Acta mettall. Mater. 40 Suppl, pp. S295-306 (1992)

8) "Deformation and Fracture Behavior of Nb in Nb_5Si_3/Nb Laminates and its Effects on Laminate Toughness." J. Kajuchi, J. Short, and J. J. Lewandowski. Acta Metall. Mater. Vol.43, No.5, pp.1955-1967

9) "The Role of Metal Plasticity and Interfacial Strength in the Cracking of Metal/Ceramic Laminates" Y. Huang, H. Zhang; Acta Metall. Mater. Vol. 43, No. 4, pp. 1523-1530

10) "Plastic Flow and Fracture of Glass", D.M. Marsh, Proc. Royal Soc. London, 1964

11) "Ceramic Armour" G. Savage; Journal of Metals and Materials, vol. 6, Aug. 1990, p. 487-492

12) "Experiments and Calculations of Jet Penetration in Glass"; B. Moran, L. Glenn, and A. Kusubov; Lawrence Livermore Nat. Lab. Report # DE91-0135672)

13) "Glass Armor and Shaped Charge Jets", Manfred Held, Propellants, Explosives, Pyrotechnics, 23, 105-110 (1998)

14) See E. Shapiro and G.E. Dieter, Metall. Trans., vol. 1, p. 1712, 1970 for maps of metal torsion deformation as a function of temperature and note viscous flow response of metals at elevated temperatures

15) "Simulation of Plate Rolling on a computerized Hot Torsion Machine and Comparison with Mill Results", I. Weiss, J. Jonas, P. Hunt, and G. Ruddle. Proc. Int. Conf. on Steel Rolling, Vol. II, ISIJ (1980), pp. 1225-1236.

16) 'Super Plasticity in Metals and Ceramics', Nieh, Wadsworth, and Sherby, Cambridge University Press, 14.1.2, pp. 242-245

17) "Engineering Materials 1", M. Ashby, D. R. H. Jones, Pergamon Press, Vol. 34; chapt. 21, pp. 197; table 21.1

18) "Deformation processes in the Vicinity of Metal-Ceramic Interfaces" Y.C. Lu, and S.L. Sass; Acta Metall. Mater. Vol. 43, No. 9, pp. 3283-3293 (1995)

19) "Design of Si_3N_4-based Ceramic Laminates by the Residual Stresses", N. Orlovskaya, J. Kuebler, V. Subbotin, and M. Lugovy; J. Mat. Science, 40 (2005) 5443-5450

20) "Deformation and Fracture Behavior of Nb in Nb5Si3/Nb Laminates and its Effect on Laminate Toughness"; J. Kajuch, J. Short, and J.J. Lewandowski; Acta Metall. Mat., 43, No. 5, pp. 1955-1967

21) "The Fracture Resistance of Metal-Ceramic Interfaces" A. G. Evans and B. J. Dalgleish; Acta Metall. Mat., 40, Suppl., pp. S295-306, 1992

22) "Stress Redistribution in Ceramic/metal Multilayers containing Cracks." Q. Ma, M. C. Shaw, M. Y. He, B. J. Dalgleish, D. R. Clarke, and A. G. Evans. Acta Metall. Mater. Vol. 43, No. 6, pp. 2137-2142

23) Ballistic Research Laboratory at Aberdeen Proving Group [Technical Report BRL-TR-3273, "Penetration of Shaped-Charge Jets into Glass and Crystalline Quartz" by Hauver, Netherwood, Blenk and Melani]

24) P. J. Hazell and S. A. Armstrong, "PERFORATION OF SPACED GLASS SYSTEMS BY THE 7.62 mm NATO BALL ROUND" 19th International Symposium of Ballistics, 7–11 May 2001, Interlaken, Switzerland

25) J. Buchar, S. Rolc, J. Voldrich, M. Lazar, and M. Stareck, "The Development of Glass Laminates Resistant to Small Arms Fire", 19th International Symposium of Ballistics, 7-11 May 2001, Interlaken, Switzerland

26) I. Horsfall, "GLASS CERAMIC ARMOUR SYSTEMS FOR LIGHT ARMOUR APPLICATIONS", 19th International Symposium of Ballistics, 7–11 May 2001, Interlaken, Switzerland

27) Guocai Wu and J.-M. Yang, "The Mechanical Behavior of GLARE Laminates for Aircraft Structures; JOM, Jan. 2005

28) R. Singleterry, and S. Thibeault, "Materials for Low-Energy Neutron Radiation Shielding" June 2000; Langley Research center, VA